AD_____

GRANT NUMBER DAMD17-94-J-4477

TITLE: Molecular Genetics of Breast Neoplasia

PRINCIPAL INVESTIGATOR: David C. Ward, Ph.D.

CONTRACTING ORGANIZATION: Yale University School of Medicine
New Haven, Connecticut 06520-8047

REPORT DATE: November 1998

TYPE OF REPORT: Final

PREPARED FOR: Commander
U.S. Army Medical Research and Materiel Command
Fort Detrick, Frederick, Maryland 21702-5012

REPORT DOCUMENTATION PAGE

Form Approved
OMB No. 0704-0188

1. AGENCY USE ONLY *(Leave blank)*	2. REPORT DATE	3. REPORT TYPE AND DATES COVERED
	November 1998	Final (29 Sep 94 - 28 Oct 98)

4. TITLE AND SUBTITLE
Molecular Genetics of Breast Neoplasia

5. FUNDING NUMBERS
DAMD17-94-J-4477

6. AUTHOR(S)
David C. Ward, Ph.D.

7. PERFORMING ORGANIZATION NAME(S) AND ADDRESS(ES)
Yale University School of Medicine
New Haven, Connecticut 06520-8047
E*Mail: david.ward@yale.edu

8. PERFORMING ORGANIZATION REPORT NUMBER

9. SPONSORING/MONITORING AGENCY NAME(S) AND ADDRESS(ES)
Commander
U.S. Army Medical Research and Materiel Command
Fort Detrick, Frederick, Maryland 21702-5012

10. SPONSORING/MONITORING AGENCY REPORT NUMBER

11. SUPPLEMENTARY NOTES
This report contains colored photographs

12a. DISTRIBUTION / AVAILABILITY STATEMENT
Approved for public release; distribution unlimited

12b. DISTRIBUTION CODE

13. ABSTRACT *(Maximum 200*

The overall objectives of this grant were a) to develop new multiparametric fluorescence in situ hybridization (M-FISH) techniques for the analysis of chromosomal abnormalities and genetic alterations in breast cells and tissues and b) to identify genes in the p14-21 region of chromosome 3 that may be implicated in the pathophysiology of breast neoplasia. We were successful in developing and validating an M-FISH karyotyping procedure in which each chromosome is uniquely identified by combinatorially fluor-labeled chromosome 'painting' probes. M-FISH was also carried out with band-specific probes as well as genomic DNA clones specific for chromosomal regions implicated in breast cancer. Unfortunately, the development of computer algorithms for 3-D image deconvolution were extremely difficult and time-consuming, thus M-FISH on surgical sections or archival specimens could not be done. We demonstrated that mRNA transcripts from the fragile histidine triad (FHIT) gene, that maps within the 3p14-21 interval was aberrant in approximately 40% of the primary breast carcinomas examined,, indicating that the FHIT gene may be involved in breast cancer progression. Finally, we have shown that comparative genome hybridization (CGH) of needle aspirates from breast tumors detect the same chromosomal changes as found in surgical specimens, facilitating evaluation of tumors prior to surgery.

14. SUBJECT TERMS	15. NUMBER OF PAGES
Breast Cancer	76
	16. PRICE CODE

17. SECURITY CLASSIFICATION OF REPORT	18. SECURITY CLASSIFICATION OF THIS PAGE	19. SECURITY CLASSIFICATION OF ABSTRACT	20. LIMITATION OF ABSTRACT
Unclassified	Unclassified	Unclassified	Unlimited

FOREWORD

Opinions, interpretations, conclusions and recommendations are those of the author and are not necessarily endorsed by the U.S. Army.

N/A Where copyrighted material is quoted, permission has been obtained to use such material.

N/A Where material from documents designated for limited distribution is quoted, permission has been obtained to use the material.

Yes Citations of commercial organizations and trade names in this report do not constitute an official Department of Army endorsement or approval of the products or services of these organizations.

N/A In conducting research using animals, the investigator(s) adhered to the "Guide for the Care and Use of Laboratory Animals," prepared by the Committee on Care and Use of Laboratory Animals of the Institute of Laboratory Resources, National Research Council (NIH Publication No. 86-23, Revised 1985).

____ For the protection of human subjects, the investigator(s) adhered to policies of applicable Federal Law 45 CFR 46.

Yes In conducting research utilizing recombinant DNA technology, the investigator(s) adhered to current guidelines promulgated by the National Institutes of Health.

Yes In the conduct of research utilizing recombinant DNA, the investigator(s) adhered to the NIH Guidelines for Research Involving Recombinant DNA Molecules.

Yes In the conduct of research involving hazardous organisms, the investigator(s) adhered to the CDC-NIH Guide for Biosafety in Microbiological and Biomedical Laboratories.

Donald C Ward March 7th/99

PI - Signature Date

Table of Contents

Appendices

A. Tables, Figures and Figure Legends for Body of Report
B. CGH profiles from 10 breast cancer patients, each analyzed as fine needle aspirates and as paraffin-embedded tissue samples.

INTRODUCTION

The development of breast cancer, as well as other neoplasias, is thought to occur by cumulative alterations in the genome, possibly acquired in an orderly fashion. These changes appear to be responsible for the passage of the disease through hyperplastic, benign, malignant, and metastatic stages of growth. Some genetic alterations are found in a variety of tumor types, while others appear to be involved in tumor tissue specificity. In breast cancer, recurrent genomic changes reportedly have been associated with many chromosomal locations and involved both amplifications and deletions of chromosomal segments as well as translocation breakpoints. However, only a few specific genes within these regions have been identified and characterized at the molecular level. P53, RB-1, BRCA-1, BRCA-2, and cathepsin D mutations and deletions have been found to predispose individuals towards malignancy. Furthermore, overexpression of the c-erb B-2/Her-2/neu oncogene has been found in a significant number of breast tumors. The functions that these genes play in regulating the normal cell cycle and the mechanisms by which their disruption leads to neoplasia are not well understood. Knowledge of genetic changes occurring during the inception and progression of tumorigenesis is necessary for the development of new diagnostic markers and therapies, rational analysis of treatment protocols, tracking remission progression, and assessing genetic risk status.

The overall objectives of this project were to develop new fluorescence in situ hybridization (FISH) techniques that would permit the analysis of multiple genetic loci simultaneously in breast tumor tissues, in chromosomes prepared from short term cultures of breast tumor cells or in tumor cell lines. Specifically, we proposed to develop chromosome "painting" probe sets that can be combinatorially labeled with different fluorescent dyes such that karyotype analysis of tumor cell chromosomes is feasible using multicolor FISH (M-FISH). In addition, we proposed to establish probe sets for specific genes and chromosomal regions implicated in the pathophysiology of breast carcinoma and to develop experimental protocols for multiplex FISH analysis of such probes in fresh or paraffin-embedded tissues. Finally, we proposed to study the role of genes mapping in the p14-21 region of chromosome 3 in the initiation, progression or metastasis of breast cancer. These objectives constituted the four tasks reported in the Statement of Work (Section G) of our original grant proposal.

The following report below outlines the progress made during the entire funding period of this proposal. We were successful in completing Task 1, Task 2a and Task 2b. Because of the lack of progress in developing a robust computer algorithm for 3-D image deconvolution of 24-color images (a task that has yet to be achieved to my knowledge by any academic laboratory or commercial software developer) we were not able to undertake Task 2c or Task 3. Instead, we substituted a study of the utility of comparative genome hybridization (CGH) to directly detect chromosomal changes in breast tumor cells obtained by fine needle aspiration. We demonstrated, for the first time, that fine needle aspirates give CGH results equivalent to paraffin embedded material obtained surgically. These results indicate that CGH from needle aspirates could facilitate the genetic evaluation of tumors prior to surgery. When coupled with an assay to determine overexpression of Her2/Neu by either FISH or immunohistochemistry, this could provide

an early indicator of patients with a poor prognosis and potential candidates for Herceptin therapy. Finally, our work relevant to Task 4 was focused on the analysis of FHIT (fragile histidine tetrad) gene transcripts. This gene maps within the 3p 14-21 interval of particular interest in breast carcinoma. We showed that approximately 40% of the FHIT mRNAs were aberrant in primary breast cancer specimens, suggesting a possible role of FHIT in the progress of a subset of breast carcinomas.

BODY

1) Multiparametric Fluorescence in situ Hybridization (M-FISH)

Assumptions

Chromosome karyotyping by conventional cytogenetic banding methods is time-consuming, expensive, and difficult to automate. The detection of recurring genetic changes in solid tumor tissues by karyotyping is particularly problematic because of the difficulty in routinely preparing metaphase spreads of sufficient quality and quantity and the complex nature of many of the chromosomal changes. Marker chromosome identification based solely on banding patterns is extremely difficult. Indeed, attempts to fully automate karyotype analysis over the past twenty years have failed because robust computer algorithms could not be developed to reliably decipher complex banding patterns, particularly those of extensively rearranged chromosomes.

Fluorescence in situ hybridization (FISH) is a powerful tool for the analysis of genes and chromosomes because of its high absolute sensitivity and its ability to provide information at the single gene/single cell level. One of the advantages of fluorescence for the detection of hybridization probes is that several targets can be visualized simultaneously in the same sample. Using either combinatorial or ratio-labeling strategies, many more targets can be discriminated that the number of spectrally resolvable fluorophores. Combinatorial labeling provides the simplest ways to label probes in a multiplex fashion since a probe fluor is either completely absent or present in unit amounts; image analysis is thus more amenable to automation, and a number of experimental artifacts are avoided (such as differential photobleaching of the fluors and the effect of changing excitation source power spectrum).

The number of useful Boolean combinations of N fluors is 2^N-1. Thus, for a single fluor A, this is only one useful combination (A=1), while for two fluors, A and B, there are three useful combinations (A=1, B=0, A=1,B=1; A=0. B=1). There are seven combinations of three fluors, 15 combinations of four fluors, 31 combinations for five fluors, and so on. To uniquely identify all 24 chromosome types in the human genome, using chromosome painting probes, five spectrally distinguishable fluors are needed. Each probe is thereby provided with a distinct spectral signature dictated by its fluor composition.

A significant limitation of M-FISH is that it provides no chromosomal banding data for the identification of chromosomal subregions. Thus, certain types of chromosome rearrangements, such as pericentric inversions, are not detectable by the current version of M-FISH nor can chromosomal translocations be assigned to specific cytogenetic bands. To circumvent this problem, we have worked on identifying an additional fluor/filter that would enable us to discriminate yet another fluorophore when incorporated into the existing fluorophore set. This has been achieved. Our ultimate goal is to present M-FISH results as similarly to conventional cytogenetics as possible; i.e., black and white (or gray scale) ideograms (in which chromosome identification is based

on the spectral signature provided by the combinatorially labeled chromosome painting probe) containing standard G-banding data (produced by inverting the R-banding images produced by hybridization of the Alu-oligonucleotide labeled with fluor).

Procedures

All of our effort during year 01 were focused on the identification of appropriate sets of spectrally resolvable fluorophores and optical filter sets that would permit the analysis of 6 to 7 fluors simultaneously and to utilize chromosomal DNA "painting" libraries, combinatorially labeled with these fluors, to carry out 24 color FISH karyotyping

A significant portion of the second year was devoted to validating the utility of M-FISH by analyzing, in a blind fashion, multiple cell lines previously subjected to conventional karyotyping. These studies have included a variety of breast carcinomas, ovarian carcinomas, squamous cell carcinomas of the head and neck, leukemias, lymphomas as well as numerous normal cell samples. While the M-FISH data show a high degree of concordance with conventional cytogenetics (>95%) there are some limitations that need to be addressed, particularly with regard to M-FISH applications in interphase nuclei, cells, and tissues. Most notable are the lack of 3-D image deconvolution software and fully automated image acquisition hardware. These limitations prevented us from carrying out the proposed studies on interphase cells and tissues during year 3 of the grant as planned. The technical aspects of M-FISH, the types of data obtained to date and the relative merits and pitfalls of M-FISH are detailed in the three publications appended to this final summary statement. These publications unequivocally demonstrate our ability to detect both simple and complex karyotypic changes by M-FISH, many of which could not be defined by conventional cytogenetics, and establish M-FISH as a useful adjunct for further defining chromosomal abnormalities in tumor cells detected using comparative genome hybridization or conventional cytogenetics.

Experimental Methods

Slide preparation
Prometaphase spreads are prepared from phytohemaglutinin (PHA, Murex) stimulated lymphocytes of healthy male donors (46, XY) following standard procedures of hypotonic treatment with 0.075M KCl and methanol/glacial acetic acid fixation (3:1). Briefly, 5 ml of blood from a healthy male donor is placed into 45 ml of RPMI culture medium, supplemented with glutamine, penicillin, streptomycin, 10% fetal bovine serum, and phytohemaglutinin (PHA, Murex). After 68 hours of culture, the blood is centrifuged and the cells are resuspended in 0.075M KCl, a hypotonic solution, causing the cells to swell. A small amount of methanol/glacial acetic acid (3:1) is added, causing the red blood cells to lyse. The remaining cells, primarily lymphocytes, are fixed with additional methanol/acetic acid and washed several times in fixative to remove cellular debris. 10-50 ul of fixed lymphocytes are placed on glass slides at approximately 23oC and 55% humidity. The nuclei of cells containing metaphase chromosomes lyse allowing the chromosomes to spread out on the slides.

Chromosomes are prepared from short term cultures of primary tumor cells or from established tumor cell lines essentially as outlined above but without pretreatment with phytohemaglutinin.

Slide pretreatment before hybridization

1. Put slides into 2xSSC for 5' on shaker.
2. Prepare dilution of RNase A stock solution (Stock solution: 10 mg/ml in 10 mM Tris-HCl pH 7.5, 15 mM NaCl diluted 1:100 in 2 x SSC) and add 200 µl to each slide and cover with a coverslip (24 x 60 mm).
3. Incubate for 60' at 37°C in a moist chamber.
4. After 60' incubation, wash 3x 5' in 2xSSC.

Pepsin treatment

1. Prewarm a coplin jar containing 100 ml of ddH_20. Add 50 ul of Pepsin stock solution (100ug/ml in ddH_20) and 1 ml of 1 M HCl.
2. Incubate the slides at 37°C for exactly 10' in the pepsin-HCl-solution.
3. Stop the reaction by adding of fresh 1xPBS.
4. Perform 2 additional wash steps in 1xPBS and one in 1xPBS / 50 mM $MgCl_2$ on shaker.

Postfixation

1. Place the slides in the formaldehyde fixative: 1% formaldehyde, PBS (phosphate buffered saline), 50 mM $MgCl_2$ for 10' at room temperature.
2. Wash in 1xPBS.
3. Dehydrate in an ethanol series (70-90-100% ethanol in ddH20) for 3 minutes each at RT.
4. Select slides with at least 10 to 20 good metaphases for hybridization.

Denaturation

1. Preheat the slide denaturation solution in the coplin jar to 70°C plus 0.5°C for every slide to be added to the jar..
2. Incubate the slides for exactly 2 minutes in the denaturation solution.
3. Dehydrate for 3 minutes in Ethanol 70% at -20°C.
4. Dehydrate for 3 minutes in Ethanol 90% at -20°C.
5. Dehydrate for 3 minutes in Ethanol 100% at -20°C.
6. Air dry slides (not on the slide warmer!).

DNA labeling by Nick Translation

Initially the chromosome DNAs were labeled by nick translation using the following protocol (1, 2), then combined to make hybridization cocktail.

The mixture for one probe (50µl):

1 µg (max. 25 µl) DNA

5 µl	10x nick-translation buffer (0.5 M Tris-HCl, 50 mM $MgCl_2$, 0.5 mg/ml BSA)
5 µl	0.1 M mercaptoethanol

5 µl 10x nucleotide mix (dATP, dGTP, dCTP each 0.5 mM)
5 µl 10x label-dUTP mix (e.g. 0.45 mM Biotin-dUTP, 0.05 mM dTTP in 0.01 M Tris-HCl, pH 8.0)
2 µl DNA-Polymerase I, E. coli, 10 U/µl
3 µl stock DNase (5U/µl, 0.075 M NaCl, 25% Glycerol) diluted 1:100-1:1000
Add sterile ddH_2O to final volume of 50 µl.
Incubate for 90 -180' at 15°C.

Check the fragment length on a 1% TBE agarose gel after 90' while the tubes are kept at -20°C. When the fragment length is about 100-500 bp, the reaction can be stopped. Originally the probes were nick-translated individually and combined to create fluor pools after labeling. Later, the DOP-PCR (Degenerate oligonucleotide-primed PCR) chromosome-specific libraries are pooled into fluor groups and labeled during DOP-PCR. The FITC pool contains chromosomes 1, 6, 7, 9, 13, 15, 17, 20, 21, 22. The Cy3 pool contains chromosomes 3, 5, 7, 9, 13, 16, 19, X, Y. The biotin pool (later detected with avidin-Cy3.5) contains chromosomes 4, 6, 7, 11, 12, 14, 15, 18, 19, 21, X. The Cy5 pool contains chromosomes 8, 9, 10, 11, 14, 16, 19, 20, 21, 22. The digoxigenin pool contains chromosomes 2, 5, 8, 12, 13, 14, 15, 17, 18, 20. Although these pools can be labeled by nick translation as above, commonly the labeled nucleotides are incorporated during the PCR reaction itself (3, 4, 5).

5 µl 10x PCR-buffer (with no $MgCl_2$, e.g., Perkin Elmer)
4 µl 25mM $MgCl_2$ (Final conc. 2mM $MgCl_2$)
2 µl 5mM dATP, dGTP, dCTP(Final conc. 200µM of each dNTP)
1 ul 5 mM fluor-labeled dUTP
1 ul 5 mM dTTP
1 µl 100µM6MW-primer (Final conc. 2 µM)
0.5 µl Taq Polymerase (2.5 units)
2 µl chromosome specific library or pooled chromosome libraries
Add sterile ddH20 to a final volume of 50 µl

Design of the degenerate oligonucleotide primer 6MW : 5'-CCG ACT CGA GNN NNN NAT GTG G-3'

PCR-Program (Thermocycler Perkin Elmer):
5' at 93°C,
five cycles of 1' at 94°C, 1.5' at 30°C,
3' transition 30-72°C
3' extension at 72°C
35 cycles 1' at 94°C,
1' at 62°C
3' at 72°C, with an addition of 1 sec/cycle to the extension step
10' at 72°C, then keep at 4°C.

Check 5 µl of PCR product on a 1% agarose gel. The length of the labeled product

should be 100-800 bp in length. If the length is excessive, incubate the probe with either DNase or the restriction endonuclease XhoI (which cuts in the Telenius primer sequence and will reduce the probe size to 100-500 bp).

M-FISH Probe Mixture
2.5-5 μg of each fluor mix
30 μg of human CotI DNA
20 μg of sheared salmon sperm DNA
1/10th volume of 3M NaOAc
2-2.5 volumes of 100% ethanol.
Store at -20°C.

Final Steps in Probe Preparation
Spin for 30 minutes at 13,000g.
Wash the pellet with 200 μl of 70% Ethanol followed by another centrifugation for 10 minutes at 13,000g.
Dry pellet in the Speedvac for 10' (lyophilization).
Resuspend of the pellet in 6 μl of deionized formamide for at least 30 minutes at 37°C.

Denaturation and Preanealing
Prior to denaturation add 6 μl of hybridization buffer (4xSSC, 20% dextran sulfate).
Denature for 5' at 78°C.
Preanneal for 30-50' at 37°C.
Place on the slides.

Hybridization
1. As soon as the slides are dry, place them one by one on the slide warmer at 37°C.
2. 10 μl of DNA-probe is dropped on each slide and the hybridization area is covered with a 18x18 mm coverslip.
3. Coverslips are sealed with rubber cement.
4. The slides are incubated for 2 to 3 days at 37°C in a moist chamber. (6).

Probe Detection
1. The coverslips are gently removed from the slides and the slides are placed in coplin jars filled with 50% formamide, 2 x SSC at 42°, three times for 5 minutes each wash.
2. The slides are washed three times for 5 minutes each wash in 0.2 x SSC, at 60°C.
3. Non-specific binding is reduced by incubating the slides for 30 minutes in 3% BSA, 2 x SSC for 30' at 37°C.
4. Suitable detection solutions are prepared by dilution of the following stock SSC:

Detection

Avidin-cy3.5. Avidin is coupled with cy3.5 by combining avidin (1 mg avidin DCS [Vector] in 1 ml of 1 M NaBorate, pH 8.5) with cy3.5 succinimidyl ester (0.5 mg , in 0.2 ml formamide, Amersham). After incubation at RT for 2 hr, the mixture is put

through a 5 ml G-25 Sephadex column in 1 M NaBorate, pH 8.5, then dialyzed against PBS before storage at 20°C. Avidin cy3.5 (1 mg/ml) is diluted 1:500 before use.

Anti-digoxigenin-cy5.5. One mg of anti-digoxigenin (anti-digoxigenin Fab fragment [Boehringer] in 1 ml of 1 M NaBorate, pH 8.5) is coupled with cy5.5 succinimidyl ester (0.5 mg in 0.2 ml formamide, Amersham). After incubation at RT for 2 hr, the mixture is put through a 5 ml G-25 Sephadex column in 1 M NaBorate, pH 8.5, then dialyzed against PBS before storage at 20°C. Use at a 1/500 dilution.

5. 200 µl of each antibody solution for each slide is pipetted onto the slide and a coverslip is applied.
6. The slides are incubated for 30 minutes at 37°C in the moist chamber.
7. The slides were washed 3 times for 5 minutes each wash in 2 x SSC, 0.1% Triton X-100.
8. The slides are incubated in a DNA counterstain solution solution (200 µg/ml of 4',6-diamino-2-phenylindole, diluted 60 µl in 90 ml of 2 x SSC) for 2 minutes.
9. After washing the slides for 10 minutes in 2 x SSC, 35 µl antifade solution (23.3 mg/ml DABCO (1,4-diazobicyclo-[2.2.2]-octane from Sigma, 20 mM Tris-HCl, pH 8.0, 90% glycerol) is applied and the slide is covered a coverslip.

Imaging

Briefly, imaging was done with a Zeiss Axioskop microscope with a high pressure 75W DC xenon arc (XBO) as an excitation source. The xenon lamp is a more stable light source in order to simplify the provision of uniform illumination free of chromatic aberration. The objective lens was a 63x 1.25NA Plan Neofluar [should be "plan" and apochromatic with a high numerical aperture]. Image exposure times had to be varied to adjust for photon flux differences.

An imaging program was developed on the basis of an image analysis package (BDS-Image) implemented on a Macintosh Quadra 900. Image shifts caused by optical and mechanical imperfections were corrected by the alignment of the gravity center [center of mass] of a single chromosome in each image according to a procedure described by Waggoner (7) and du Manoir (8). The DAPI image was used to define the morphological boundary of each chromosome. Accurate chromosome segmentation was achieved by using a pre-filtering of an image through a top-hat filter (8,9). The mode of the gray level histogram of the top-hat filtered DAPI image was used as the threshold. For each fluor background was eliminated by subtracting the interchromosomal fluorescence intensity from the chromosomal fluorescence. The mean of the intrachromosomal fluorescence intensities was used to calculate the threshold for the indivudal segmentation mask of each fluor. Individual DNA targets were assigned distinct gray values depending on the "Boolean signature of each probe", i.e. combination of fluors used to label this DNA probe. In a final step a look-up-table was used to assign each DNA target a pseudocolor depending on this gray value.

Results

Selection of resolvable fluors and high contrast filters.
The limited spectral bandwidth available for fluorescence imaging (~350-800 nm), and the extensive overlap between the spectra of organic fluors, makes separating multiple fluors spectroscopically a significant technical challenge. Choice of the fluors and filters was based on computer modeling of their contrast parameters using digitized excitation and emission spectra of a number of common fluors, the transmittance spectra of interference filters and dichroic beamsplitters from several optical supply houses (Omega, Ealing, Oriel, Zeiss), and the power spectra of the high pressure mercury arc, high pressure xenon arc, the Hg-Xe arc, the quartz tungsten-halogen lamp and various laser excitation sources. Excitation and emission contrast ratios were computed for every fluor relative to its two nearest spectral neighbors. Filters were then selected to achieve >90% discrimination. This level of contrast is not generally achievable using either excitation selection or emission selection alone, no matter how narrow the filter bandwidths. Thus excitation selection and emission selection were applied simultaneously. Excitation contrast was favored whenever possible, to avoid unnecessary wasting of fluorescence photons (and hence unproductive photobleaching of the fluor).

The chosen fluor set consisted of 4'-6-diamidino-2-phenylindole (DAPI, a general DNA counterstain), fluorescein (FITC), and the cyanine dyes Cy3, Cy3.5, Cy5, Cy5.5 and Cy7. The absorption and emission maxima, respectively, for these fluors are: DAPI (350nm; 456nm), FITC (490nm; 520nm), Cy3 (554nm; 568nm), Cy3.5 (581nm; 588nm), Cy5 (652nm; 672nm), Cy5.5 (682nm; 703nm) and Cy7 (755nm; 778nm). The excitation and emission spectra, extinction coefficients and quantum yield of these fluors are described in detail elsewhere. All fluors were excited with a 75W Xenon arc .

To attain the required selectivity, filters with bandwidths in the range of 5-15 nm (cf. approximately 50 nm or more for "standard" filter sets) were required. Further, it was necessary to both excite and detect the fluors at wavelengths far from their spectral maxima. Emission bandwidths were made as wide as possible. For low-noise detectors such as the cooled CCD camera used here, restricting the excitation bandwidth has little effect on attainable signal to noise ratios; the only drawback is increased exposure time.

Epifluorescence filter cubes constructed using the bandpass and dichroic filters were tested experimentally for spectral contrast between adjacent fluors. Good contrast (>92%) was attained in practice for all fluors except the Cy5/Cy 5.5 pair, which was marginal (80-90%). For this reason, Cy 5.5 was omitted from the combinatorial labeling experiments described below. It is vital to prevent infra-red light emitted by the arc lamp from reaching the detector; CCD chips are extremely sensitive in this region. Thus, appropriate IR blocking filters were inserted in the image path immediately in front of the CCD window, to minimize loss of image quality.

Software for analysis of combinatorially labeled probes.
Multi-fluor combinatorial labeling depends on acquiring and analyzing the spectral signature of each probe, i.e. the intensity values of each of the component fluors in the six

imager channels. Critical features are accurate alignment of source images, correction of chromatic crosstalk, and quantitation of the intensity of each fluor. To circumvent manual image manipulation we developed the necessary software to achieve these functions. This software carries out the following steps in sequential order:
1) correction of geometric image displacements caused by wedging in the emission interference filters, and by mechanical noise, 2) calculation of a DAPI segmentation mask to delineate all chromosomes in a metaphase spread, 3) calculation and subtraction of background intensity values for each fluor, calculation of a threshold value, and creation of a segmentation mask for each fluor. 4) use of the segmentation mask of each fluor to establish a "boolean" spectral signature of each probe, 5) display the material hybridizing to each chromosome probe next to the DAPI image to facilitate chromosome identification 6) create a composite gray value image, where the material from each chromosome is encoded with a gray value and 7) final presentation of the hybridization results using a look-up table (LUT) that assigns a pseudocolor to each such gray value.

Color karyotyping of normal human chromosomes.
To test the feasibility of karyotyping chromosomes by M-FISH, chromosome painting probes representing the 22 autosomes and two sex chromosomes were combinatorially labeled, mixed, and cohybridized to normal metaphase spreads prepared from peripheral blood lymphocytes. In the case of chromosomes 3, 5 and 11 separate p and q arm probes were used; thus a total of 27 different fluor combinations were tested in this experiment. The DNA probes were generated by microdissection and subsequent PCR amplification and labeled by nick translation. As expected, probes labeled with equal amounts of different fluors did not give equal signal intensities for each fluor, reflecting the fact that the filter sets were selected to maximize spectral resolution rather than throughput. To diminish signal intensity differentials, probe concentrations for the hybridization mix had to be established carefully in a large number of control experiments.

Figure 1 shows a metaphase spread after hybridization with the 27 probe cocktail. The fluorescence source images for DAPI, FITC, Cy3, Cy3.5, Cy5 and Cy7 are shown in the left column of the figure while the segmentation masks computed for each fluor are shown in the right column. After subtracting the interchromosomal fluorescence background from the chromosomal fluorescence, the mean of the intrachromosomal fluorescence intensities was used to calculate the threshold for creating the individual segmentation mask of each fluor. Discrimination of hybridization positive and hybridization negative chromosomes was not problematic and was accomplished within a second or two. Figure 2 shows a typical distribution of the relative fluorescence intensity values for a single fluor, Cy3.5, that documents the signal differential between hybridization positive and hybridization negative pairs of homologous chromosomes; all chromosomes showing fluorescence intensities above the threshold are represented in the Cy3.5 mask.

Each of the fluor segmentation masks is interrogated by the computer program in order to establish the fluor composition of all chromosomes. For example, as described in Experimental Methods, chromosome 7 material should be labeled with FITC, Cy3 and Cy3.5 while chromosome 9 material is labeled with FITC, Cy3 and Cy5. Each of the

individual chromosomes (or chromosomal segments) identified in the fluor masks on the basis of their fluor composition (i.e. its boolean spectral signature) can be displayed on the computer monitor next to the DAPI image of the metaphase spread. This provides a simple means for the operator to confirm chromosome identity and to assess any chromosomal abnormalities seen in the final gray value or pseudocolored composite images.

Figure 3a shows the metaphase spread in Figure 1 as a pseudocolored image while Figure 3b illustrates the karyotype generated on the basis of the spectral signature of each chromosome. Note that the p and q arms of chromosomes 3, 5, and 11 are labeled differentially, reflecting the use of the arm-specific probes. The karyotype is that expected for a normal male cell. Multiple chromosome spreads were analyzed in a similar fashion and all indicated a normal karyotype as expected. The high efficiency of the chromosome painting achieved and the reproducibility of these results through many additional experiments using either 24 or 27 color labeling protocols indicated that karyotype analysis by M-FISH was indeed feasible.

Analysis of chromosomal abnormalities by M-FISH.
To further test the utility of M-FISH for karyotype analysis, we examined a set of five patient samples in which various chromosomal alterations had been detected by conventional cytogenetic banding techniques. These samples were provided by the Yale University Clinical Cytogenetics Laboratory and were analyzed in a blind fashion using a pool of 24 whole chromosome painting probes. Figure 4 shows the karyotypes determined by M-FISH for each of the five patient specimens. The chromosomal abnormalities observed were as follows: BM2486, a 5;8 translocation (Fig. 4a); 10608, a 2;14 translocation (Fig. 4b); BM2645, a 2;3 translocation plus a deletion in 6q (Fig. 4c); BM2527, a 15;17 translocation (Fig. 4d), and BM3149, a 3;5 and a 6;12 translocation, loss of one copy of chromosomes 5 and 12 and trisomy of chromosome 8 (Fig. 4e). In each case, the chromosomal alterations seen by M-FISH were identical to those identified by cytogenetic banding. Furthermore, using the G-banding pattern generated by the DAPI fluorescence and measuring the fractional chromosome length of the translocation chromosomes, it was possible to infer the cytogenetic band implicated in the translocation breakpoints using fractional chromosome length/cytogenetic band conversion charts which again agreed with the cytogenetic data. In some instances, e.g. BM2486, BM2645 and BM2527, where the chromosomes are highly condensed there is an additional color generated at the site of the translocation breakpoints. This is due the blending of colors by fluorescence flaring at the junctions of the individual chromosome painting probe domains. This color blending is not observed when more extended, e.g. prometaphase chromosomes, are examined (e.g. sample 10608), or when the fluor composition of both translocation chromosomes have only a single fluor difference. For example in BM2527 (Fig. 4d) chromosome 15 was labeled with FITC, Cy3.5 and Cy7, while chromosome 17 was labeled with FITC and Cy7 only; in this translocation no color blending is observed. Color blending also occurs at sites where two different chromosomes overlap in the spread. However, by examining several spreads potential problems in chromosome characterization can be avoided.

We next studied a pair of cell lines HTB43 and SCC15, derived from patients with squamous cell carcinoma of the head and neck. These cell lines possessed sufficiently extensive chromosomal rearrangements that much of their chromosome complement were designated as "marker" chromosomes when analyzed by a board certified cytotechnologist using conventional cytogenetic banding procedures. The G-banded karyotype of one HTB43 cell is shown in Figure 5a. The karyotype of this cell line as revealed by M-FISH is illustrated in Figures 5b. The chromosomal partners in numerous chromosomal translocations are readily identifiable and some of the chromosomal rearrangements are extremely complex (see chromosome 5 and 15). Many but not all metaphase spreads for SCC15 demonstrated some double minute chromosomes (DMs), thus demonstrating the usefulness of M-FISH to identify DMs.

Comparative genome hybridization (CGH) was also done on cell lines HTB43 and SCC15 to determine those chromosomal regions that were over- or underrepresented in the tumor lines (data not shown). Both cell lines have a large number of different clones. Since CGH provides a summary of data for all clones one would not necessarily expect that the M-FISH data from a small number of metaphase spreads would correlate exactly with these relative copy number karyotypes. However, even with this caveat, there was a very close similarity between the M-FISH and CGH data concerning the relative abundance of whole chromosomes or chromosome segments. Since the CGH data indicated that chromosome 3p was underrepresented in these cell lines while 3q, 5p, and 11q arms were overrepresented, the use of the arm specific probes for these chromosomes in M-FISH facilitated the comparative evaluation.

M-FISH with band-specific probes and YAC clones

A set of three band specific probes from chromosome 6 were used with 19 non chimeric YAC clones and two whole chromosome painting probes (for chromosomes X and 8) in order to determine if M-FISH could be done efficiently using regionally localized and genetically less complex probe mixtures. The result of this experiment, shown in Fig. 6, demonstrates that both band specific clone pools and individual YAC clones with inserts as small as 0.5 Mb can be imaged and their spectral signatures correctly identified by our computer algorithms. While the ultimate sensitivity of M-FISH has yet to be established, it should be possible to assemble probe panels to address a broad spectrum of specific biological and clinical questions.

Previous studies have shown that G or R banding profiles can be generated by hybridization with oligonucleotides complementary to LINE or SINE (Alu) sequences. We have used Cy5.5 for such banding since Cy 7 has recently become unavailable. By adding Cy5.5 as a sixth fluor one can now do M-FISH karyotyping complete with G or R banding profiles a la conventional cytogenetics. We have taken delivery of a prototype microscope imaging sytem that is fully automated (autofocus, metaphase finder, autofilter wheel changer, and automated chromosome color classification). With further implementation of 3-D image deconvolution software we will be in position to do the cell and tissue analyses that we proposed. Unfortunately, for this grant we were ahead of the technology development which is just now beginning to deliver the tools needed to undertake these studies.

2) Studies on the Expression of the FHIT gene

Assumptions

One of the stated tasks in our grant proposal was to investigate the possible role in breast carcinomas of genes mapping in the 3p14-21 region of the genome. Many molecular and cytogenetic studies have indicated that the 3p14-21 area may harbor one or more putative tumor supressor genes important in the progression of breast carcinoma (10, 11), lung cancers (12), renal cell carcinoma (13), cervical carcinoma (14), as well as thyroid (15), and head and neck cancers (16). Recently a candidate gene has been isolated that appears to span the t(3;8) translocation in familial renal cell carcinoma and the 3p14.2 fragile site (17). This gene, designated FHIT (fragile histidine triad), is a member of the histidine triad family of enzymes and has been found to be highly conserved over evolution sharing 60-70% homology with a gene found in Saccharomyces pombe (diadenosine 5',5'''-P1,P4-tetraphosphate (Ap4) asymmetrical hydrolase) which cleaves the Ap4A substrate asymmetrically into ATP and AMP. FHIT expression abnormalities were originally described in digestive tract tumors (esophagus, stomach, and colon). Alterations in the genome and its expression have also been observed in lung cancer (18), and more recently in breast cancer cell lines, as well as some primary breast tumors (19), and head and neck tumors (20).

Procedure

The intriguing initial studies on FHIT abnormalities prompted us to examine the expression of the FHIT gene in 27 primary breast tumors, predominantly of the intraductal and invasive type. We used both reverse transcriptase-polymerase chain reaction (RT-PCR) and RNase mismatch cleavage (RMC) assays, coupled with DNA sequencing, to determine if deletions or insertions occurred in FHIT transcripts isolated from these breast tumors.

Experimental Methods

Patients

See Table 1 for complete clinical descriptions

RNA extraction and reverse transcription

Total and poly(A+) mRNA was extracted from breast tumor tissue using TRIzol Reagent (Gibco BRL). Fresh tumor specimens were frozen immediately after excision and stored at either -70°C or in liquid nitrogen prior to RNA extraction. Samples were sectioned by microtome and judged to be between 70-99% tumor cells by hematoxylin and eosine (H&E) staining. Several sections cut by microtome immediately following the section used for H&E analysis were used for RNA preparation with TRIzol. After isolation the RNA was solubilized in RNase free water, 20-40 Units of RNAsin (Promega) was added prior to storage at -70°C. Reverse transcription was performed in 20 µl final volume containing 20M Tris-HCL (pH 8.4), 50mM KCl, 5mM $MgCl_2$, 10mM DTT, 1mM dNTPs, 500 ng oligo(dT) or 5mM random hexamer, 200 units SUPERSCRIPT II (Life Technologies Inc., Gaithersburg, MD), and 5µg of RNA. Primers and RNA were incubated at 70°C for ten minutes and then chilled on ice. After addition of buffer, DTT,

dNTPs, and MMLV-RT reactions were incubated at room temperature for ten minutes, and then at 42°C for sixty minutes. MMLV-RT enzyme was inactivated at 70°C for fifteen minutes prior to using the first strand synthesis for PCR amplification.

PCR amplification

The design of oligonucleotides used for generating RT-PCR products has been previously described (17). Two microliters of first strand synthesis was used for first round PCR amplification with a final volume of 100 µl. Primers 5U2 and 3D2 were used at a concentration of 0.8mM in 1X PCR buffer, 1.5mM MgCl2, 200mM dNTPs and 1.25 Units Taq polymerase (Perkin Elmer Cetus). Reaction conditions consisted of one cycle of denaturation at 95°C for 3 minutes, thirty cycles of 94°C for 20 seconds, 60°C for 30 seconds, 72°C for 1 minute, and a final extension at 72°C for 5 minutes using a Perkin Elmer Cetus PCR thermocycler model 9600. Two microliters of the amplified product was used directly for a second round of PCR using nested primers 5U1 and 3D1 (14). The cycling conditions for second round PCR were the same as first round PCR described above. As an internal control for each case, b actin primers (5' GGT CAC CCA CAC TGT GCC CAT CTA CG 3' and 5' GGA TGC CAC AGG ACT CCA TGC CCA G 3') were used to amplify a 289bp fragment of the human b actin gene. In a limited number of cases the genome was screened directly using primers that amplify exons 3, 4, and 5 of the FHIT gene. These primers have been described elsewhere (17). The primers used for the RNase digestion assay were designed to incorporate T7 and SP6 phage promoters onto 5U1 and 3D1 respectively (T7-5U1: 5' TAA TAC GAC TCA CTA TAG GGT AGT GCT ATC TAC ATC 3' and SP6-3D1: 5' ATT TAG GTG ACA CTA TAG GAT GAT TCA GTT CCT CTT GG 3'). The PCR products were resolved on an ethidium bromide stained 0.8% agarose gel (SeaKem LE).

RNase digestion assay

A Mismatch Detect II kit was purchased from Ambion. The procedure outlined in the kit is an adaptation of Myers et al. (20) and Winter et al.(21). The method works on the principle that mismatches in RNA hybrids may be cleaved by RNase A. Briefly, RT-PCR is performed as described above. Phage promotors T7 and SP6 are incorporated into the second pair of nested primers (T7-5U1 and SP6-3D1). After transcribing the PCR product the single stranded test "sense" RNA was hybridized to single stranded wild type "antisense" RNA. The duplexes were digested with three proprietary RNase solutions as described in the kit. The products were visualized by gel electrophoresis in 2% high resolution agarose (Ambion). Wild type and mutant p53 primers were supplied in the kit as controls. The wild type FHIT PCR fragments generated by nested primers was sequenced prior to use.

Sequencing of RT-PCR products

RT-PCR products from all primary tumors positive for Fhit aberrant transcription by Rnase digestion assay were cloned into pCR 2.1 (an Invitrogen TA cloning vector). Plasmid DNA was prepared using Qiagen Plasmid Preparation kits. Multiple Fhit fragments were sequenced in both directions for each tumor.

Results and Discussion

We analyzed RNA from the 27 primary breast tumors described in Table 1. Use of primers 5U1 and 3D1 (see Material and Method Section) resulted in the amplification of a small portion of the 5' untranslated region and essentially all of the coding region (exons 3 through 9 and a portion of exon 10) in 26 of the 27 cases. As an internal control and to assess RNA quality, a 289 bp fragment from the human Beta actin gene was routinely amplified using the same PCR reaction mixtures and PCR conditions. Full length fragment was obtained in a reproducible manner when doing RT-PCR using RNA prepared from normal human peripheral blood lymphocytes. Four of 27 cases screened amplified both full length FHIT fragment and deletion products. BCD truncated PCR products were sequenced directly and found to lack exons 5, 6, 7, and 8 and contained multiple base substitutions as well. The "full length" BCD Fhit fragments was sequenced after subcloning as described above. It was found to contain a C to T transition at +265 and a T to C transition at +294 (Table 2). Both BCD substitutions in the full-length fragment represent polymorphisms that have previously described (23). In our study, one or more of these polymorphisms was found in five of nine primary breast tumors sequenced. This frequency is comparable with earlier reports.

Amplification product for case BC2 was not obtained in two out of three RT-PCR attempts, while robust amounts of b-actin product were generated with appropriate primers. In one RT-PCR attempt with case BC2, Fhit fragment was generated and used in Mismatch Analysis. This fragment digested in the presence of Mismatch Rnase solution, indicating that its sequence was not normal. Attempts to clone this Fhit fragment for sequencing were not successful dur to the repeated inability to generate RT-PCR amplification products.

Aberrant Fhit transcripts were found by both RT-PCR and mismatch analysis in four cases: BCD, BC2, BC3, and BC16 . The BC3 Fhit fragment had multiple characteristic alterations in four out of seven clones sequenced (57%) suggesting heterozygosity (Fig. 12). The sequence coding for the conserved histidine triad from BC3 had substitutions of five amino acids. The predicted protein sequence from BC3 sequence alignments is truncated by 23 amino acids. In case (BC-16, Fig.10b) all amplification products were clearly or slightly larger than wild type, indicating insertions. The presence of mismatched bases was confirmed in BC-16 by RNase digestion and by sequence analysis. All BC16 clones sequenced had a T to C transition at _+294. Half of the BC16 clones had a A to G transition in the 5' untranslated region at -111 suggesting heterozygosity. Cases BC7, BC22, BC26, BC28, and BC31 all contained a 7-11 bp deletion at +452 in the 3' untranslated region of the Fhit RT-PCR fragment.

Occasionally low levels of transcripts clearly longer than the normal FHIT transcript were seen (BC-10 and BC-13); however, these were not tabulated as insertions into transcripts because they were not observed consistantly. Since amplification of the FHIT fragment from BC-15 RNA yielded wild type length fragment without larger or smaller fragments in the same experiment, stringency was considered sufficient.

Aberrant FHIT transcripts were found by both RT-PCR and mismatch analysis in four cases: BC-D, BC-3, BC-7 and BC-16. A deletion transcript was detected by RT-PCR in case BC-13 using primer sets 5U1 & 3D1 and T7-5U1 & SP6-3D1, however, a small fragment was not detected by mismatch analysis. In general, fragments under 400 bp were not detected using the RNase digestion assay. A 100 bp DNA ladder (Gibco BRL) treated in the same manner as test and control amplification products also could only be visualized at approximately 400 bp. The Mismatch Detect II kit while not having the sensitivity to pick up small deletion transcripts clearly had the ability to distinguish one or two basepair mismatches in the full length FHIT fragment from abnormal tissue.

Controls were used to verify the different steps of mismatch analysis. Nested primers supplied by Ambion that amplified a 781 bp fragment from wild type and mutant p53 codons 111-371 were hybridized using all possible permutations of sense and antisense transcripts and promoters. After digestion with the RNase solutions (I, II, and III) supplied with the kit, expected cleavage patterns were observed (data not shown). Wild type FHIT fragment from normal peripheral blood was routinely used as control along side test samples. To check promoter efficacy as well as polymerase activity, T7 and SP6 transcription reactions were carried out in the same tube using wild type p53 as template. After hybridization, aliquots of this reaction mixture were digested with RNase solutions I, II, and III. Titration experiments also were done to show that all reactions contained approximately equal RNA concentrations. Non-isotopic mismatch analysis is a qualitative assay, however success depends on similar levels of RNA synthesis of the two strands generated for hybridization. Empirically, the T7 promoter seemed a stronger promoter than SP6 when transcribing mutant templates, so the SP6 promoter was routinely used to generate wild type FHIT antisense strand.

In ten out of twenty-seven cases analyzed by mismatch analysis, a full length RT-PCR transcript appeared to have one or more mismatch basepairs detectable by at least one of the three RNase solutions supplied with the Ambion kit. Sequence analysis of nine full-length Fhit transcripts used in Mismatch Analysis is presented in Table 3. In addition to alterations resutling in polymorphisms seven out of nine cases were found to have changes that either directly affected the coding region or the 5' or 3' untranslated regions of the gene. In total, evidence exists by RT-PCR and Rnase Digestion assays that as many as ten out of twently-seven primary breast tumors screened (37% of total cases) may have had affected Fhit transcripts (Table 3).

The presence of aberrant FHIT transcripts did not correlate with a particular TNM classification, tumor stage or tumor size (Table 1). Four of eight tumors of T1 classification were positive for FHIT transcription anomalies (50%); Four of fourteen T2 tumors were positive (29%), two of three T3 tumors (66%) and one of two T4 tumors were positive (50%). The node status of twenty-two of the twenty-seven patients screened also was assessed. Nine of the patients screened had no metastatic homolateral axillary nodes (No). Twelve of the patients screened had movable homolateral axillary metastatic nodes, not fixed to one another or other structures (N1), one patient had nodes that were fixed to one another or other structures (N2). Five of the No group were positive for FHIT expression anomalies (56%), five of the N1 group were FHIT positive

(42%); the other two positive FHIT cases were not assessed. Normal FHIT expression was found in one case with N2 node status. One case with metastatic lesions had normal Fhit expression. Staging based on TNM classification showed three out of seven Stage I tumors positive for aberrant FHIT expression (43%), four out of thirteen Stage II (31%), three out of six stage III (100%), and one stage IV (0%) had normal expression. Nuclear grading led to the finding that 55% of positive cases were in Nuclear group II, 27% of the cases were in Nuclear group III. 18% of the cases were not assessed. In Histological grouping 27% of the cases were in grade II, 55% of the cases in grade III, and 18% were not assessed.

Estrogen and progesterone receptor status and flow cytometry reports were available for ten of the twelve cases positive for aberrant FHIT transcription. Nine out of these ten cases (90%) were either estrogen or progesterone receptor negative (six were estrogen and progesterone receptor negative, one estrogen receptor negative and progesterone receptor positive, two were estrogen receptor positive and progesterone receptor negative). Seven out of these ten cases (67%) had parameters from flow cytometric studies indicating predominantly adverse prognoses. Aneuploidy in cell populations ws assessed by DNA indices greater than 1.0. Seven Fhit positive cases had DNA indices greater than 1.0, however five of the seven cases had a low percentage of cells in S phase. Four positive Fhit cases had DNA indices equal to 1.0, the percentage of cells in S phase in these cases was also low.

3. CGH Studies of Breast Carcinomas

Assumptions

Progress in the cytogenetic characterization of solid tumors, e.g., breast cancer and gynecological tumors, has been relatively slow because of the technical difficulties in culturing tumor cells and obtaining metaphase spreads of sufficient quality to allow cytogenetic analysis. Furthermore, the complex nature of many of the genetic aberrations in tumors makes their precise identification based only on banding patterns extremely difficult (24). There is a strong need for new analytical methods not only to detect genetic changes in cancer, but also to investigate the effects of chemotherapy and hormone therapy on the gene level in order to understand therapy resistance. One recently developed tool - Comparative Genomic Hybridization (CGH) - has the potential to identify such change, and CGH was used in the studies described below.

Comparative Genomic Hybridization (CGH), developed in 1992 (25, 26), was the first molecular cytogenetic tool that allowed comprehensive analysis of the entire genome. It has now become one of the most popular genome scanning techniques, especially among cancer researchers (27). Equal amounts of differentially fluorophore labeled tumor and normal DNA are hybridized simultaneously to normal metaphase chromosomes. Regions of gains and losses in the tumor DNA are identified by an increase or decrease in the color ratio of the two fluorochromes. This approach has obvious advantages over the conventional cytogenetic method in avoiding the need for cultured tumor cells. Indeed, genomic DNA is the only source required from the tumor specimen, because genetic

imbalances are detected on normal reference chromosomes. Therefore, even tumor DNA from archived specimens (paraffin blocks) can be used. The sensitivity of this technique is limited by the resolution of the hybridization target, the metaphase chromosomes. Genetic changes can be detected and mapped on chromosomes when the size of the involved region exceeds 5-10 Mb (28). Changes affecting smaller regions are only detectable in the case of high-level amplifications. The total amount of amplified DNA (amplicon size multiplied by level of amplification) is estimated to be at least 2 Mb for becoming detectable (29). In many cases, this is already sufficient to provide a starting point for the search of novel genes implicated in cancer.

Because oncogenes and drug resistance genes are known to be upregulated by DNA amplification, it has been speculated that DNA amplification sites in cancer could pinpoint locations of novel genes with important roles in cancer progression (25). This hypothesis appears to be gaining support in the literature.

There are at least six genes whose amplification in cancer were discovered based on leads from CGH analysis. Among these is the telomerase gene at 3q26 in ovarian and cervical cancers (30), and the AIB1 (steroid receptor co-activator) (31) and BTAK (serine/threonine kinase) (32) genes involved in breast and other cancers. Overall, it is likely that many more novel gene amplifications occurring in the development of cancer will emerge in future studies.

Losses of genetic material discovered by CGH often coincide with regions previously reported to undergo loss of heterozygosity. The detection of novel small deletions by CGH could lead to the identification of new tumor suppressor genes, as suggested by a recent example from studies of hereditary cancer predisposition in the Peutz-Jegher syndrome with deletions in 19p (33). This encourages cancer geneticists to use CGH analysis for achieving rapid identification of chromosomal regions that might contain other genes responsible for familial cancers.

Tumor progression implies the gradual transition of a localized, slow growing tumor to an invasive, metastatic and treatment refractory cancer. This progression is thought to be caused by a complex stepwise accumulation of genetic changes affecting critical genes. By providing genome-wide information of clonal genetic alterations, CGH is extremely useful in the analysis of the biological basis of tumor progression as, for example, shown in cervical cancer development (gain of 3q) (34) and breast cancer progression (35, 36).

Procedures

Three specific questions were addressed using CGH. First a set of 10 tumors was analyzed to determine whether the few breast cancer tumor cells obtained by a fine needle aspiration are sufficient for a reliable CGH investigation. Paraffin embedded material of the same tumor, which is usually available in much greater abundance, was used as a control source for the CGH assay. Ten tumors were analyzed by two different hybridizations each: one from paraffin embedded material and one from fresh frozen needle aspirate.

Secondly, CGH analysis of primary tumors and their lymph node metastases in six premenopausal breast cancer patients was undertaken. The aim of this study is to determine the specific genetical differences between primary tumors and their lymph node metastases, if any. Our hypothesis would predict an increasing number of aberrations during the progression of a tumor. It would be of clinical interest to know what kinds of genetic changes occur early (e.g., in the primary tumor) and which ones are unique or markedly changed in a metastasizing tumor.

Finally, CGH analysis of breast and ovarian carcinomas of the same patient was undertaken. The aims of analyzing breast and ovarian tumors occurring in the same patient are: a) to determine whether the profile of genetic changes in this group differs from the genetic changes in the group of patients with sporadic breast or ovarian cancer and b) to compare the genetic alterations in breast and ovarian tumors in the same woman (i.e., are they two independent tumors or metastases, one derived from each organ).

Experimental Methods

Patients and Controls

For the comparison of tissue sections from paraffin embedded blocks to material from needle aspirates, materials were obtained from ten patients presenting at the department of Gynecology in Zurich in the years 1996/1997 with a newly diagnosed breast cancer. The clinical description of each patient is included in Table 4. For each breast cancer one fresh frozen fine needle aspirate and 10 thick sections (15 μm) from the formalin fixed and paraffin embedded tumor, containing >80% of malignant cells, were obtained for CGH investigations. In addition, one fine needle aspirate was prepared for cytological evaluation. Then the specimen was routinely processed for histopathological examination and determination of hormone receptor status. Blood was collected from normal male volunteers for preparation of reference DNA and also from female volunteers for normal control samples.

Preparation of Reference DNA

Genomic reference DNA for the CGH experiments is obtained from blood of healthy donors (male or female) following standard protocols using 155 mM NH_4Cl, 10 mM $KHCO_3$, 0.1 mM Na_2EDTA lysis buffer with 4 to 5 centrifugation steps at 230g (1010 rpm on Beckmann GS-6 at 4°C), proteinase K digestion (40 μl 100 mg/ml in 5 ml SE buffer with 250 μl 20% SDS) and finally a Phenol/Chloroform/isoamyl alcohol extraction.

Tumor DNA extraction

All tumor samples - whether paraffin embedded or fresh frozen specimens or fresh frozen fine needle aspirates - have to be evaluated by a pathologist or cytologist to determine the quality and the proportion of cancer cells (at least 50%). A high percentage of normal cells and necrotic tissue will severely decrease the chance for a successful CGH experiment. The quality of the DNA depends on two factors: the kind of fixation (e.g.,

frozen section versus formalin fixation) and the duration of fixation (very important for formalin fixation). Frozen sections yield high molecular weight DNA. Tissue fixed in buffered formalin (4% phosphate buffered saline) yields mildly degraded high molecular weight DNA. DNA from unbuffered formalin tissues is usually severely degraded. However, even DNA degraded to less than 1 kb can be used for CGH experiments. Dependent on the tumor size, the cell content and the duration of the formalin fixation about 10 thick cuts (15-20 μm) of paraffin embedded material is necessary to extract enough DNA for direct use in CGH. In smaller tumors (in paraffin block) tissue microdissection may be necessary to eliminate normal cell contaminants before DNA extraction and amplification by universal primer PCR (5, 37,38). When this DOP-PCR amplification is used, even the analysis of small subregions of tumors (minimum of 2000 cells, about 15-20 ng DNA), or as few as 10 unfixed cells (70 pg DNA), is possible. The standard protocol we have used for DNA preparation is presented below.

Dewaxing (paraffin embedded tissue):

1. Incubate paraffin embedded tissue sections in Eppendorf tubes.
2. 3 x 15' in 1 ml of Xylene at 55 - 60° C with 2nd centrifugation (13,000g) before pipetting.
3. Incubate 2 x 5' in 1 ml of 100% Ethanol at room temperature with 2nd centrifugation (13,000g) before pipetting.
4. Air dry tissue at room temperature (RT).
5. Incubate tissue sections in 1 ml of 1M NaSCN at 37°C for DNA nucleohistone complex dissociation (all samples) (36):
6. Wash cells three times in 1 ml of DNA isolation buffer (75 mM NaCl, 2.5 mM EDTA, 0.5% Tween 20).

Proteinase K digestion:

Incubate in 1 ml of DNA isolation buffer (see step 6) + 50 μl Proteinase K (10 mg/ml) overnight on rotory shaker at 55°C. For paraffin embedded material usually a total incubation time of 3 to 5 days is needed (every day 50 μl of fresh Proteinase K is added).

Phenol/Chloroform/Isoamyl alcohol (PCI) extraction:

8. Distribute the the content of each tube into 3 tubes before the extraction.
9. Add to each tube equal amounts (around 400 μl) of commercially available Tris-saturated Phenol after equilibration to pH 7.8 to 8.0.
   Mix the solution gently for 10' on the rotory shaker until an emulsion forms.
10. Centrifuge for 5' at 13,000g.
    Transfer the upper aqueous phase (with most of your DNA) to a fresh tube for the further procedure.
    Keep the organic phase and interface the first time for step 11.
    Repeat steps 9 and 10 once, then go to step 11.
11. Back extraction of the organic phase and interface of step 10:
    Add equal amounts of TE (pH 7.8) to each tube.
    Mix the solution gently for 10' on the rotory shaker until an emulsion forms.
12. PCI extraction (2x):
    Add to each tube equal amounts (around 400 μl) of fresh PCI solution (Phenol:Chloroform: Isoamyl alcohol 25:24:1).

Mix the solution gently for 10' on the rotory shaker until an emulsion forms
Centrifuge at 5' at 13,000g.
Repeat step 12 once, then go to step 13

13. Incubate in 40 µl of 3M NaOAc (1/10 of tube content) and 800-1000 µl of 100% Ethanol (2-2.5 x tube content) overnight at -20°C.
14. Centrifugate 30', 13,000g at 4°C.
15. Wash the pellet with 200 µl of 70% Ethanol at -20°C followed by another centrifugation of 10' at 13,000g at 4°C.
16. Speedvac for 10' (lyophilization).
17. Resuspension of the pellets (3 original and 3 back extraction tubes for 1 probe) in 10-20 µl of TE buffer (pH 7.5), second wash with 10 µl of TE buffer each, and collect in 1 original (80 µl) and 1 back extraction tube (50 µl).
18. Dissolve at 37°C for at least 1 hour. Store at 4°C.

Tumor DNA quality assessment

To assess the quality of the extracted DNA, 5-8 µl of the DNA (1/10 of the total amount) and 1.5 µl of gel loading buffer III from Sambrook (40) is placed on a 1% Agarose TAE minigel with ethidium bromide (0.5 µg/ml) and started to run at 100 mAmp (110-120 Volt) for 30-40'. For size comparison 3 µl Lambda-HindIII-DNA-Marker from Biolabs (500 ng/µl) is used. The gel is photographed with an ultraviolet transilluminator system (Fluor-5 Multlimager from Bio Rad) which detects minimal amounts of about 20 ng of genomic DNA (therefore 200 ng total amount of DNA). Both the extent of DNA degradation and the level of RNA contamination can be determined by this gel assay. This information is important for determining which DNA purification steps are to be used and for establishing the DNAse concentration required for the nick-tranlsation reactions used to fluorophore label the DNA.

Tumor DNA quantification

The precision of the CGH assay depends very much on the cohybridization of equal amounts of DNA. Therefore the exact quantification of these small amounts of DNA is crucial. The usual spectrophotometric assay is not useful, because the minimal amount of DNA in the cuvette has to be at least 1 µg (OD 0.1 = 5 ug/ml = 5 ng/µl in 300 µl solution) which sometimes exceeds the total DNA available for some samples. Therefore a much more sensitive method of DNA measurement is employed. The Picogreen dsDNA Quantification of Molecular Probes (41, 42) is a new assay based on a ultrasensitive nucleic acid fluorescence dye for the quantification of doublestranded DNA in solution. Minimal concentrations of 250 pg/ml can be detected. In our samples with a total DNA volume between 50 and 80 µl amounts of 2.5 to 4 ng total DNA can be measured using the Fluor-5 Multimager from Bio Rad (excitation at 480 nm, emission at 520 nm). With every 96-well-plate a standard curve from 5 dilutions of Lambda-DNA is determined.

Additional DNA purification

To have optimal conditions for the nick-translation or especially the DOP-PCR amplification reactions, the extracted DNA is usually repurified. For this purpose the commercially available DNA purification Compass Kit of American Bioanalytical

showed the best results (43). However, it should be noted that up to 40-50% of DNA can be lost with this procedure, so extreme caution should be practiced. The final resuspension volume is dependent on the DNA content (10 µl + 2 µl/µg DNA) and usually lies around 12 to 16 µl per 5 x 10 µm tissue sections.

DNA labeling by Nick Translation

The purified genomic tumor DNA or the DOP-PCR amplification products are labeled with biotin-11-dUTP, whereas the reference DNA is labeled with digoxigenin-11-dUTP, both using standard nick-translation procedures (1, 2).

The mixture for one probe (50µl):

1 µg DNA (max. 25 µl)
5 µl 10x nick-translation buffer (0.5 M Tris-HCl, 50 mM $MgCl_2$, 0.5 mg/ml BSA)
5 µl 0.1 M mercaptoethanol
5 µl 10x nucleotide mix (dATP, dGTP, dCTP each 0.5 mM, Biolabs)
5 µl 10x Biotin-11-dUTP mix (0.45 mM Biotin-dUTP, 0.05 mM dTTP in 0.01 M Tris-HCl, pH 8.0) for tumor DNA
or
5 µl 10x Digoxigenin-11-dUTP mix (0.25 mM Digoxigenin-dUTP, 0.25mM dTTP in 0.01 M Tris-HCl, pH 8.0) for reference DNA
2 µl DNA-Polymerase I, E. coli, 10 U/µl (Biolabs 209L)
3 µl stock DNase (5U/µl, 0.075 M NaCl, 25% Glycerol) diluted 1:100-1:1000
Add sterile ddH_2O to final volume of 50 µl.
Incubate for 90 -180' at 15°C.

Check the fragment length on a 1% TBE agarose gel after 90' while the tubes are kept at -20°C. When the fragment length is about 100-500 bp, the reaction can be stopped. If the fragment sizes are still too large, additional DNase and DNA polymerase are added and the nick-translation reaction is incubated for an additional period of time (variable: 30 to 60') at 15°C. If the DNA is not or almost not digested, purify probe and start again.

Prepare for each probe a 1 ml G-50 Sephadex column:
Column buffer: 10 mM Tris-HCl, 1 mM EDTA, 0.1% SDS pH 7.2, autoclaved
Sephadex solution: 30 g Sephadex G-50 in 300-400 ml column buffer (some supernatant will stay on top) is autoclaved together for 30'.

Pull out plugger of syringe and pack glass wool (with gloves and sterile forceps) into syringe until 0.1 ml mark is reached.

Wash 2x with 100% Ethanol.

Wash 2x with ddH2O.

Add the Sephadex solution without bubbles and spin. Repeat filling until the column reaches the 1 ml mark (usually 2-3 times).

Hang the syringes into 15 ml tubes, add 100 µl of column buffer and spin them for 5' in the clinical centrifuge level 5 (3375 rpm = 1323g). Repeat until the received fluid in the tube equals the added 100 µl.

Add 100 µl of column buffer and let them sit on the bench for a short time or

cover them with saran wrap and keep them at 4°C. Spin the columns a last time just before use.

5. Stop the reaction with 1.5 µl of EDTA 0.5 M and 0.5 µl of SDS 10% for 15' at 68°C.
6. Remove free nucleotides by running the nick-translated probes over the G-50-Sephadex column (into a new Eppendorf tube with cut off lid) for 5' in the clinical centrifuge level 5 (3375 rpm = 1323g).
7. Store probes at -20°C.

DNA preparation before hybridization
CGH Probe Mixture
Ethanol precipitate overnight at -20°C of the following mixture:

500 ng	Biotin-labeled tumor DNA
500 ng	Digoxigenin-labeled reference DNA
50 µl	human Cot-1-DNA(Gibco 15279-037) (=50 µg)
20 µl	sonicated salmon sperm DNA (=20 µg)
1/10 volume	3M NaOAc
2-2.5x volume	ethanol 100% at -20°C

(total volume about 400-500 µl)

All aspects of hybridization including slide preparation, probe denaturation and annealing, hybridization, washes and detection steps are done in the same manner as for M-FISH. The only exception is the composition of the detection mix (avidin-FITC and anti-digoxigenin rhodamine).

CGH Image Acquisition
Image acquisition for the preliminary data has been carried out with a fluorescence microscope AX 70 from Olympus equipped with a triple color epifluorescence filter cube (U-M00050) in combination with computer hardware and a cooled CCD camera from Applied Imaging Corporation controlled by their software Cytovision(tm).

For each metaphase spread 3 different gray scale images (one for each of the 3 fluorochromes) are collected. The optimal exposure time, brightness and dark invert noise level is evaluated (automatic or manual) for each exposure and the images were saved as raw data files (44).
CGH Image Analysis
The raw data of 5 to 10 metaphases per case have to be prepared before semi-automated karyotyping and CGH analysis can be carried out. In the inverted DAPI image (similar to an inverted Giemsa banding) on the computer screen touching chromosomes have to be split, cross-overs must be excluded, and axis and centromeres have to be positioned exactly. Then an automated karyotype is generated. This karyotype has to be reviewed and corrected carefully.

When the karyotype is accepted, the Cytovision(tm) program from Applied Imaging generates the CGH profiles for each chromosome in calculating the red-green-ratio at

every spot along the chromosomal axis. The profiles of different metaphases of the same case can be merged to a sum profile with annotation of the 95% confidence interval at every spot.

Some remarks for the interpretation of these profiles: When the test DNA expresses a trisomy, the ratio of test DNA versus control DNA would be 3 to 2 (or 1.5 to 1) at the location of the trisomy. When there is a monosomy, the expected ratio would be 1 to 2 (or 0.5 to 1). To consider these values (0.5 and 1.5) as limits for positive or negative results would be wrong, because there is always a contamination with some normal cells. In case of a contamination with 50% normal cells a trisomy would appear as a 1.25 to 1 ratio, a monosomy as a 0.75 to 1 ratio. These two values are marked as red (0.75) and green (1.25) limit lines on both sides of the balanced 1 line in the profiles. When the curve passes one of these lines, most likely this is due to a real chromosomal aberration depending on the confidence interval at this spot. Because the percentage of contamination with normal cells cannot be assessed exactly, it is not possible to determine the exact copy number in a case of amplification, only an estimation (8, 26, 29, 45).

Results and Discussion

Initial Studies to Validate CGH Protocol

A set of control experiments was done to optimize the CGH protocol before initiating an extensive study of multiple breast tumors. These studies included negative (normal to normal cell) controls, a positive control (a brain tumor cell line with a well characterized CGH profile) and three test breast tumors. Negative and positive controls were included in all subsequent experiments.

Negative control: DNA was purified from a normal control and divided into two aliquots for labeling. One aliquot was labeled with biotin and one with digoxigenin. Both biotin and digoxigenin labeled reference DNAs were co-hybridized to normal metaphase chromosomes. As expected, the ratio of biotin to digoxigenin signals gave a medium profile value of 1 with a narrow 95% confidence interval. Exceptions were noted in the heterochromatin rich centromeric regions of chromosome 1, 3, 9, 16, 21, 22 and Y, which have to be excluded from consideration in CGH.

Positive control: Brain tumor cell line KB/7D with known CGH profile was hybridized against normal reference DNA. Only five analyzable metaphases could be found, resulting in a 95% confidence interval wider than desired. The major previously known aberrations could still be found: amplifications in 5p, 6p, 12p, 16p, 17q and Xp, and deletions in 4q, 10, 18q and Yq.

Breast Cancers: In all cases, female tumor DNA was hybridized against male reference DNA on male chromosomes. Therefore, the X (totally green: 1.5) and Y chromosomes (totally red: 0.5) served as internal controls in every metaphase.

Tumor A: Seven metaphases were karyotyped using the inverted DAPI image and a profile of FITC versus rhodamine intensity with quite narrow 95% confidence interval

was obtained. The most prominent alteration was an almost total loss of the q-arm of chromosome 13 (13q13-q34). The tumor suppressor gene BRCA 2 (47) is one example of a gene mapping within this chromosomal region (13q12 -13). Major amplifications also were found on chromosome 1: telomeric on the short arm (1p36.3-33) as well as on the long arm (1q21-23 and 1q42-44). Smaller amplifications were detected telomeric on chromosome 2 (2p25-24), telomeric on chromosomes 6 (6q27), 10 (10q25-26), 11 (11q24-25) and 15 (15q26), the whole q-arm of chromosome 19 and part of the long arm of chromosome 22 (22q13). In addition a deletion was found on chromosome 6 (6q16-22). Altogether 12 aberrations on 9 different chromosomes could be visualized.

Tumor B: Of this small (T1), but already metastasizing, tumor, seven metaphases could be analyzed resulting in a good 95% confidence interval. The most prominent amplification was found on the long arm of chromosome 1 (1q12-42). Other amplifications were observed on 16p12-q11.2, 19p13.3-13.2, 17p11.2 and 17q25, as well as telomeric on 4p16, 5p15.3 and 9q34. Altogether there were found 8 amplifications and no deletions on 7 chromosomes. These are fewer aberrations than normally seen in that stage of disease (48, 49).

Tumor C: In this early breast cancer (stage I) 10 metaphases could be evaluated that led to an excellent 95% confidence interval. The amplification on chromosome 1 (1q12-44) with color change in the proximal part of the p-arm and another amplification more distal on 1p34.1-34.3 are obvious. Other amplifications are seen on 11q12-13 where the PRAD-1 oncogene is located (50) and on chromosome 20 (20q13.1-13.3) that is already known to be related to breast cancer (28). Deletions are found on 11q22-25 where the ATM tumor suppressor gene is located (52, 53) and on 6q15-21. Altogether in this early tumor stage 6 aberrations on 4 chromosomes were identified.

Study 1: Comparison of CGH on paraffin embedded versus fresh frozen needle aspirate samples.
In nine of ten cases both kinds of material sources - fresh frozen fine needle aspirated cells and paraffin embedded tissue sections - led to interpretable CGH results. In one case only the paraffin embedded material worked. The ratio profiles of different breast cancers each exhibited unique features, but the profiles of DNA isolated from the two different material sources yielded similar fluorescence ratio profiles. Detectable differences appear mainly in the 95% confidence intervals. In four out of nine cases, needle aspirates showed better results, in four cases the paraffin embedded material was superior, and case showed equivalent results.

A summary of the results is presented in Figure 7 and Table 4. Amplifications are noted as a bar on the right-hand side of the chromosome icon and deletions as a bar on the left-hand side. Thick bars stand for highly amplified or deleted regions. On top of each bar the case number is noted. The suffix 'a' refers to paraffin embedded material, suffix 'b' to material from fine needle aspirates. Most frequently amplifications in 1q, 16p and 17q as well as deletions in 13q and 14q, 16q and 17p could be found. For illustration purposes the metaphase hybridization images and the CGH profiles of case I are given in Figures 8 to 11. Figure 8 shows hybridization data using needle aspirate derived tumor DNA,

while Figure 9 shows results obtained with DNA from the corresponding formalin-fixed, paraffin-embedded tissue block. The CGH profiles obtained for the needle aspirate and fixed tissue are given in Figures 10 and 11,.respectively. Note that both sources of DNA give the same CGH profiles and each illustrate the complete spectrum of chromosomal abnormalities described above.

Each material source presents its own difficulties. The formalin fixed, paraffin embedded material suffers from unquantifiable damage and degradation of the DNA. This reduces the yield of DNA suitable for nick-translation and hybridization, which may be seen as an irregular profile with many spikes and a decreased 95% confidence interval value. The quality of the DNA depends mainly on two factors: the duration of fixation (more than 48 to 72 hours in formalin is bad) and, more importantly, the kind of fixation (46). Tissue fixed in buffered formalin (4% phosphate buffered saline) yields mildly degraded high molecular weight DNA.

A sufficient amount of pure, undegraded, high molecular weight DNA can be obtained from 10^4 to 10^5 cells of fresh frozen needle aspiration. However, because of the different in nuclear/cytoplasmic density between tumor and normal fibroblasts, a small number of contaminating normal cells may contribute a proportionally large amount of non-tumor DNA. This may smooth out an otherwise sharp and characteristic profile and broaden the 95% confidence interval. While DNA amplification with degenerate oligonucleotide primed polymerase chain reaction (DOP-PCR) could be used to increase the amount of available DNA, DOP-PCR has been avoided whenever possible, both in order to minimize sequence biases during amplification and to establish the feasibility of using needle aspirates directly.

Study 2: CGH on primary tumors and their lymph node metastases in premenopausal breast cancer patients (20 cases).
Of the twenty cases obtained, six have been analyzed in detail while data from the remaining 14 cases are still being evaluated. The preliminary data from the first six cases are summarized in Figure 12. Amplifications are again noted as a bar on the right-hand side of the chromosome icon and deletions as a bar on the left-hand side. Blue color represents aberrations in the primary cancer, and red color stands for chromosomal changes in the lymph node metastases. Thick bars stand for highly amplified or deleted regions. On top of each bar the specimen number is noted. The corresponding pairs of primary tumors and metastases are named in a small table within the figure. In contradiction to our hypothesis there generally were found equal numbers of aberrations at basically the same locations in the primary tumors as in their corresponding lymph node metastases. Most frequently amplifications in 7p, 9p, 16p and 17q as well as deletions in 13q, 16q, 17p, 19p and q, 20q and 21q could be found. As an interesting exception the deletions in 19p seem to occur predominantly in lymph node metastases.

Study 3: CGH on breast and ovarian tumors from the same patients (10 cases).
Ten patients that have had both a breast and an ovarian tumor diagnosed within an 18 month interval have now been investigated in detail. The profiles for these patients have been appended (Figures 13-23).

The cases analyzed to date showed similar profiles for breast and ovarian cancers. Amplifications for 1q, 16p, and 17q were seen in comparable frequency and extent in both tumor types, although in the literature gains in 16p and 17q are mentioned as typical of breast cancers only (27). Gains in 6p and 22q were only seen in ovarian cancers, although aberrations (deletions) in 22q would be expected in breast 6 cancers. Amplification in 2q, 3q, and 4q 18p, and 19p were seen predominantly in ovarian cancers.

CONCLUSIONS

The work supported by the grant has resulted in the development of a novel method for karyotyping human chromosomes and identifying the complex chromosomal rearrangements that occur in most solid tumors, including breast carcinomas. Spectral karyotyping thus proves a valuable tool to complement conventional methods for cancer cell cytogenetics. Multiplex analysis of chromosomes or specific genes in interphase nuclei of cells and tissues should be feasible in the near future with the development of appropriate multicolor 3-D image deconvolution software. Our studies also have shown that aberrant transcripts from the Fhit gene occur in a significant percentage (>40%) of breast tumors of intraductal and invasive ductal type. These observations further support the hypothesis the Fhit gene may play an important role in the pathophysiology of breast cancer. Finally, we have shown that comparative genomic hybridization using DNA from the limited number of breast cancer cells obtained by fine needle aspiration can identify chromosomal abnormalities with high efficiency and thus may be used to assess chromosome integrity prior to surgical procedures.

REFERENCES

1. Lichter, P., Cremer, T. Chromosome analysis by non-isotopic in situ hybridization. In: Rooney, D.E., Czepulkowski, B.H., ed. Human Cytogenetics: A practical approach. 2nd ed. Oxford, Washington DC: IRL Press, 1992: 157-192, vol. 1.

2. Moch, H., Presti, J.C., Jr., Sauter, G., et al., (1996) Genetic aberrations detected by comparative genomic hybridization are associated with clinical outcome in renal cell carcinoma. Cancer Res. 56 (1) 27-30.

3. Telenius, H., Pelmear, A.H., Tunnacliffe, A., Carter, N.P., Behmel, A., Ferguson-Smith, M.A., Nordenskjšld, M., Pfragner, R., and Ponder, B.A.J. (1992a) Cytogenetic analysis by chromosome painting using DOP-PCR amplified flow-sorted chromosomes. Genes, Chromosomes & Cancer 4:257-263.

4. Telenius, H., Carter, N.P., Bebb, C.E., Nordenskjšld, M., Ponder, B.A.J., Tunnacliffe, (1992b) Degenerate oligonucleotide-primed PCR: general amplification of target DNA by a single degenerate primer. Genomics 13:718-725.

5. Speicher, M.R., Jauch, A., Walt, H., du Manoir, S., Reid, T., Jochum, W., Sulser, T., and Cremer, T. (1995) Correlation of microscope phenotype with genotype in a formalin-fixed, paraffin-embedded testicular germ cell tumor with universal DNA amplification, comparative genomic hybridization, and interphase cytogenetics. Am. J. Pathol. 146(6) 1332-1340.

6. Husler, M.G Molekular-zytogenetische Untersuchung eines Dysgerminoms mittels Comparativer, Genomischer Hybridisierung (CGH) und Vergleich mit dem Seminom des Hodens. Frauenklinik des Universitatsspitals Zurich, 1996.

7. Waggoner A, Debasio R, Conrad P, Bright GR, Ernst L, Ryan K, Nederlof M, Taylor D (1989) Multiple spectral parameter imaging. Methods Cell Biol 30:449-478

8. du Manoir, S., Schršck, E., Bentz, M., Speicher, M.R., Joos, S., Ried, T., Lichter, P., Cremer, T. (1995) Quantitative analysis of comparative genomic hybridization. Cytometry 9:21-49

9. Smith TG Jr, Marks WB, Lange GD, Sheriff WH Jr, Neale EA (1988) Edge detection in images using Marr-Hildreth filtering techniques. J Neurosci Methods 26:75-81

10. Devilee,P., van den Broek, M., Kuipers-Dijkshoorn, N., Kolluri, R., Khan, P.M., Pearson, P.L., Cornelisse, C.J. At least four different chromosomal regions are involved in loss of heterozygosity in human breast carcinoma. Genomics, 5:554-560 (1989).

11. Pandis, N., Jin, Y., Limon, J., Bardi, G., Idvall, I., Mandahl, N., Mitelman, F., Heim, S. Interstitial deletion of the short arm of chromosome 3 as a primary chromosome abnormality in carcinomas of the breast. Genes, Chromosomes, and Cancer 6(3):151-155 (1993).

12. Naylor, S.L., Johnson, B.E., Minna, J.D., Sakaguchi, A.Y. Loss of heterozygosity of chromosome 3p markers in small-cell lung cancer. Nature 329 (6138): 451-454 (1987).

13. Kovacs, G., Erlandsson, R., Boldog, F., Ingvarsson, S., Muller-Brechlin, R., Klein, G., Sumegi, J. Consistent chromosome 3p deletion and loss of heterozygosity in renal cell carcinoma. Proc. Natl. Acad. Sci., USA 85(5):1571-1575 (1988).

14. Yokota, J., Tsukada, Y., Nakajima, T., Gotoh, M., Shimosato, Y., Mori, N., Tsunokawa, Y., Sugimura, T., Terada, M. Loss of heterozygosity on the short arm of chromosome 3 in carcinoma of the uterine cervix. Cancer Res. 49(13):3598-3601 (1989).

15. Herrmann, M.A., Hay, I.D., Bartelt, D.H. Jr., Ritland, S.R., Dahl, R.J., Grant, C.S, Jenkins, R.B. Cytogenetic and molecular genetic studies of follicular and papillary thyroid cancers. J. Clin. Invest. 88(5):1596-1604 (1991).

16. Latif, F., Fivash, M., Glenn, G., Tory, K., Orcutt, M.L., Hampsch, K., Delisio, J., Lerman, M., Cowan, J., Beckett, M., Weichselbaum, R. Chromosome 3p deletions in head and neck carcinomas: statistical ascertainment of allelic loss. Cancer Res. 52(6):1451-1456 (1992).

17. Ohta, M., Inoue, H., Cotticelli, M.G., Kastury, K., Baffa, R., Palazzo, J., Siprashvili, Z., Mori, M., McCue, P., Druck, T., Croce, C.M., Huebner, K. The FHIT gene, spanning the chromosome 3p14.2 fragile site and renal carcinoma-associated t(3;8) breakpoint, is abnormal in digestive tract cancers. Cell 84(4):587-597 (1996).

18. Sozzi, G., Veronese, M.L., Negrini, M., Baffa, R.,Cotticelli, M.G., Inoue, H., Tornielli, S., Pilotti, S., De Gregorio, L., Pastorino, U., Pierotti, M.A., Ohta, M., Huebner, K., Croce, C.M. The FHIT gene at 3p14.2 is abnormal in lung cancer. Cell 85(1):17-26 (1996).

19. Negrini, M., Monaco, C., Vorechovsky, I., Ohta, M., Druck, T., Baffa, R., Huebner, K., Croce, C.M. The FHIT gene at 3p14.2 is abnormal in breast carcinomas. Cancer Res. 56: 3173-3179 (1996).

20. Virgilio, L., Shuster, M., Gollin, S.M., Veronese, M.L., Ohta, M., Huebner, K., Croce, C.M. FHIT gene alterations in head and neck squamous cell carcinomas. Proc. Natl. Acad. Sci. USA 93: 9770-9775 (1996).

21. Myers, R.M., Larin, Z., Maniatis, T. Detection of single base substitutions by ribonuclease cleavage at mismatches in RNA:DNA duplexes. Science 230(4731):1242-1246 (1985).

22. Winter, E., Yamamoto, F., Almoguera, C., Perucho, M. A method to detect and characterize point mutations in transcribed genes. Proc. Nat. Acad. Sci. USA 82:7575-7579 (1985).
23. Mao, L., Fan, Y-H., Lotan, R., Hong, WK. (1996) Frequent abnormalities of Fhit, a candidate tumor suppressor gene, in head and neck cancer cell lines. Cancer Res. 56 5128-5131.

24. Geleick, D., Muller, H., Matter, A., Torhorst, J., and Regenass, U. (1990) Cytogenetics of breast cancer. Cancer Genet. Cytogenet. 46 (2) 217-229.

25. Kallioniemi, A., Kallioniemi, O.P., Sudar, d., Rutovitz, D., Gray, J.W., Waldman, F., and Pinkel, D. (1992) Comparative genomic hybridization for molecular cytogenetic analysis of solid tumors. Science 258 (5083) 818-821.

26. du Manoir, S., Speicher, M.R., Joos, S., Schršck, E., Popp, S., Dšhner, H., Kovacs, G., Robert-Nicoud, M., Lichter, P., and Cremer, T. (1993) Detection of complete and partial chromosome gains and losses by comparative genomic in situ hybridization. Hum Genet 90:590-610.

27. Forozan, F., Karhu, R., Kononen, J., Kallioniemi, A., Kallioniemi, O.P (1997) Genome screening by comparative genomic hybridization. Trends in Genetics 13 (10) 405-409.

28. Kallioniemi, A., Kallioniemi, O.P., Piper, J., Tanner, M., Stokke, T., Chen, L., Smith, H.S., Pinkel, D., Gray, J.W., and Waldman, F. (1994) Detection and mapping of amplified DNA sequences in breast cancer by comparative genomic hybridization. Proc. Natl. Acad. Sci. USA 91 (6) 2156-2160.

29. Piper, J., Rutovitz, D., Sudar, D., Kallioniemi, A., Kallioniemi, O.P., Waldman, F.M., Gray, J.W., and Pinkel, D. (1995) Computer image analysis of comparative genomic hybridization. Cytometry 19 (1) 10-26.

30. Soder, A.I., Hoare, S.F., Muir, S., Going, J.J., Parkinson, E.K., Keith, W.N. (1997) Amplification, increased dosage, and in situ expression of the telomerase RNA gene in human cancer. Oncogene 14 (9) 1013-1021.

31. Anzick, S.L., Kononen, J., Walker, R.L., Azorsa, D.O., Tanner, M.M., Guan, X.Y., Sauter, G., Kallioniemi, O.P., Trent, J.M., and Meltzer, P.S. (1997) AIBI, a steroid receptor coactivator amplified in breast and ovarian cancer. Science 277 (5328) 965-968.

32. Sen, S., Zhou, H., and White, R.A. (1997) A putative serine/threonine kinase encoding gene BTAK on chromosome 20q13 is amplified and overexpressed in human breast cancer cell lines. Oncogene 14 (18) 2195-2200.

33. Hemminki,A., Tomlinson, I., Markie, D., Jarvinen, H., Sistonen, P., Bjorkqvist, A.M., Knuutila, S., Salovaara, R., Bodmer, W., Shibata, D., de la Chapelle, A., and Aaltonen,

L.A. (1997) Localization of a susceptibility locus for Peutz-Jeghers syndrome to 19p using comparative genomic hybridization and targeted linkage analysis. Nat. Genet. 15 (1) 87-90.

34. Heselmeyer, K., Macville, M., Schrock, E., et al., (1997) Advanced-stage cervical carcinomas are defined by a recurrent pattern of chromosomal aberrations revealing high genetic instability and a consistent gain ofchromosome arm 3q. Genes Chromosomes Cancer 19 (4) 233-240.

35. Kuukasjarvi, T., Karhu, T., Tanner, m., Kahkonen, M., Schaffer, A., Nupponen, N., Pennanen, S., Kallioniemi, A., Kallioniemi, O.P., and Isola, J. (1997) Genetic heterogeneity and clonal evolution underlying development of asynchronous metastasis in human breast cancer. Cancer Res. 57 (8) 1597-1604.

36. Nishizaki, T., DeVries, S., Chew, K., Goodson, W.H., Ljung, B.M., Thor, A., and Waldman, F.M. (1997) Genetic alterations in primary breast cancers and their metastases: direct comparison using modified comparative genomic hybridization. Genes Chromosomes Cancer 19 (4) 267-272.

37. Speicher, M.R., du Manoir, S., Schrock, E., et al., (1993) Molecular cytogenetic analysis of formalin-fixed, paraffin-embedded solid tumors by comparative genomic hybridization after universal DNA amplification. Hum. Mol. Genet. 2 (11) 1907-1914.

38. Kuukasjarvi, T., Tanner, M., Pennanen, S., Karhu, R, Visakorpi, T., and Isola, J. (1997) Optimizing DOP-PCR for universal amplification of small DNA samples in comparative genomic hybridization. Genes, Chromosomes Cancer 18 (2) 94-101.

39. Hopman, A.H., van Hooren, E., van de Kaa, C.A., Vooijs, P.G., Ramaekers, F.C. (1991) Detection of numerical chromosome aberrations using in situ hybrization in paraffin sections of routinely processed bladder cancers. Mod. Pathol. 4 (4) 503-513.

40. Sambrook, J., Fritsch, E.F., Maniatis, T. (1989) Molecular cloning: A laboratory manual. (2^{nd} ed) New York: Cold Spring Harbor University Press, v. 1-3.

41. Ahn, S.J., Costa, J., Emanuel, J.R. (1996) PicoGreen quantitation of DNA: effective evaluation of samples pre- or post-PCR. Nucleic Acids Res. 24 (13) 2623-2625.

42. Marie, D., Vaulot, D., Partensky, F. (1996) Application of the novel nucleic acid dyes YOYO-1, YOPRO-1 and PicoGreen for flow cytometric analysis of marine prokaryotes. Appl. Environ. Microbiol. 62 (5) 1649-1655.

43. Vogelstein,B., Gillespie, D. (1979) Preparative and analytical purification of DNA from agarose. Proc. Natl. Acad. Sci. USA 76 (2) 615-619.

44. du Manoir, S., Kallioniemi, O.P., Lichter, P., Piper, J., Benedetti, P.A., Carothers, A.D., Fantes, J.A., Garc'a-Sagredo, J.M., Gerdes, T., Giollant, M., Hemery, B., Isola, J.,

Maahr, J., Morrison, H., Perry, Stark, M., Sudar, D., van Vliet, L.J., Verwoerd, N., Vrolijk, J. (1995) Hardware and software requirements for quantitative analysis of comparative genomic hybridization. Cytometry 9:4-9

45. Lundsteen, C., Maahr, J., Christensen, B. et al., (1995) Image analysis in comparative genomic hybridization. Cytometry 19 (1) 42-50.

46. Ben-Ezra, J., Johnson, D.A., Rossi, J., Cook, N., and Wu, A. (1991) Effect of fixation on the amplification of nucleic acids from paraffin-embedded material by polymerase chain reaction. J. Histochem. Cytochem. 39 (3) 351-354.

47. Wooster, R. Neuhausen, S.L., Mangion, J. et al. (1994) Localization of a breast cancer susceptibility gene, BRCA2, to chromosome 13q12-13. Science 265 (5181) 2088-2090.

48. Isola, J.J., Kallioniemi, O.P., Chu, L.W., Fuqua, S.A., Hilsenbeck, S.G., Osborne, C.K., and Waldman, F.M. (1995) Genetic aberrations detected by comparative genomic hybridization predict outcome in node-negative breast cancer. Am. J. Pathol. 147 (4) 905-911.

49. Ried, T., Just, K.E., Holtgreve-Grez, H., du Manoir, S., Speicher, M.R., Schrock, E., Latham, C., Blegen, H., Zetterberg. A., Cremer, T., et al. (1995) Comparative genomic hybridization of formalin-fixed, paraffin-embedded breast tumors reveals different patterns of chromosomal gains and losses in fibroadenomas and diploid and aneuploid carcinomas. Cancer Res. 55(22): 5415-5423.

50. Lammie, G.A., Peters, G. (1996) Chromosome 11q abnormalities in human cancer. Cancer Cells 3 (11) 413-420.

51. Voreschovsky, I., Rasio, D., Luo, L., Monaco, C., Hammarstrom, L., Webster, A.D., Zaloudik, J., Barbant,-Brodani, G., James, M., Russo, G., et al. (1996) The ATM gene and susceptibility to breast cancer: analysis of 38 breast tumors reveals no evidence for mutation. Cancer Res. 56 (12) 2726-2732.

52. Savitsky, K., Sfez, S., Tagle, D.A., et al. (1995) The complete sequence of the coding region of the ATM gene reveals similarity to cell cycle regulators in different species. Hum. Mol. Genet. 4 (11) 2025-2032.

PUBLICATIONS RESULTING FROM SUPPORT OF THIS GRANT

1) Speicher, M.R., Ballard, S.G., and Ward, D.C. (1996) Karyotyping human chromosomes by combinatorial multi-fluor FISH. Nature Genet. 12 368-375.

2) Speicher, M.R., and Ward, D.C. (1996) The coloring of cytogenetics. 2 (9) 1046-1048.

3) Speicher, M.R., Ballard, S.G., and Ward, D.C. (1996) Computer image analysis of combinatorial multi-fluor FISH. Bioimaging 4 52-56.

4) Burki, N.G., Caduff, R., Walt, H., Moll, C., Pejovic, T., Haller, U., Ward, D.C. (1999) Comparative genomic hybridization (CGH) of fine needle aspirates from breast carcinomas. Lab Invest., in press.

Personnel who received financial support from this Grant
Patricia Bray-Ward, Ph.D.
Mimi Kucherlapati, Ph.D.
Nicole Burke, M.D.
Tanja Pejovic, M.D.
David C. Ward, Ph.D.

APPENDIX A

Table 1. Clinical and Histological data on Primary Breast Tumors from 27 patients.

CASE	AGE	DIAGNOSIS	a)TNM	STAGE	NUCLEAR Gp	Histol. Gp	FHIT Transcripts
BC-A	47	intraductal and invasive ductal carcinoma	T2aN1	II	III/III	III/III	Normal
BC-B	73	intraductal and invasive carcinoma	T1Nx	IV	III/III	III/III	Normal
BC-C	66	intraductal and invasive carcinoma	T1No	I	III/III	III/III	Normal
BC-D	38	extensive intraductal carcinoma	T1N1	I	II/III	III/III	Aberrant
BC-2	56	intraductal and invasive ductal carcinoma	T2No	II	II/III	III/III	Aberrant
BC-3	39	intraductal and invasive ductal carcinoma	T2N1	II	II/III	II/III	Aberrant
BC-6	48	intraductal and invasive ductal carcinoma	T1N1	I	II/III	II/III	Normal
BC-7	39	invasive ductal carcinoma	T3N1	III	n.a.	n.a.	Aberrant
BC-8	41	intraductal and invasive ductal carcinoma	T2No	II	II/III	II/III	Normal
BC-10	53	intraductal and invasive ductal carcinoma	T3N1	III	II/III	II/III	Normal
BC-13	66	intraductal and invasive ductal carcinoma	T2No	II	II/III	II/III	Aberrant
BC-15	39	invasive ductal carcinoma	T2N1	II	III/III	III/III	Normal
BC-16	85	invasive ductal carcinoma	T3Nx	III	III/III	III/III	Aberrant
BC-17	36	invasive ductal carcinoma	T2N1	II	III/III	II/III	Normal
BC-18	55	intraductal and infiltrating carcinoma	T1No	I	II/III	II/III	Normal
BC-19	62	medullary carcinoma	T1No	I	III/III	III/III	Aberrant
BC-22	59	intraductal and invasive ductal carcinoma	T1No	I	III/III	III/III	Aberrant
BC-23	49	intraductal and invasive ductal carcinoma	T2No	II	III/III	III/III	Normal
BC-24	76	intraductal and invasive ductal carcinoma	T2Nx	II	III/III	II/II	Normal
BC-25	35	intraductal and invasive ductal carcinoma	T2N1	II	III/III	III/III	Normal
BC-26	47	intraductal and infiltrating ductal carcinoma	T2N1	II	II/III	III/III	Aberrant
BC-27	31	invasive ductal carcinoma	T2N1	II	III/III	III/III	Normal
BC-28	73	invasive ductal carcinoma-lobular comp	T1Nx	I	II/III	II/III	Aberrant
BC-29	79	metastatic carcinoma	T2N2	III	III/III	III/III	Normal
BC-30	59	intraductal and invasive ductal carcinoma	T2No	II	II/III	II/III	Normal
BC-31	33	anaplastic carcinoma	T4N1	III	n.a.	n.a.	Aberrant
BC-31	57	intraductal and invasive anaplastic carcinoma	T4Nx	III	III/III	III/III	Normal

Table 2. Sequences of Abnormal FHIT Transcripts Assessed by Mismatch Analysis

CASE	RT-PCR TRANSCRIPTS	MISMATCH TRANSCRIPTS	SEQUENCE ALTERATION	EFFECT
BCD	ABNORMAL	ABNORMAL	C to T: +265; T to C: +294	POLYMORPHISMS
BC2	ABNORMAL (0)	ABNORMAL	N.D.	N.D.
BC3	ABNORMAL	ABNORMAL	Multiple*	Truncated Protein*
BC7	ABNORMAL	N.D.	7-11 bp deletion: +452	3' UNTRANSLATED REGION
BC13	ABNORMAL	NORMAL	N.D.	N.D.
BC15	NORMAL	ABNORMAL	N.D.	N.D.
BC16	ABNORMAL	ABNORMAL	A to G: -111	5' UNTRANSLATED REGION
			T to C: + 294	POLYMORPHISM
BC19	NORMAL	ABNORMAL	T to C: +294	POLYMORPHISM
BC22	NORMAL	ABNORMAL	T to C: +294	POLYMORPHISM
			7-11 bp deletion: +452	3' UNTRANSLATED REGION
BC26	NORMAL	ABNORMAL	C to T: +265; T to C: + 294	POLYMORPHISMS
			7-11 bp deletion: +452 **	3' UNTRANSLATED REGION
BC28	NORMAL	ABNORMAL	7-11 bp deletion: +452	3' UNTRANSLATED REGION
BC31	NORMAL	ABNORMAL	7-11 bp deletion: +452	3' UNTRANSLATED REGION

* Details are given in Fig. 4
** Details are given in Fig. 5

Table 3. Alteration of Fhit transcripts in primary breast tumors

Mutation	Primary Tumors/Total Cases (%)
Deletion[a]	4/27 (15%)
Insertion[a]	1/3 (4%)
Mismatch detection	10/27 (37%)
Total Cases[a and/or b]	12/27 (44%)

[a] by RT-PCR
[b] by Mismatch detection assay

Table 4 **Summary of data to each of the 10 cases**

Case	Age	Menopause	pTNM	Histology	Grading	ER	PR	Aberrations found by CGH
I	71	postmenop.	$T_2N_0M_0$	inv. papillary	1	4+	+	1p-, 1q++, 2pq-, 6p+, 6q-7p+, 8p+, 11p+, 11q-, 14q-15q-, 16p+, 16q-, 17p-17q+, 18p-, 19q+, 20q+21q-
III	43	premenop.	$T_2N_{1(2/14)}M_0$	inv. ductal DCIS	1	2+	4+	1q++, 14q-, 16p+, 16q-20p+
IV	77	postmenop.	$T_3N_{1biii(6/15)}M_x$	inv. ductal	3	-	-	1q++, 4q+, 5q+, 6q+, 10q-11p-, 12q+, 13q+, 17q-20q-
V	45	premenop.	$T_2N_{0(0/16)}M_0$	inv. ductal DCIS	3	3+	+	1q+, 2q-, 3q-, 4p-, 5q-, 8p-8q++, 9q-, 10q-, 13q-, 14q+15q-, 17p-, 19pq+, 20pq+21pq+, 22p+, 22q-
VII	85	postmenop.	$T_2N_{0(0/20)}M_0$	inv. ductal	1	3+	3+	1q+, 4q+, 15q+, 16p+, 16q-17p-, 22q-

Case	Age	Menopause	pTNM	Histology	Grading	ER	PR	Aberrations found
VIII	73	postmenop.	$T_2N_{1b(1/22)}M_0$	inv. ductal DCIS	2	3+	3+	1p-, 1q+, 6p+, 8q-, 11q- 14q-, 16p+, 16q-, 17p- 17q+, 18q-, 21q-, 22q-
IX	76	postmenop.	$T_{1c}N_{0(0/24)}M_0$	inv. ductal	1	4+	2+	1q+, 9p+, 12q+, 13q-, 14q- 16p+, 16q-, 18p-, 20p- 22q+
X	47	postmenop.	$T_2N_{1(5/20)}M_0$	mucinous DCIS	3	+	+	1q+, 5q+, 6q+, 10p+, 12p+ 13q-, 16p+, 16q-, 18p+
XI	41	premenop.	$T_2N_{1biv(6/35)}M_0$	inv. ductal DCIS	3	-	-	1q+, 3q+, 5q+, 10q-, 11q+ 13q-, 15q+, 16p-, 16q+ 17p-, 19q+, 20pq+, 22q+
XII*	82	postmenop.	$T_4N_{1biii(17/25)}M_0$	inv. ductal DCIS	2	2+	2+	2q-, 3q-, 5q+, 6q-, 7q-, 8q- 10q-, 14q-, 19q-

From the unmentioned cases II and VI there was not material of both sources available and therefore they were excluded from further investigation. In case XII* reliable results could be obtained only from the paraffin embedded material.

Premenop. premenopausal diagnosis
Postmenop. postmenopausal diagnosis
inv. invasive cancer
DCIS ductal carinoma in situ of the breast
ER estrogen receptor status: 25% postive staining +, 25-50% 2+, 50-75% 3+, >75% 4+
PR progesteron receptor status: 25% postive staining +, 25-50% 2+, 50-75% 3+, >75% 4+

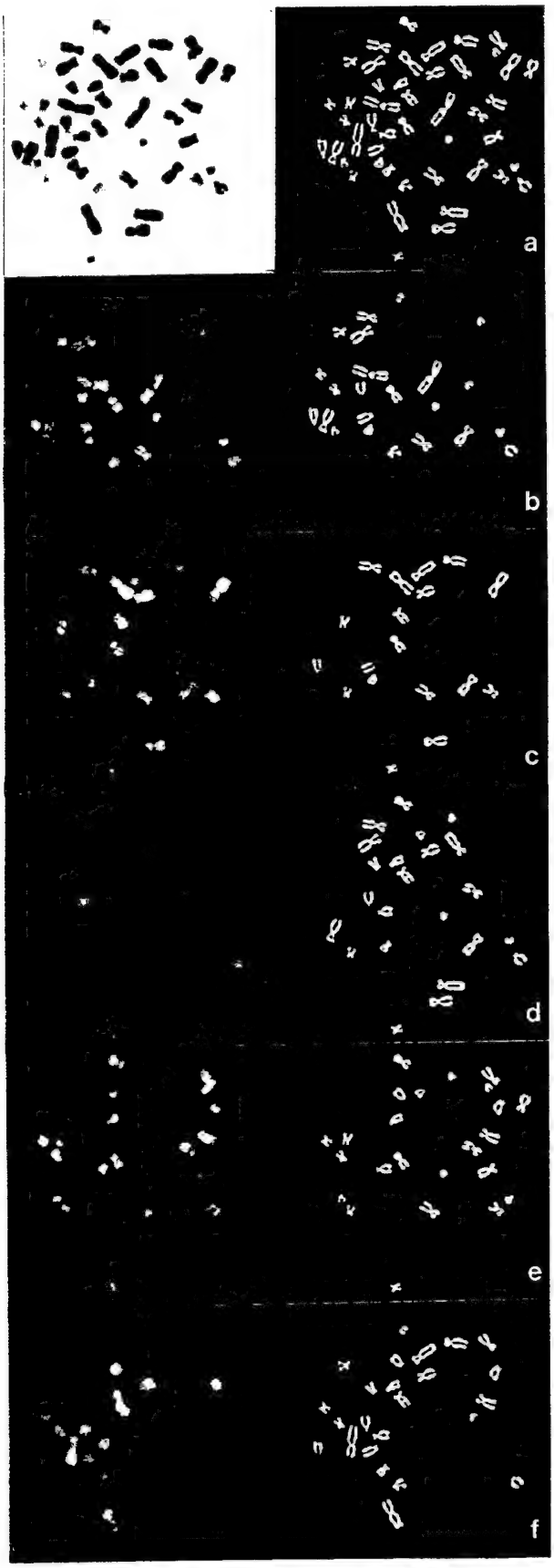

Figure 1

Figure 2

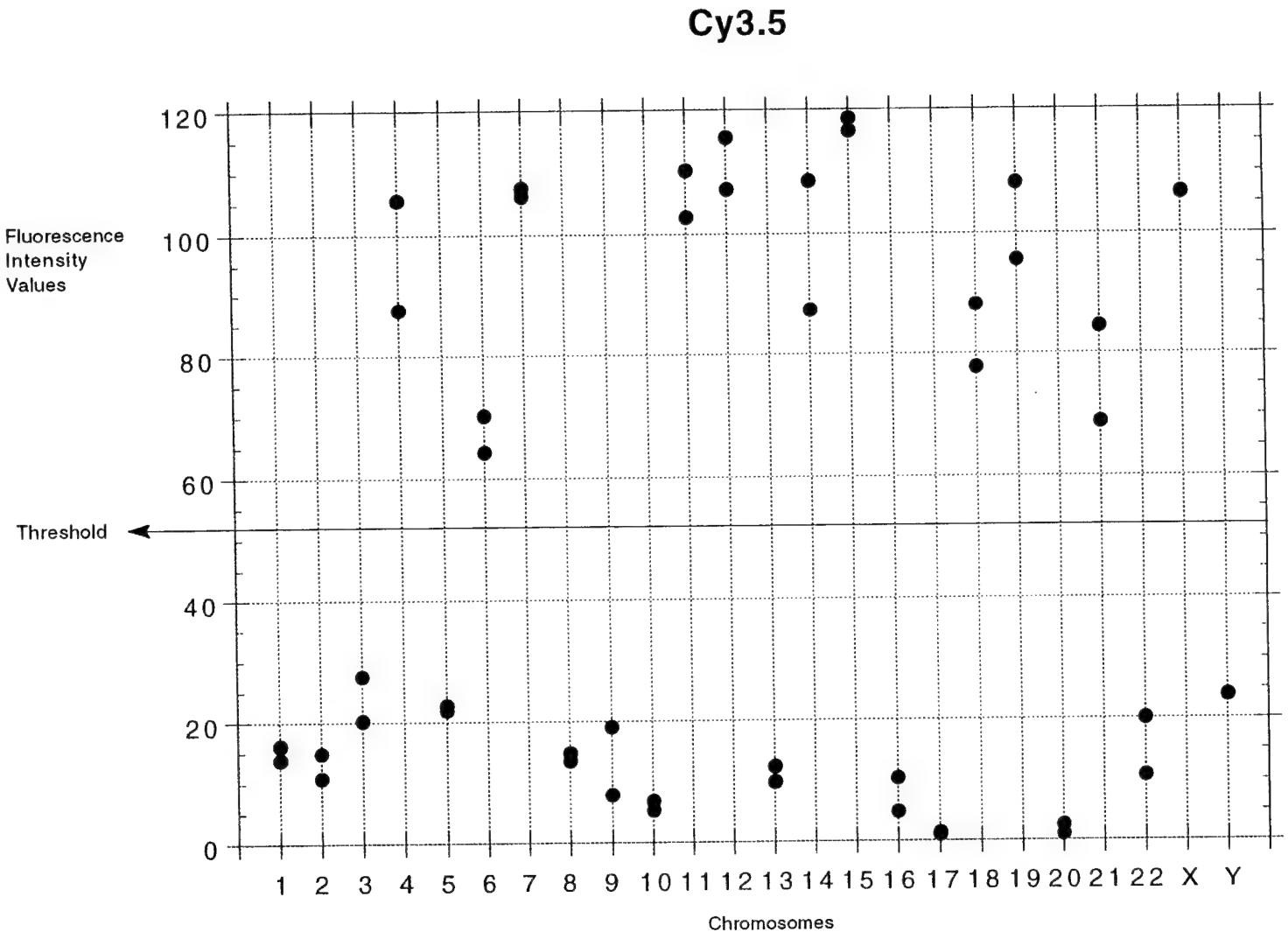
Cy3.5
Fluorescence Intensity Values
120
100
80
60
Threshold
40
20
0
1 2 3 4 5 6 7 8 9 10 11 12 13 14 15 16 17 18 19 20 21 22 X Y
Chromosomes

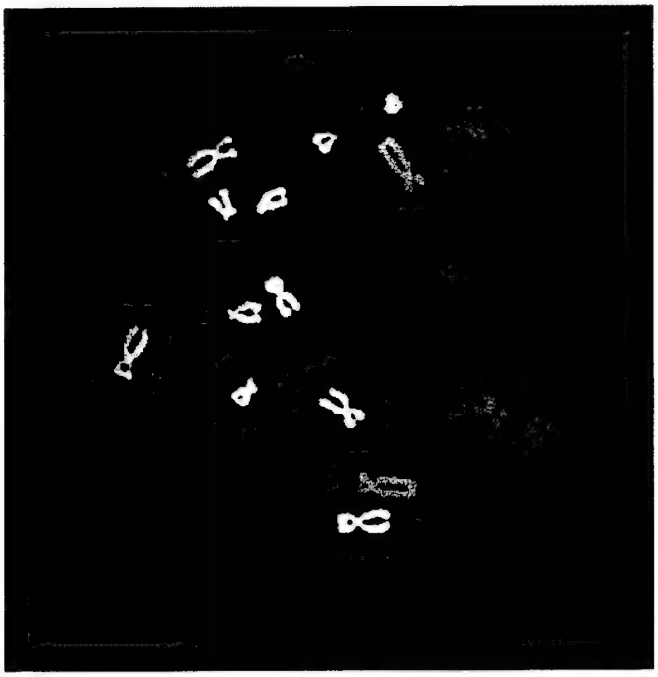

Figure 3a

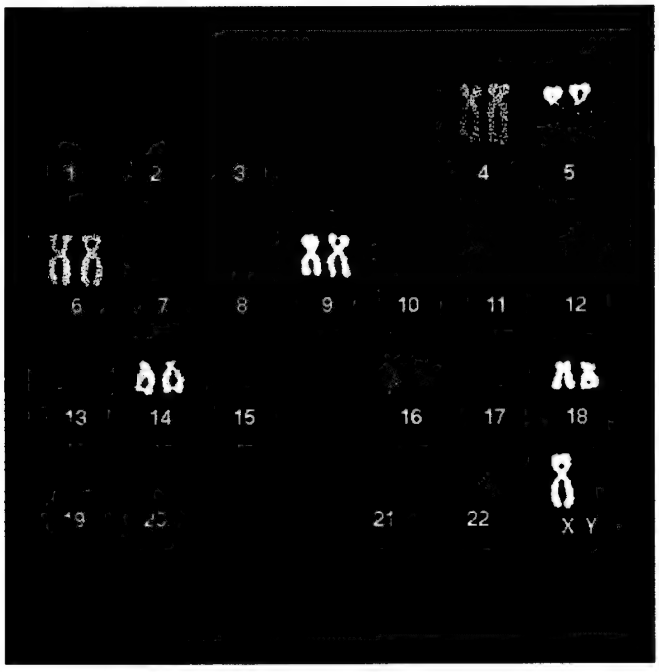

Figure 3b

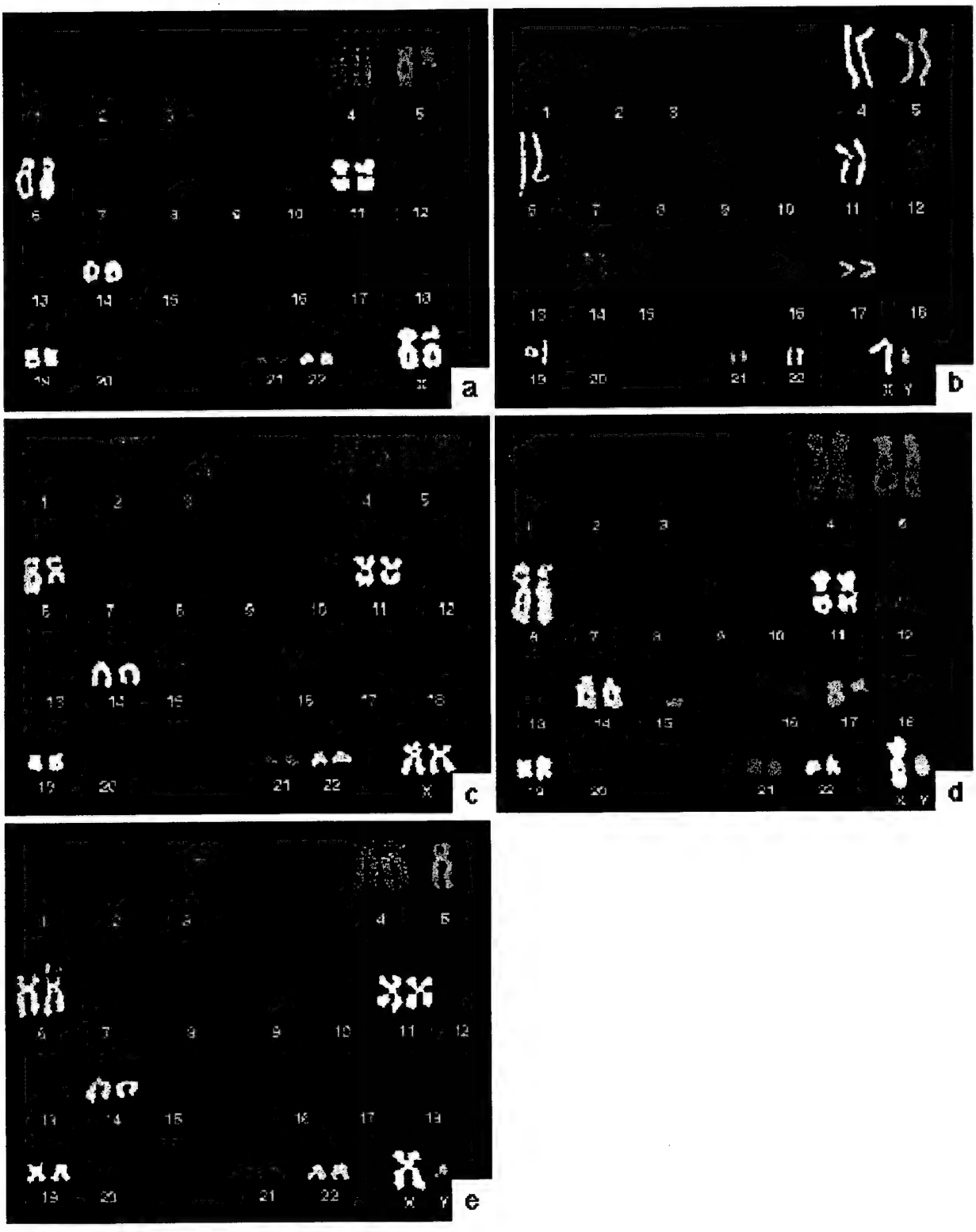

Figure 4

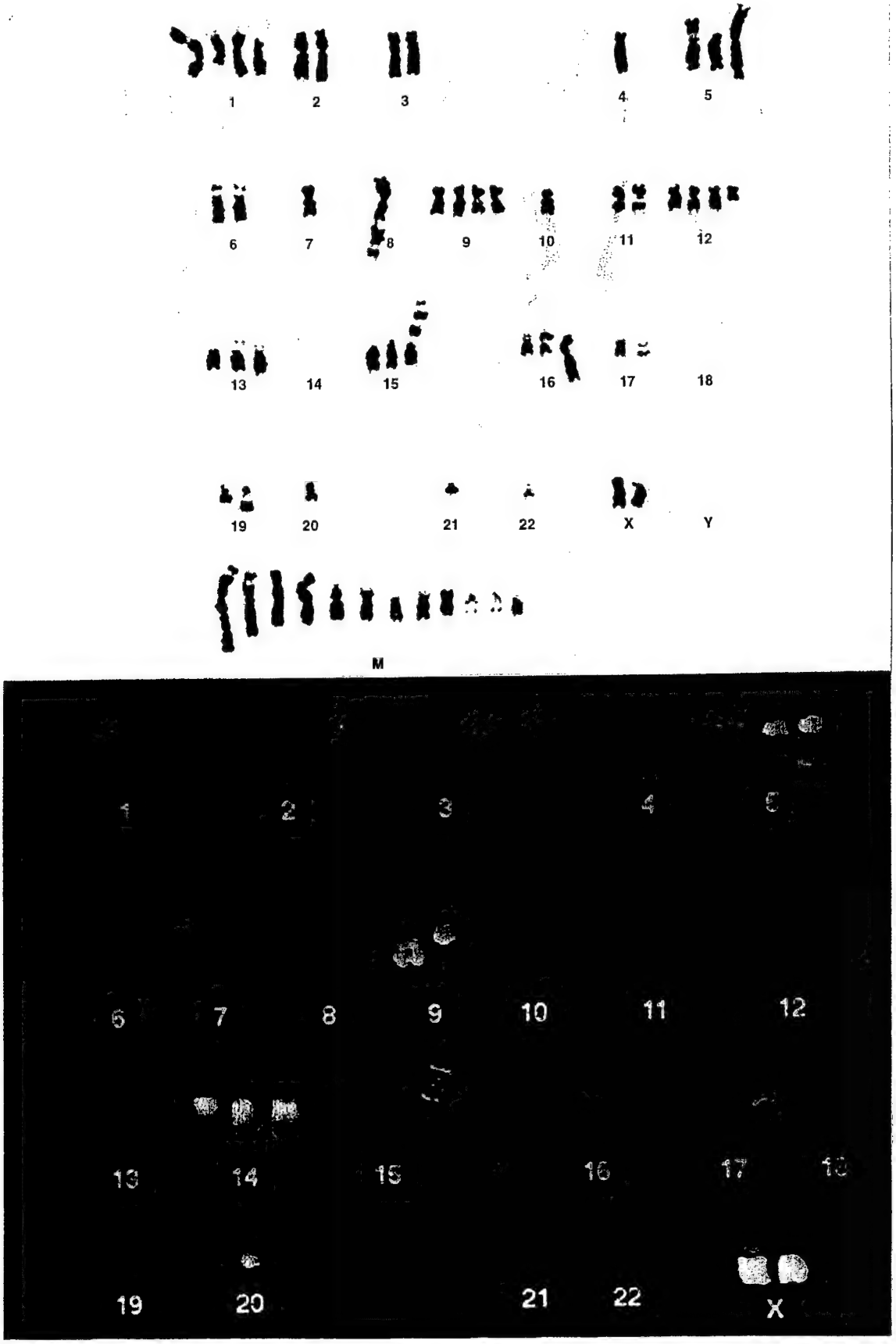

Figure 5a and 5b

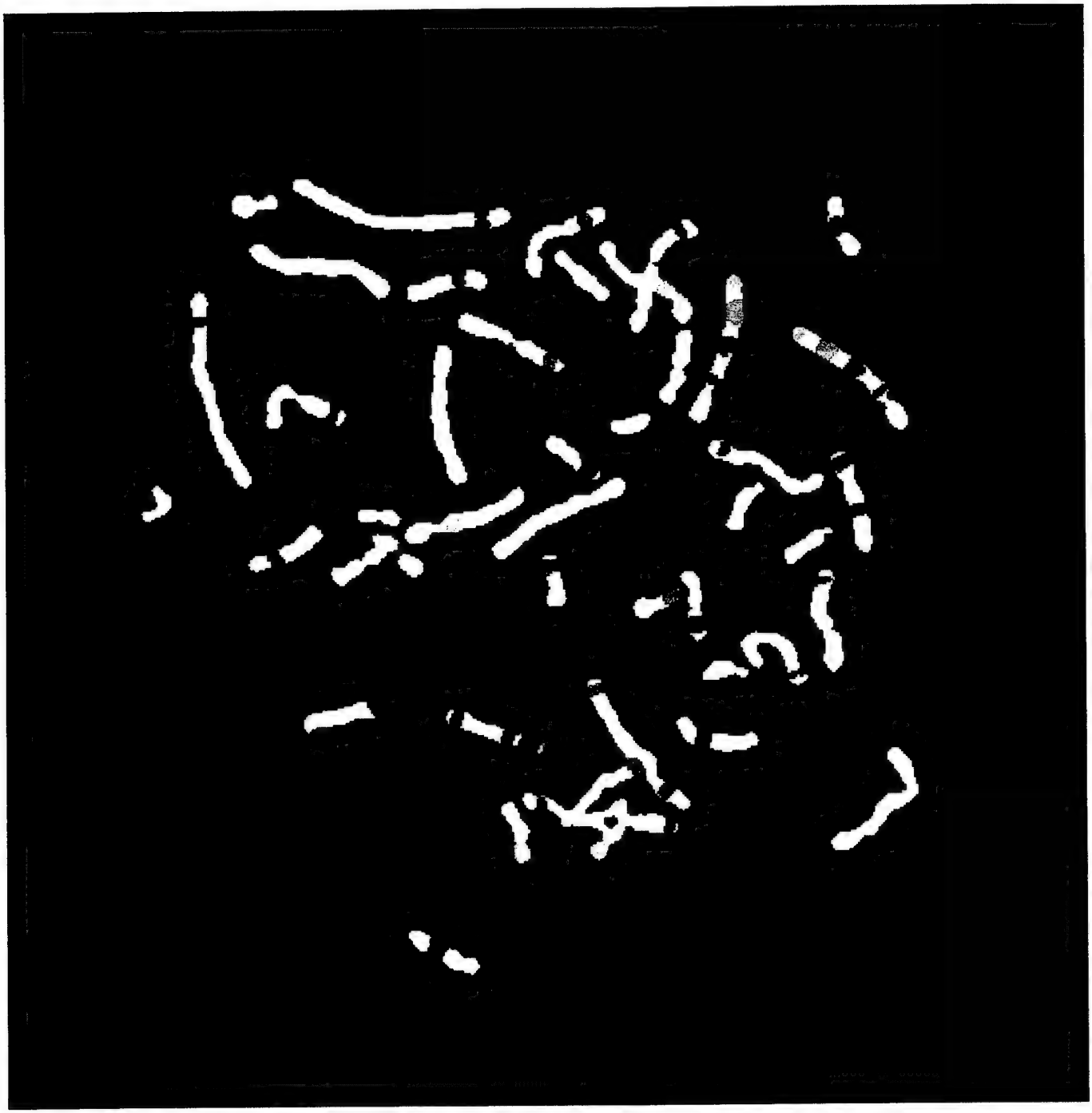

Figure 6

Summary of the CGH results of 10 breast cancers

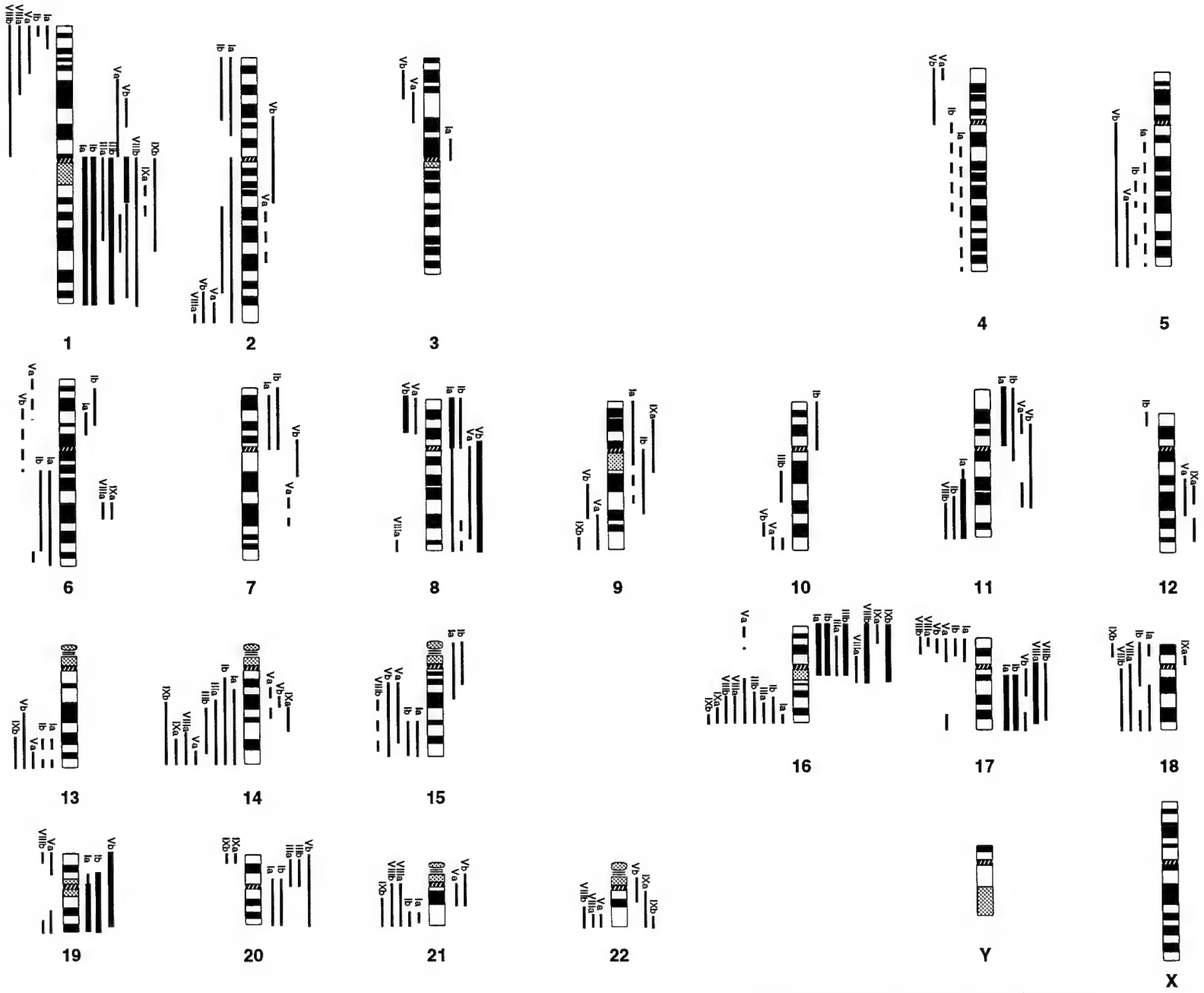

Figure 7

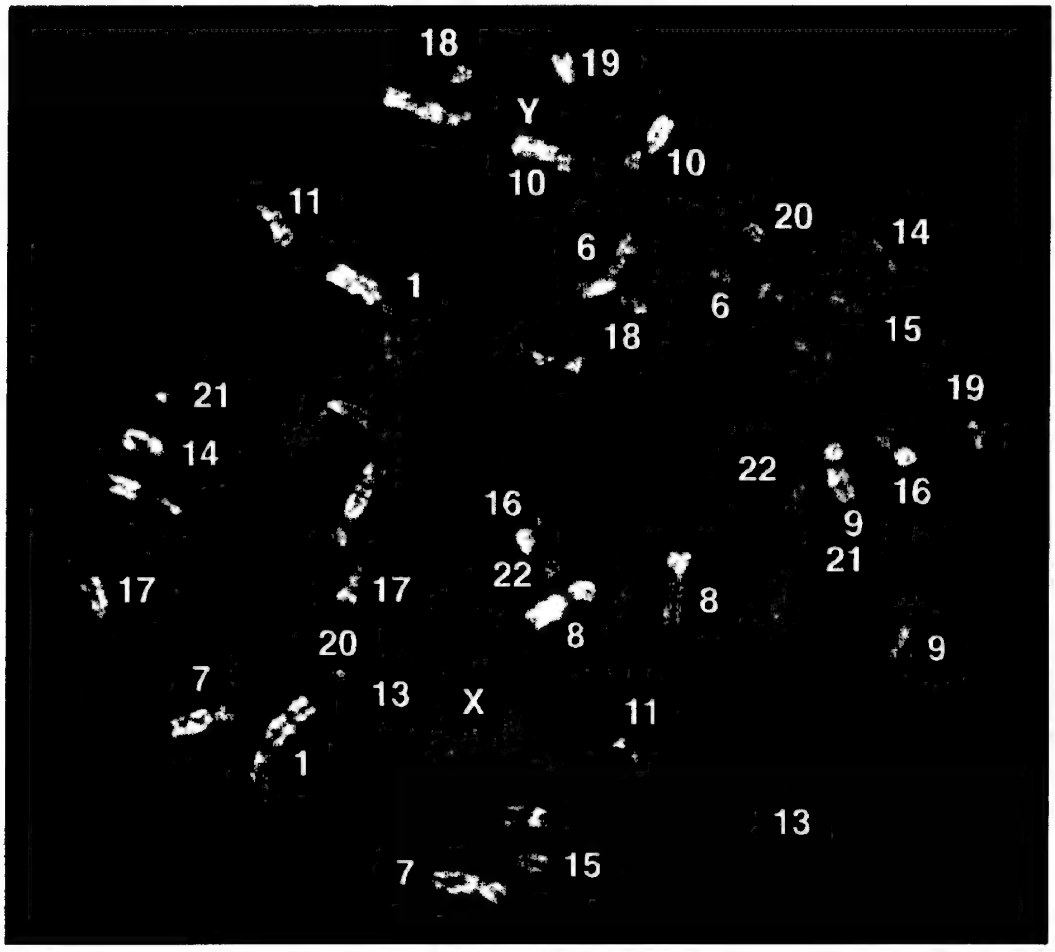
18
19
Y
10
10
11
20
14
6
1
6
18
15
21
19
14
22
16
16
9
21
17
17
22
8
8
20
9
7
13
X
11
1
13
7
15

Figure 8

Figure 9

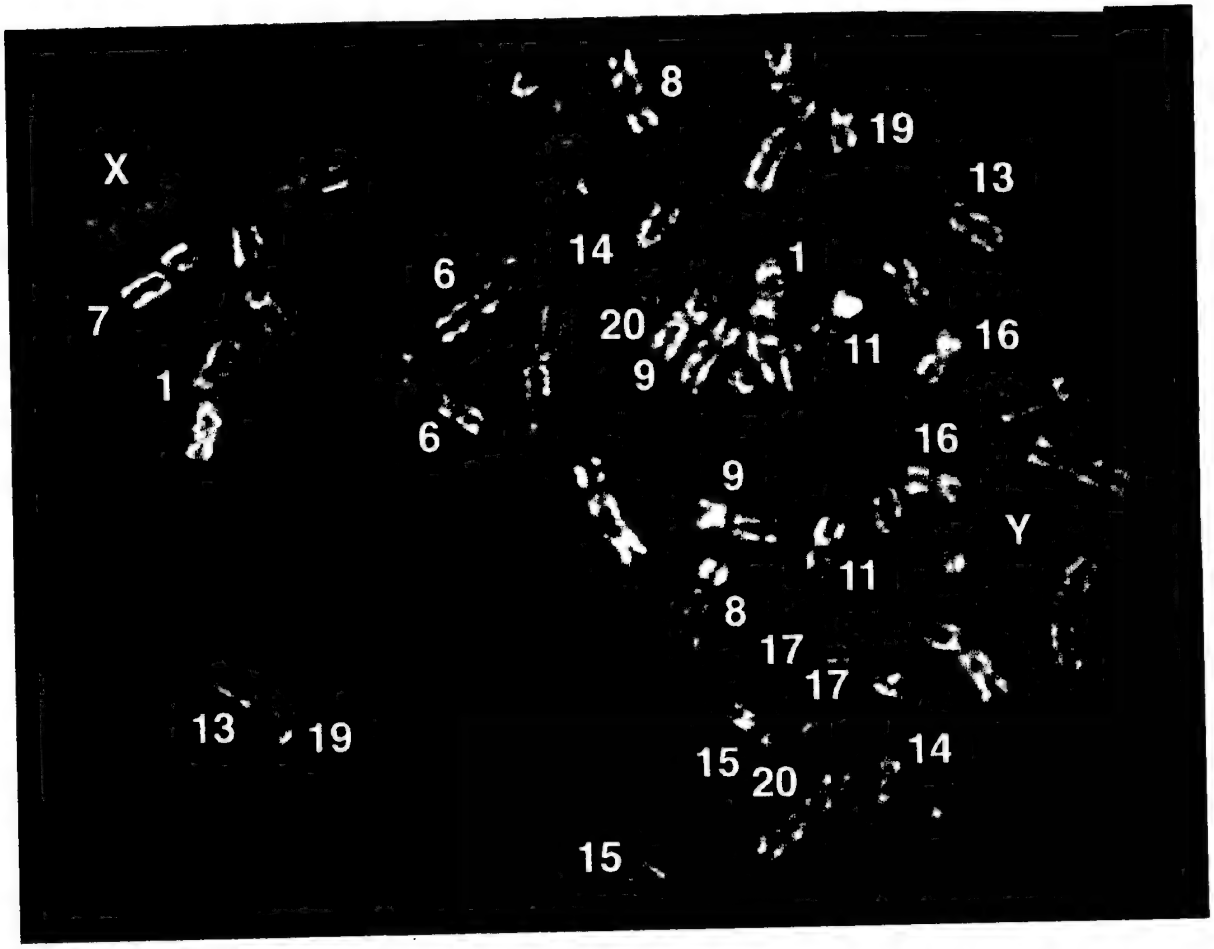

Figure 10

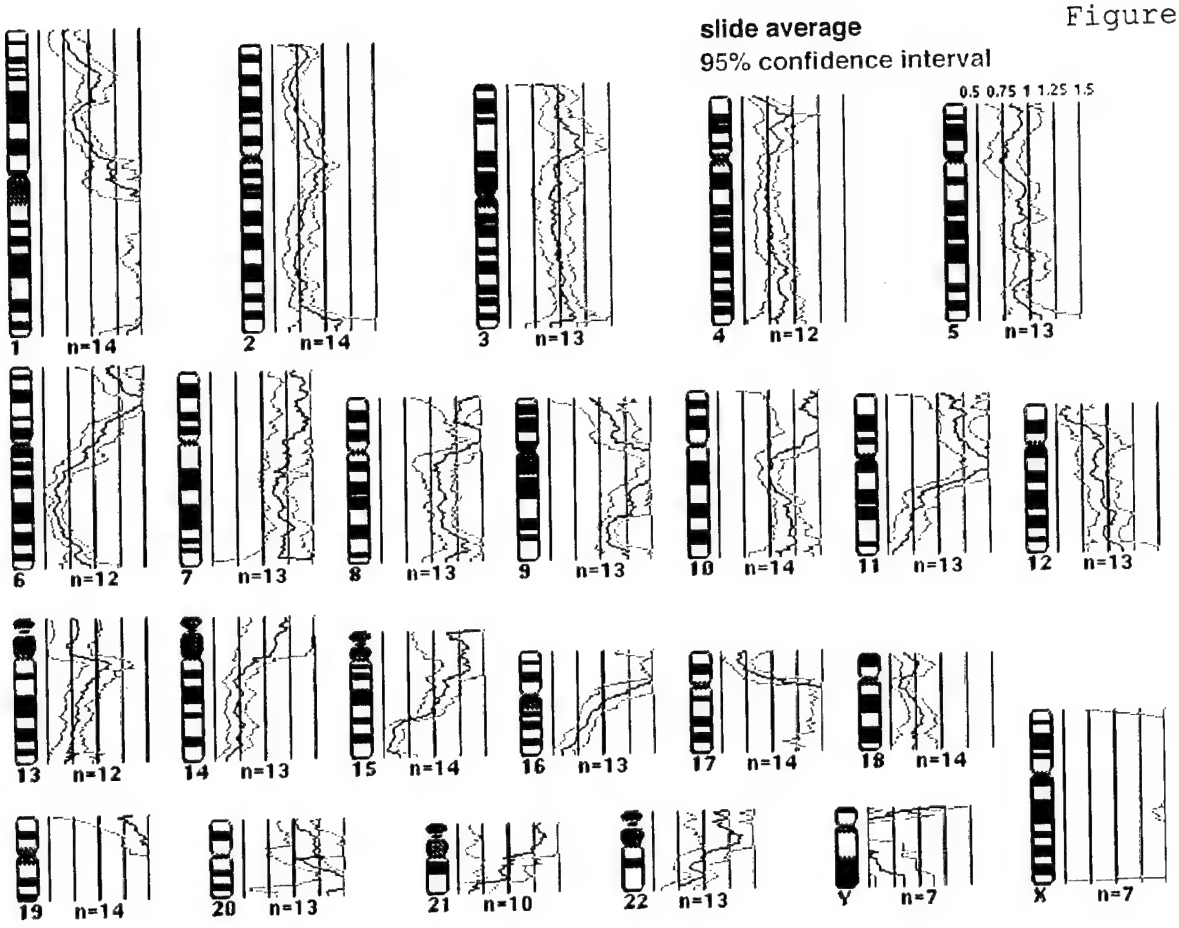
slide average
95% confidence interval
0.5 0.75 1 1.25 1.5
1 n=14
2 n=14
3 n=13
4 n=12
5 n=13
6 n=12
7 n=13
8 n=13
9 n=13
10 n=14
11 n=13
12 n=13
13 n=12
14 n=13
15 n=14
16 n=13
17 n=14
18 n=14
19 n=14
20 n=13
21 n=10
22 n=13
Y n=7
X n=7

Figure 11

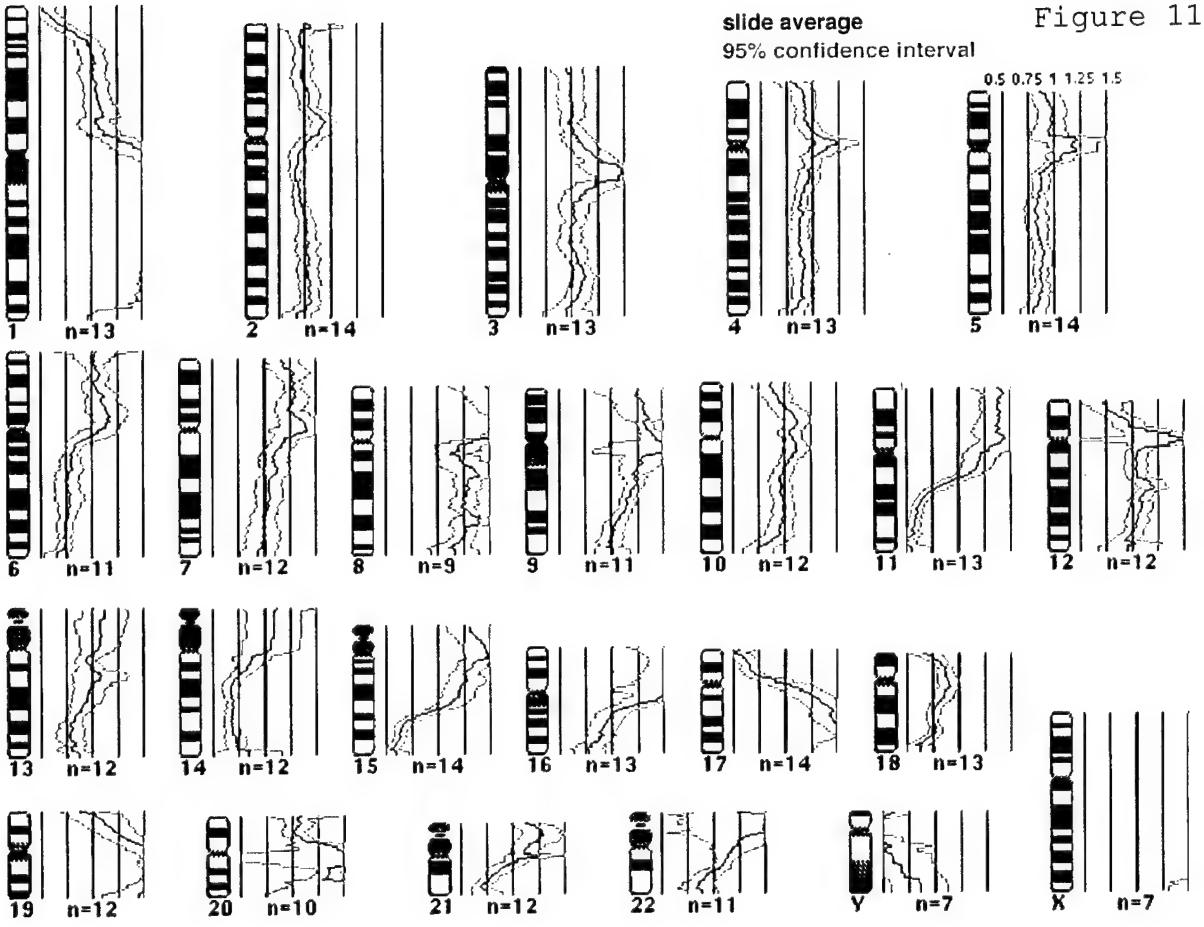
slide average
95% confidence interval
0.5 0.75 1 1.25 1.5
1 n=13
2 n=14
3 n=13
4 n=13
5 n=14
6 n=11
7 n=12
8 n=9
9 n=11
10 n=12
11 n=13
12 n=12
13 n=12
14 n=12
15 n=14
16 n=13
17 n=14
18 n=13
19 n=12
20 n=10
21 n=12
22 n=11
Y n=7
X n=7

APPENDIX B

Profile Breast cancer BO-1

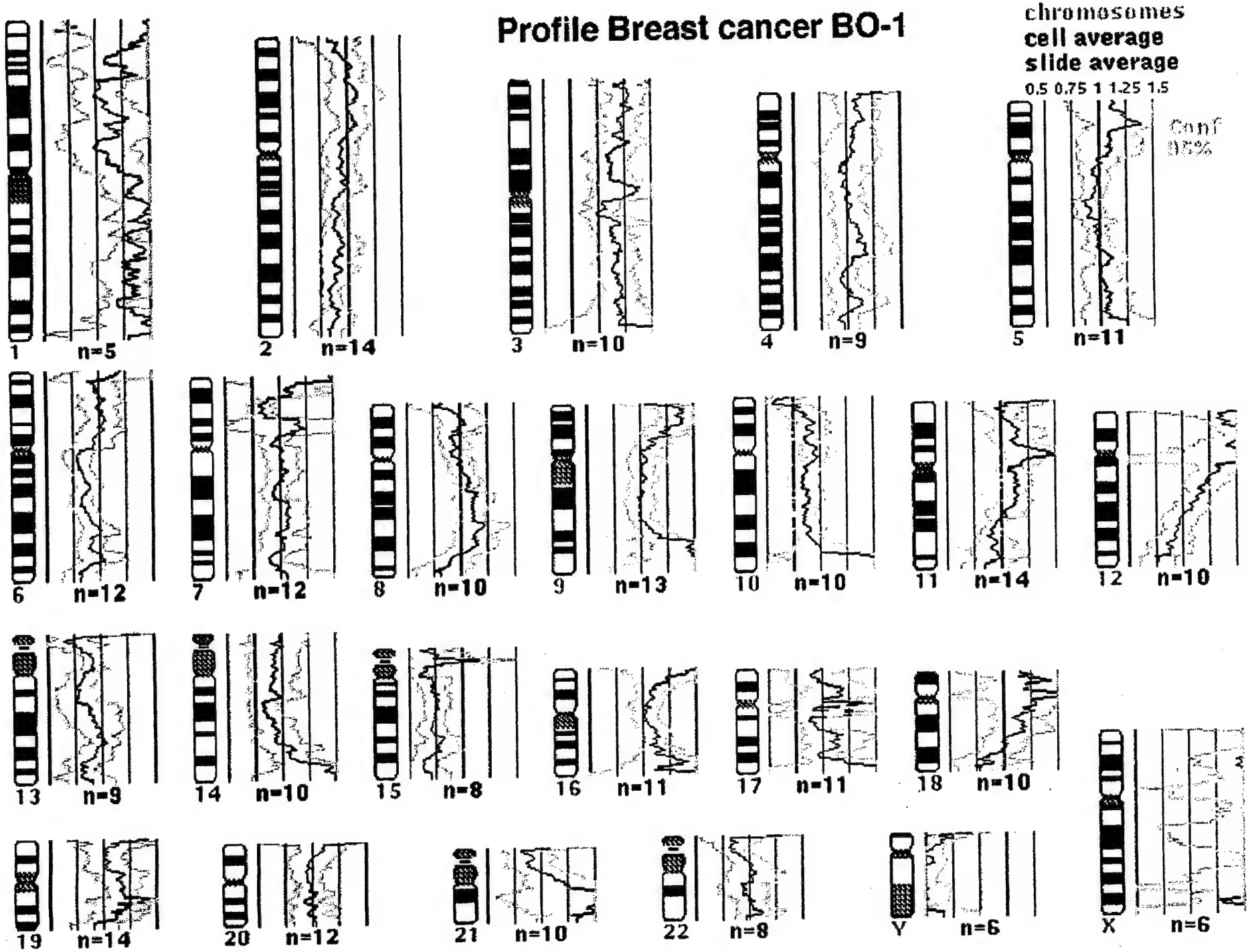

Profile Ovarian cancer BO-1

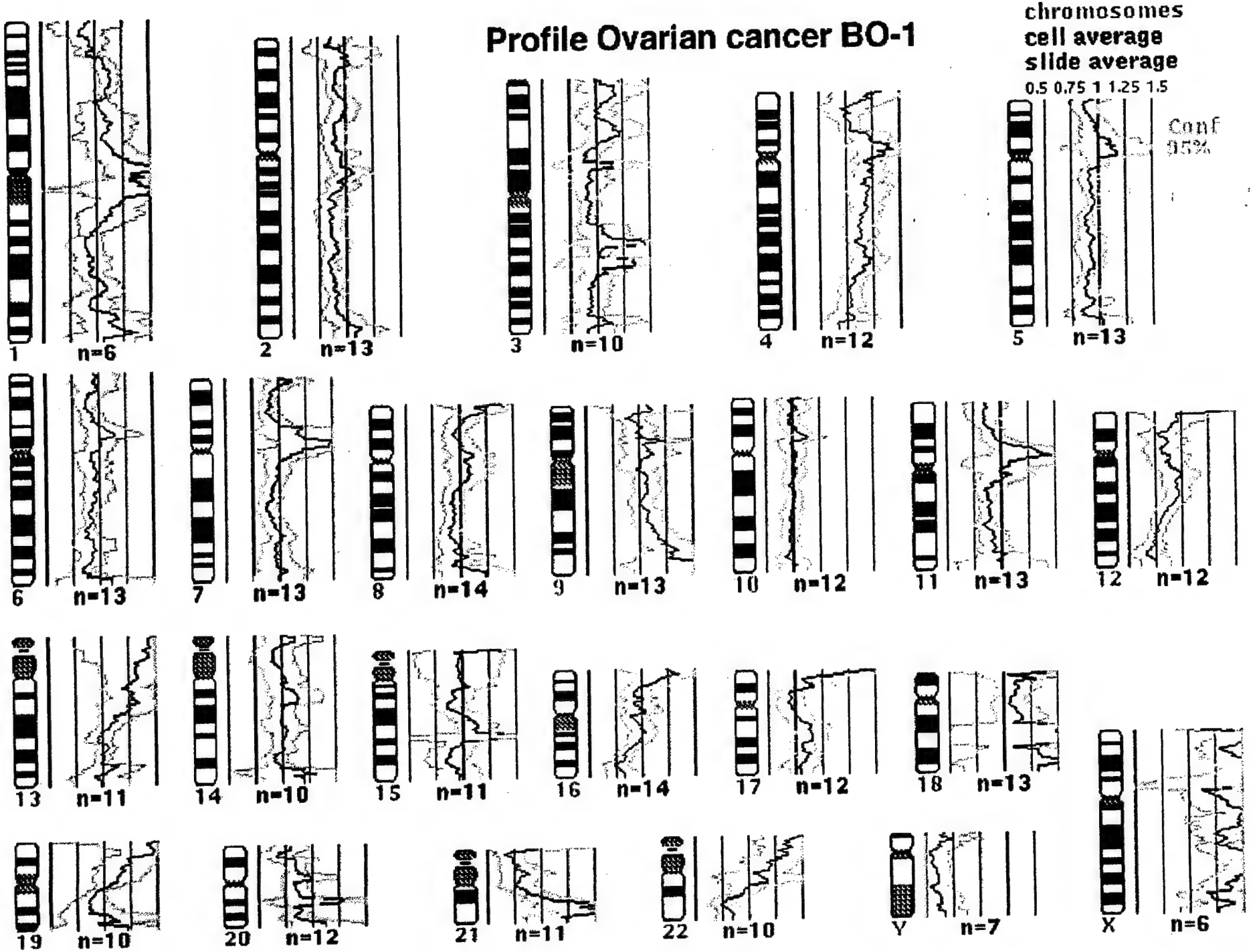

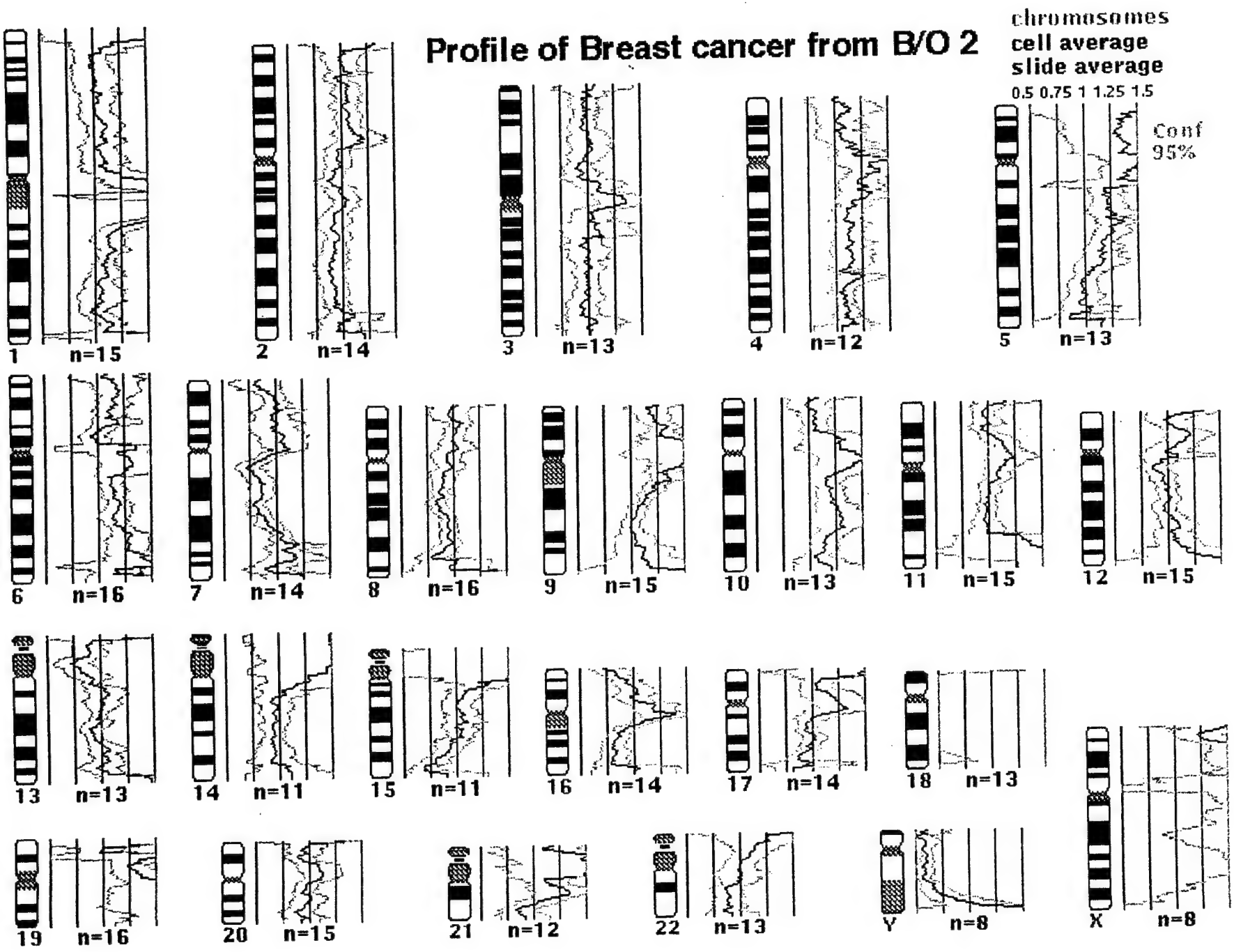
Profile of Breast cancer from B/O 2
chromosomes
cell average
slide average
0.5 0.75 1 1.25 1.5
Conf 95%
1 n=15
2 n=14
3 n=13
4 n=12
5 n=13
6 n=16
7 n=14
8 n=16
9 n=15
10 n=13
11 n=15
12 n=15
13 n=13
14 n=11
15 n=11
16 n=14
17 n=14
18 n=13
19 n=16
20 n=15
21 n=12
22 n=13
Y n=8
X n=8

Profile Ovarian cancer BO-2

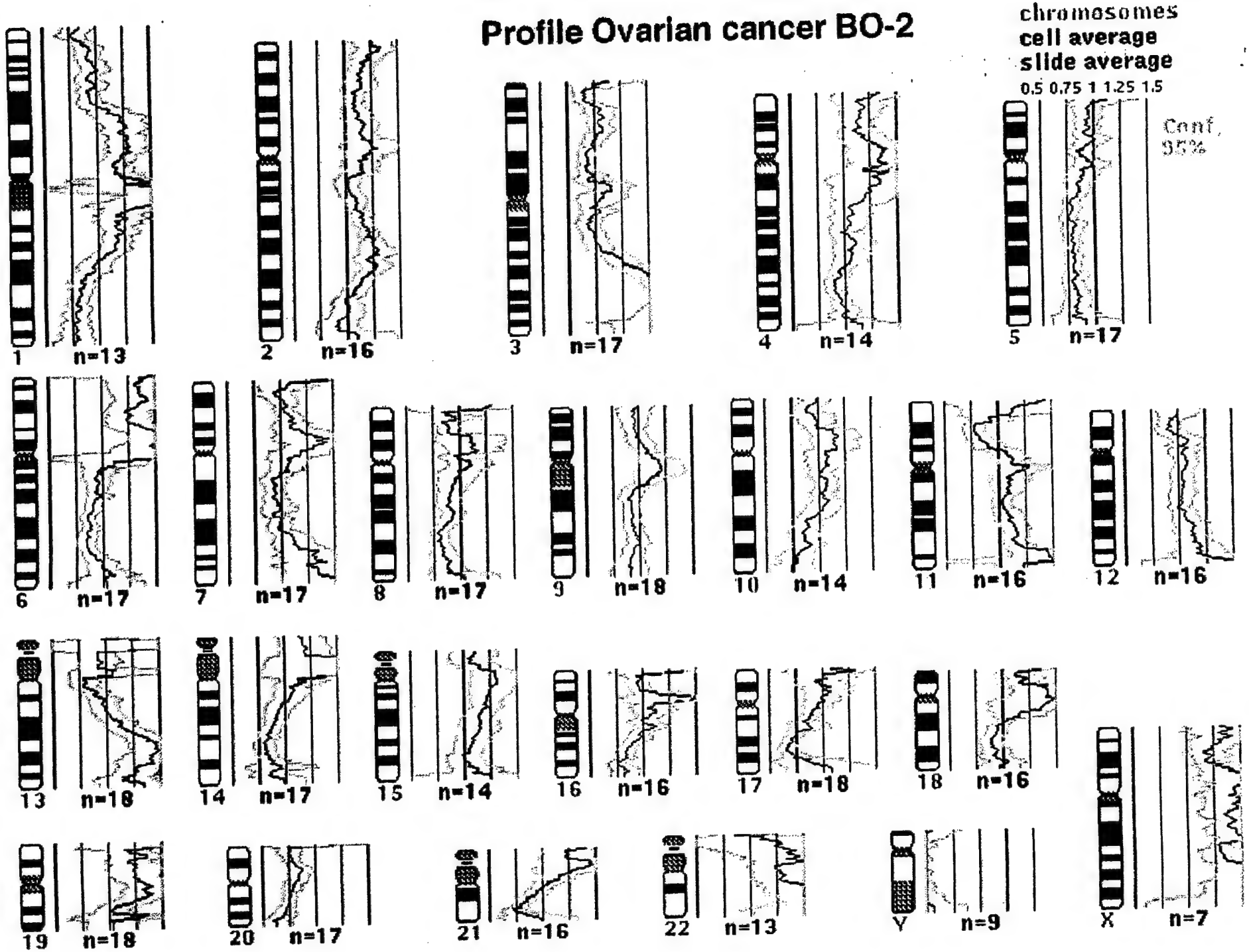

Profile Breast cancer BO-3

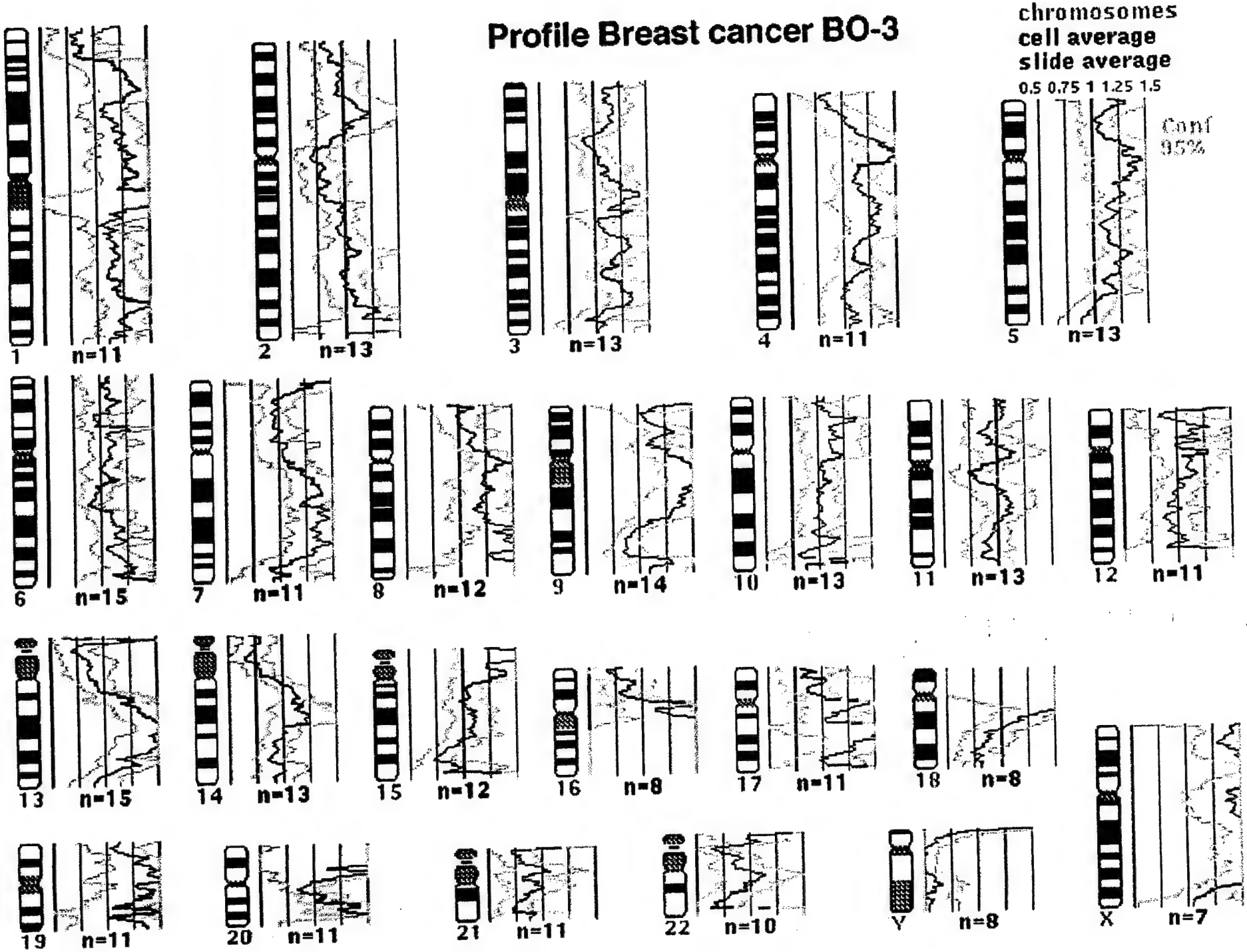

Profile Ovarian cancer BO-3

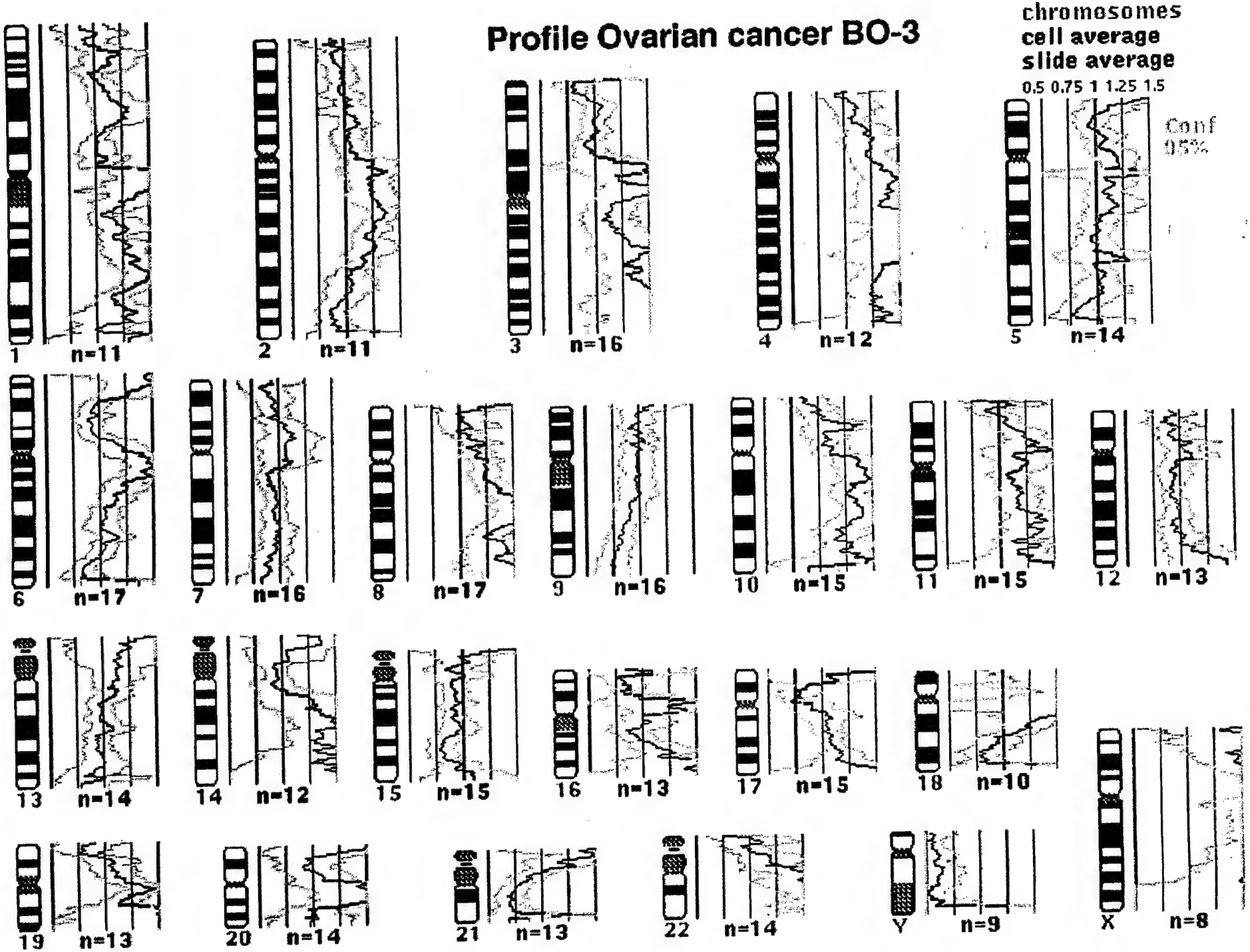

Profile Breast cancer BO-6

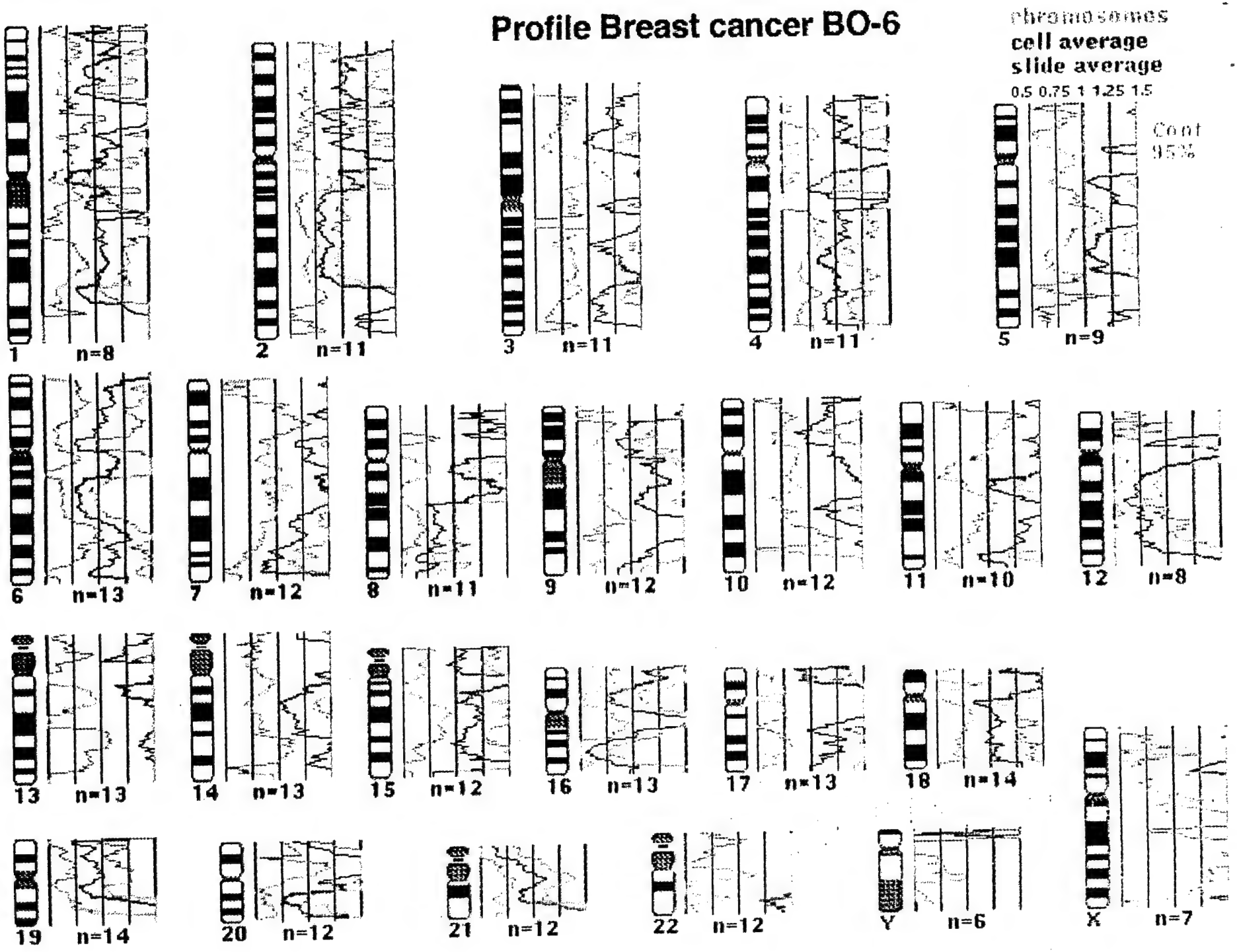

Profile Ovarian cancer BO-6

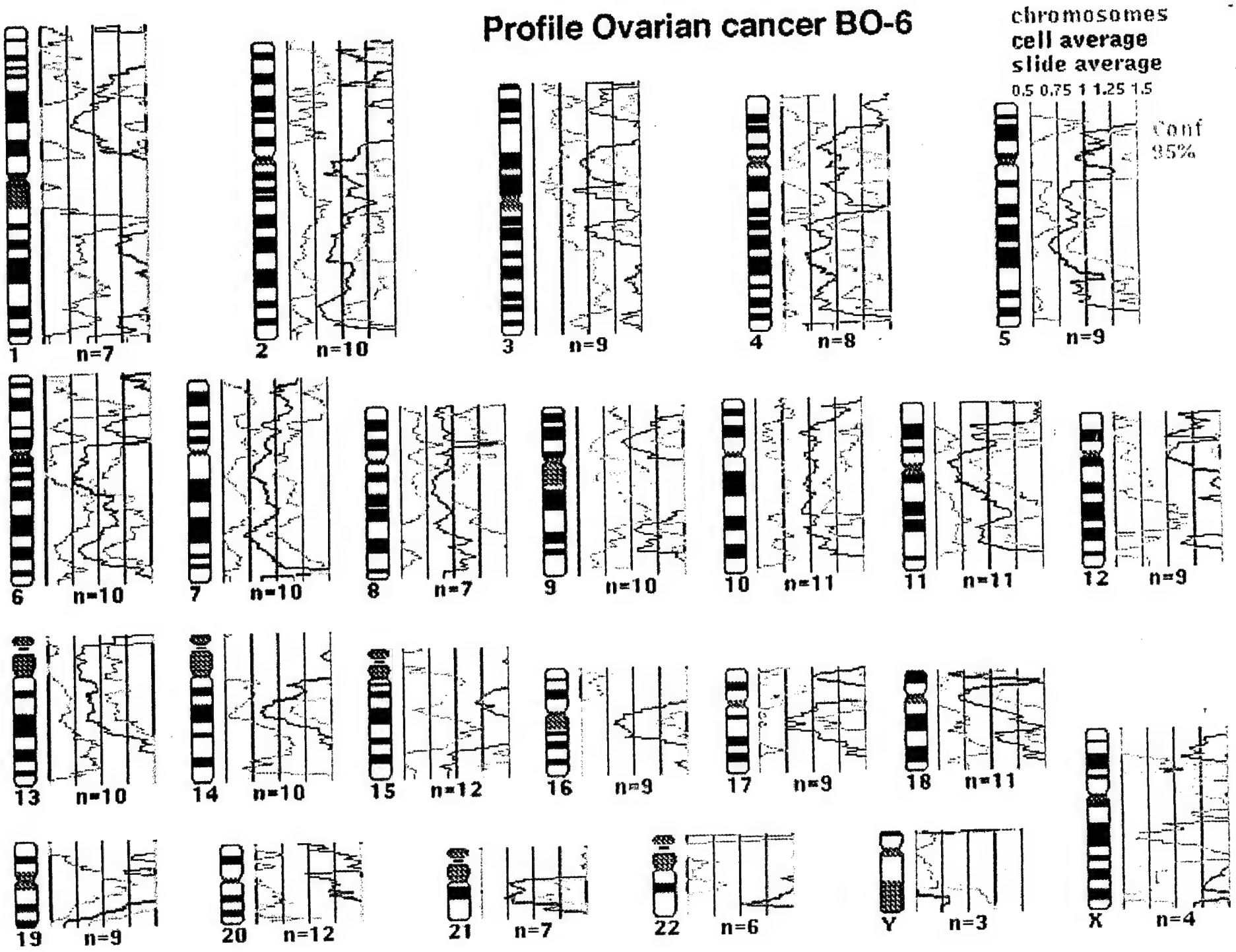

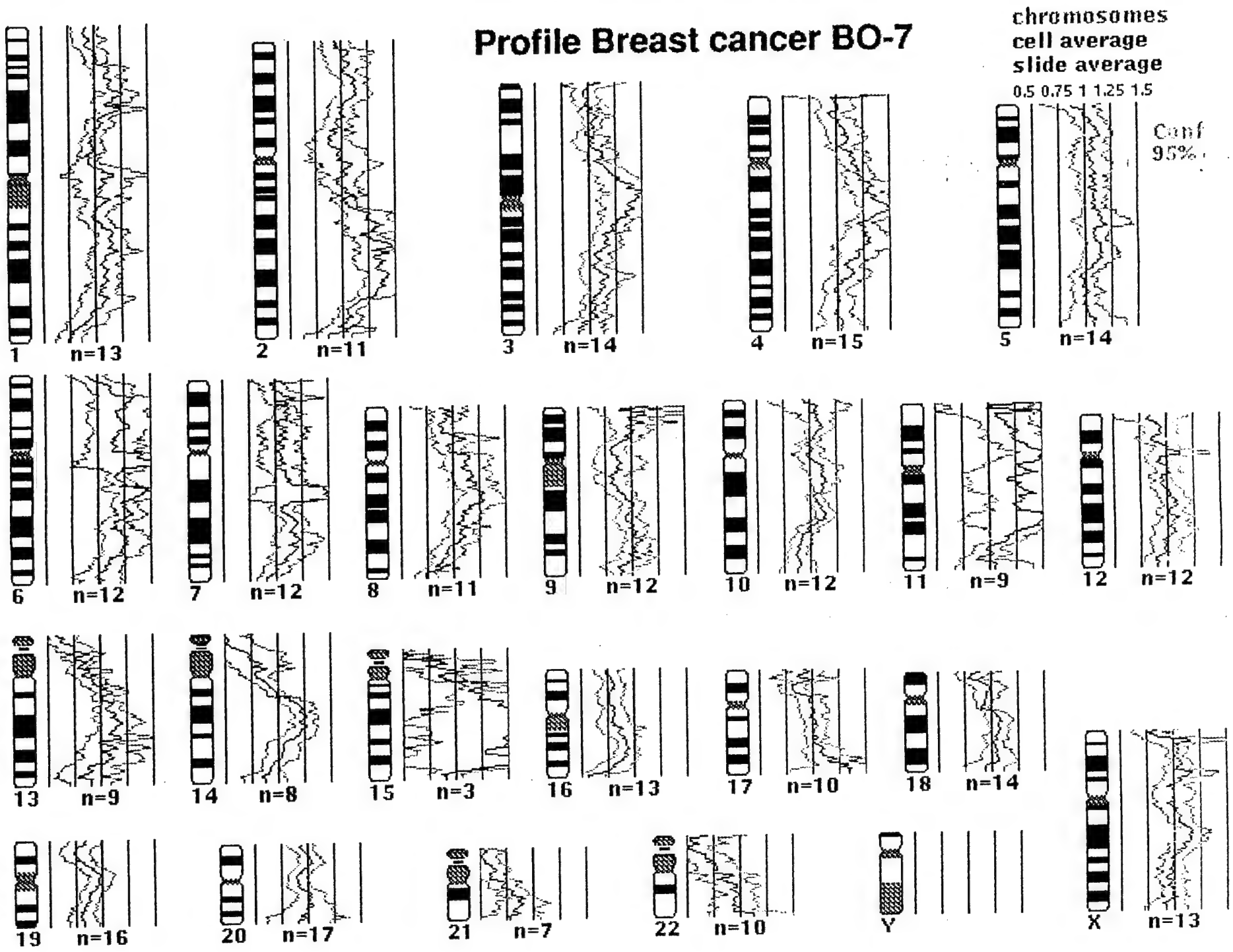
Profile Breast cancer BO-7
chromosomes
cell average
slide average
0.5 0.75 1 1.25 1.5
Conf
95%
1 n=13
2 n=11
3 n=14
4 n=15
5 n=14
6 n=12
7 n=12
8 n=11
9 n=12
10 n=12
11 n=9
12 n=12
13 n=9
14 n=8
15 n=3
16 n=13
17 n=10
18 n=14
19 n=16
20 n=17
21 n=7
22 n=10
Y
X n=13

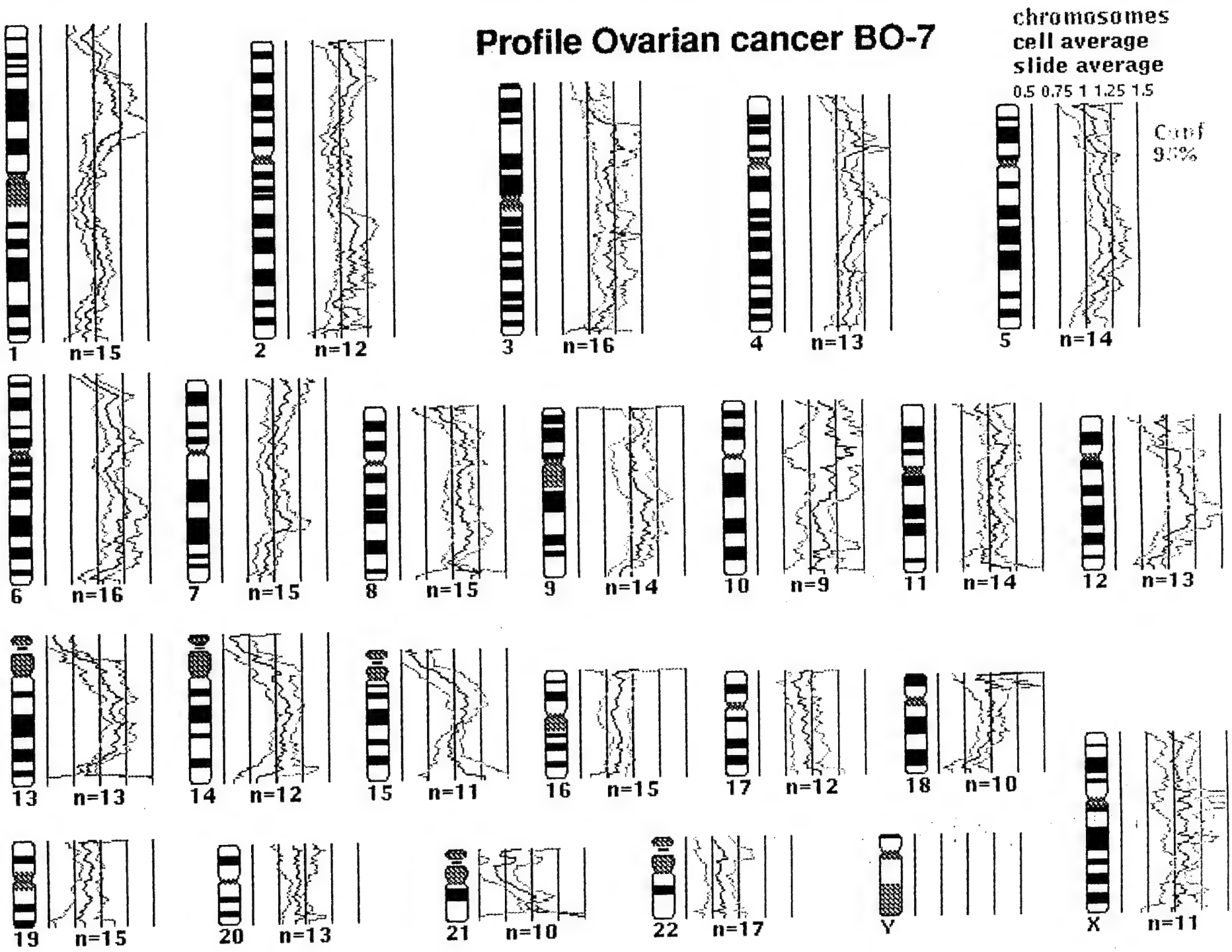
Profile Ovarian cancer BO-7
chromosomes
cell average
slide average
0.5 0.75 1 1.25 1.5
Conf
95%
1
n=15
2
n=12
3
n=16
4
n=13
5
n=14
6
n=16
7
n=15
8
n=15
9
n=14
10
n=9
11
n=14
12
n=13
13
n=13
14
n=12
15
n=11
16
n=15
17
n=12
18
n=10
19
n=15
20
n=13
21
n=10
22
n=17
Y
X
n=11

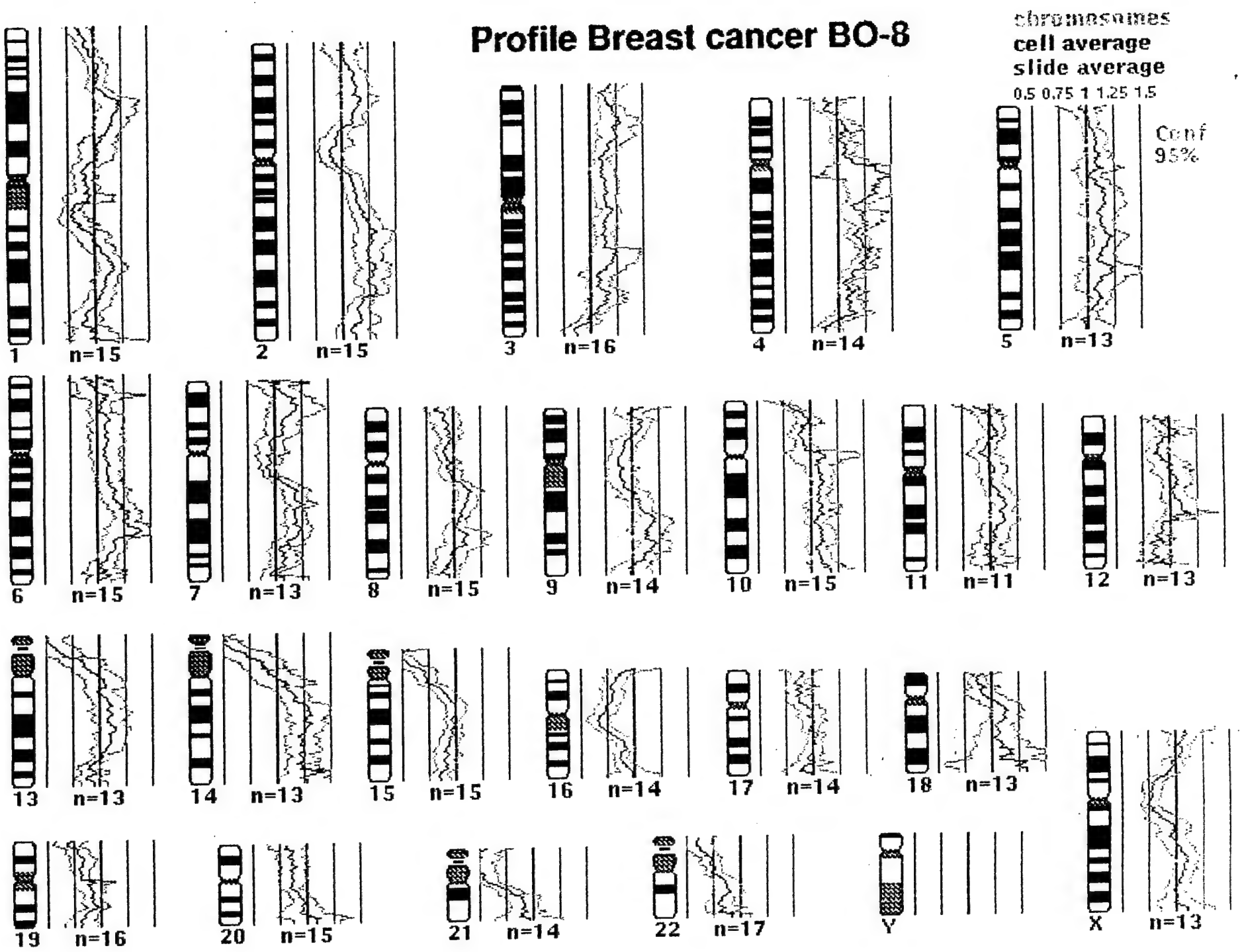
Profile Breast cancer BO-8
chromosomes
cell average
slide average
0.5 0.75 1 1.25 1.5
Conf 95%
1 n=15
2 n=15
3 n=16
4 n=14
5 n=13
6 n=15
7 n=13
8 n=15
9 n=14
10 n=15
11 n=11
12 n=13
13 n=13
14 n=13
15 n=15
16 n=14
17 n=14
18 n=13
19 n=16
20 n=15
21 n=14
22 n=17
Y
X n=13

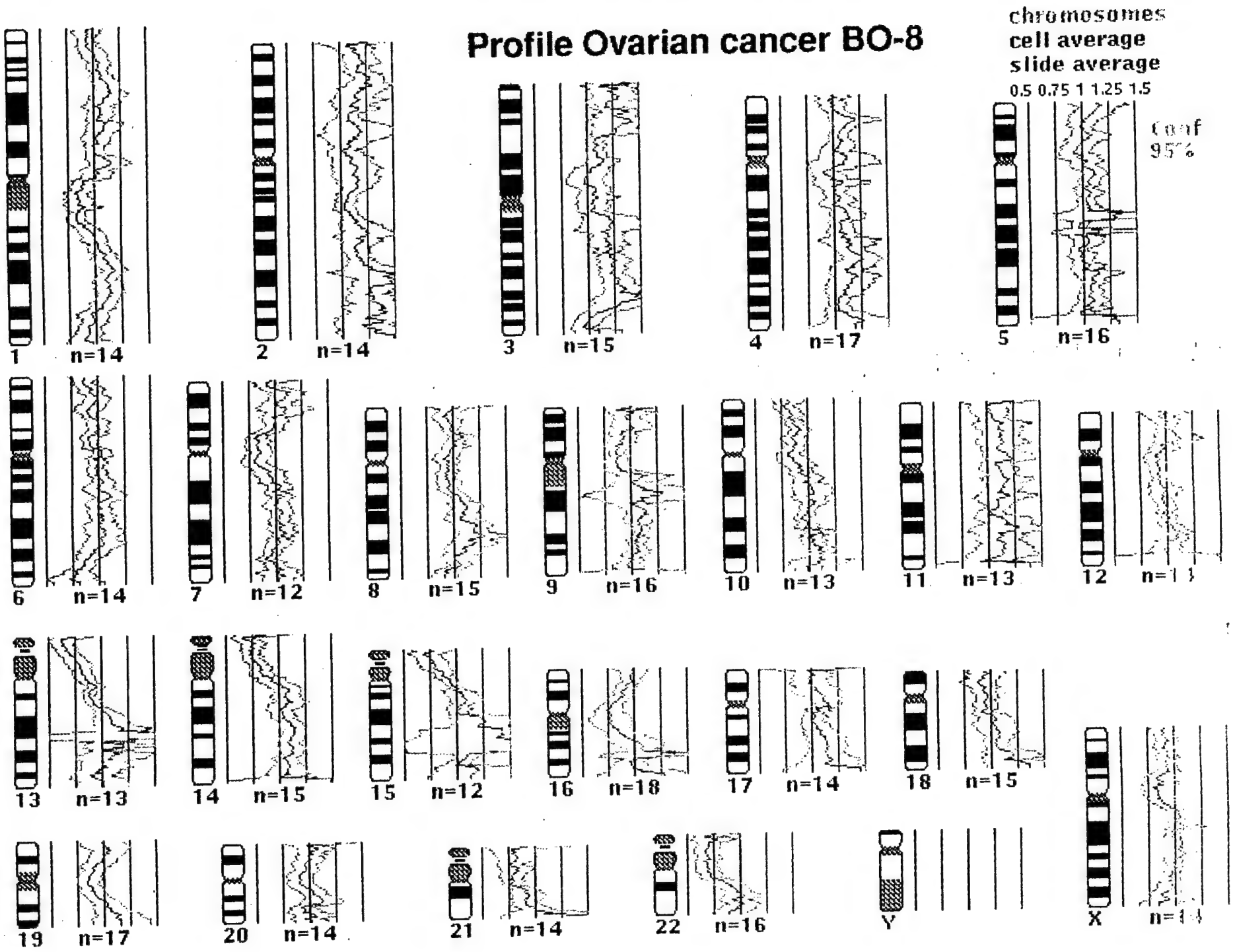
Profile Ovarian cancer BO-8
chromosomes
cell average
slide average
0.5 0.75 1 1.25 1.5
Conf
95%
1
n=14
2
n=14
3
n=15
4
n=17
5
n=16
6
n=14
7
n=12
8
n=15
9
n=16
10
n=13
11
n=13
12
n=11
13
n=13
14
n=15
15
n=12
16
n=18
17
n=14
18
n=15
19
n=17
20
n=14
21
n=14
22
n=16
Y
X
n=14

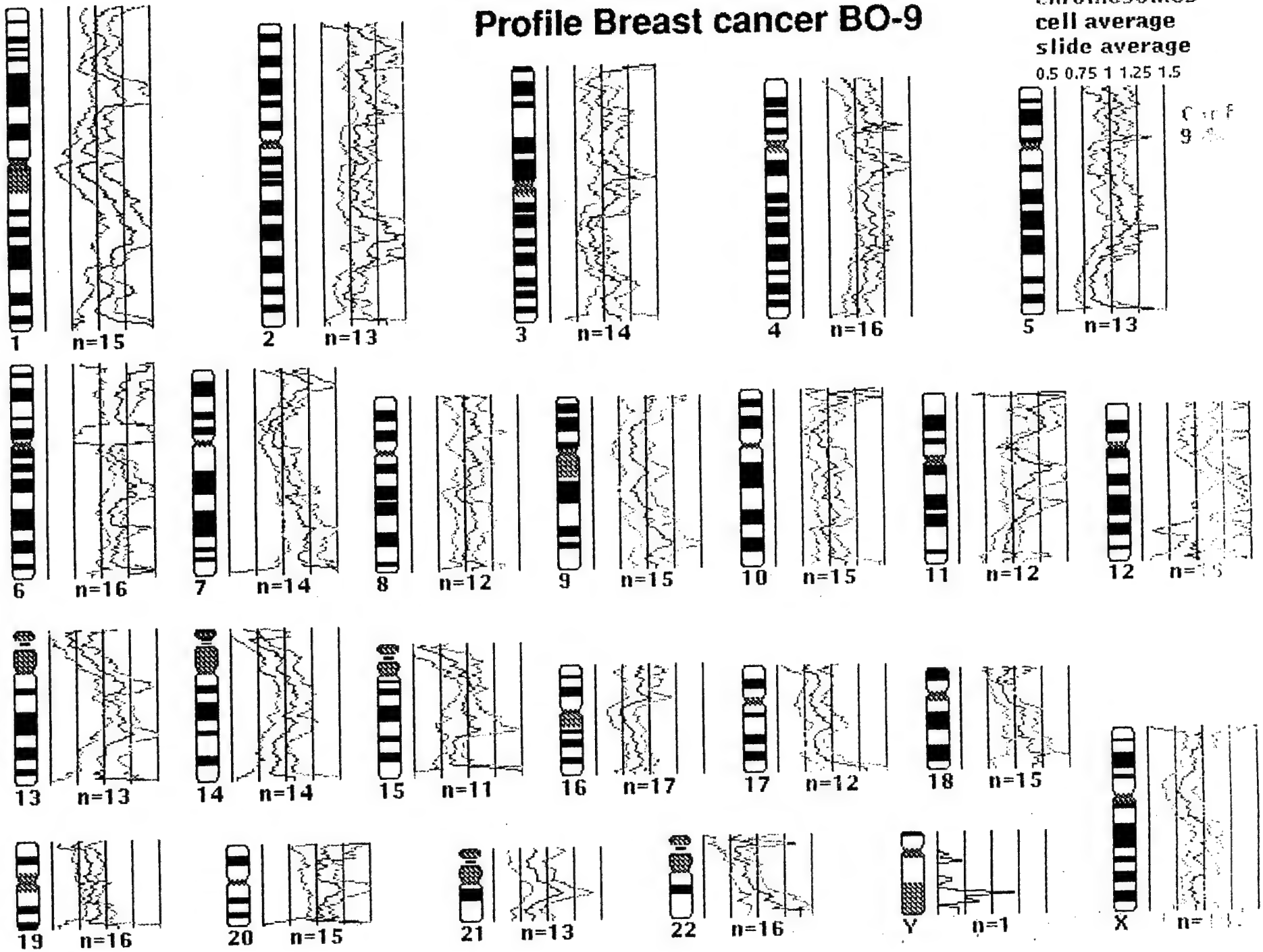
Profile Breast cancer BO-9
chromosomes
cell average
slide average
0.5 0.75 1 1.25 1.5
1 n=15
2 n=13
3 n=14
4 n=16
5 n=13
6 n=16
7 n=14
8 n=12
9 n=15
10 n=15
11 n=12
12
13 n=13
14 n=14
15 n=11
16 n=17
17 n=12
18 n=15
19 n=16
20 n=15
21 n=13
22 n=16
Y n=1
X

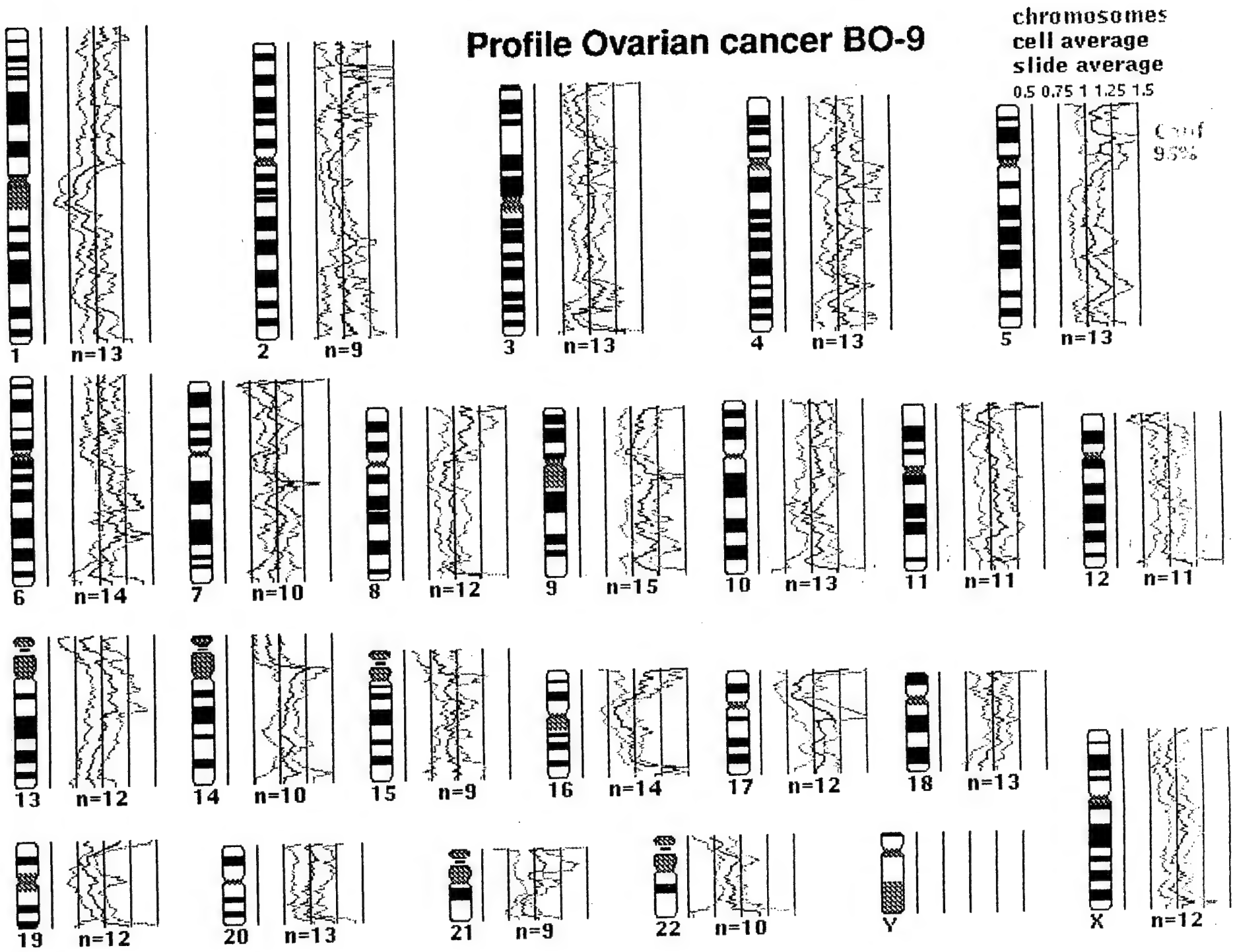
Profile Ovarian cancer BO-9
chromosomes
cell average
slide average
0.5 0.75 1 1.25 1.5
1
n=13
2
n=9
3
n=13
4
n=13
5
n=13
6
n=14
7
n=10
8
n=12
9
n=15
10
n=13
11
n=11
12
n=11
13
n=12
14
n=10
15
n=9
16
n=14
17
n=12
18
n=13
19
n=12
20
n=13
21
n=9
22
n=10
Y
X
n=12

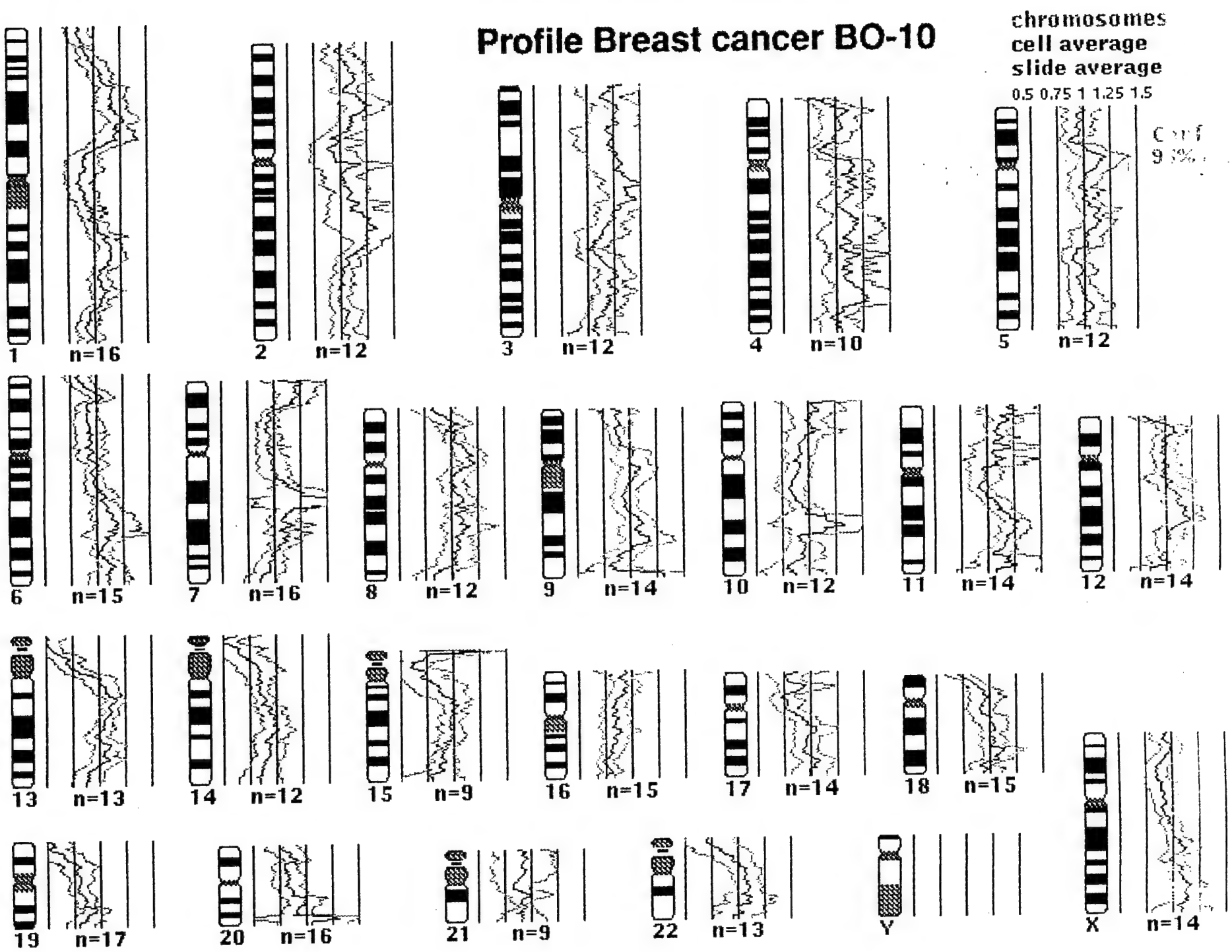
Profile Breast cancer BO-10
chromosomes
cell average
slide average
0.5 0.75 1 1.25 1.5
1 n=16
2 n=12
3 n=12
4 n=10
5 n=12
6 n=15
7 n=16
8 n=12
9 n=14
10 n=12
11 n=14
12 n=14
13 n=13
14 n=12
15 n=9
16 n=15
17 n=14
18 n=15
19 n=17
20 n=16
21 n=9
22 n=13
Y
X n=14

Profile Ovarian cancer BO-10

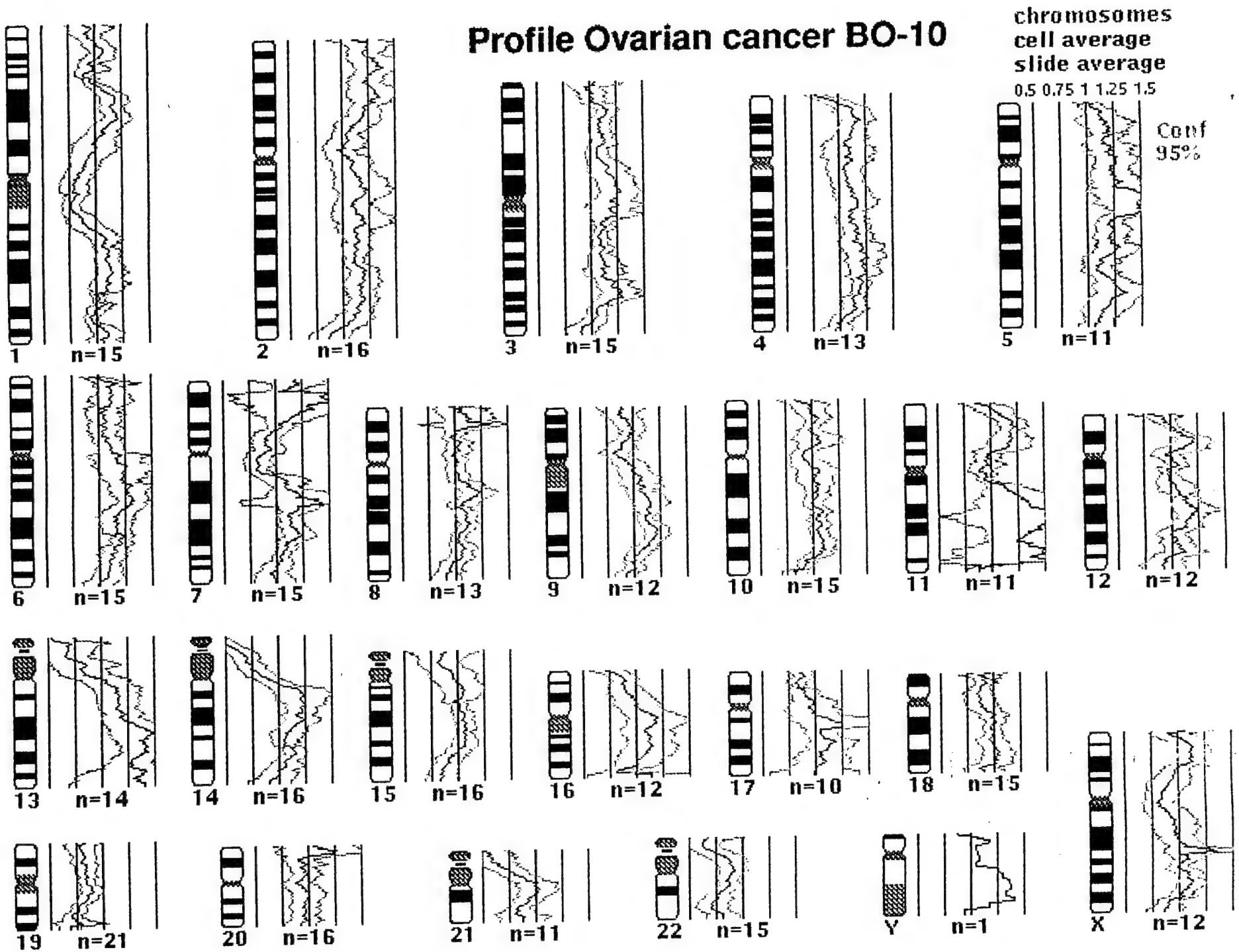

Profile Breast cancer BO-11

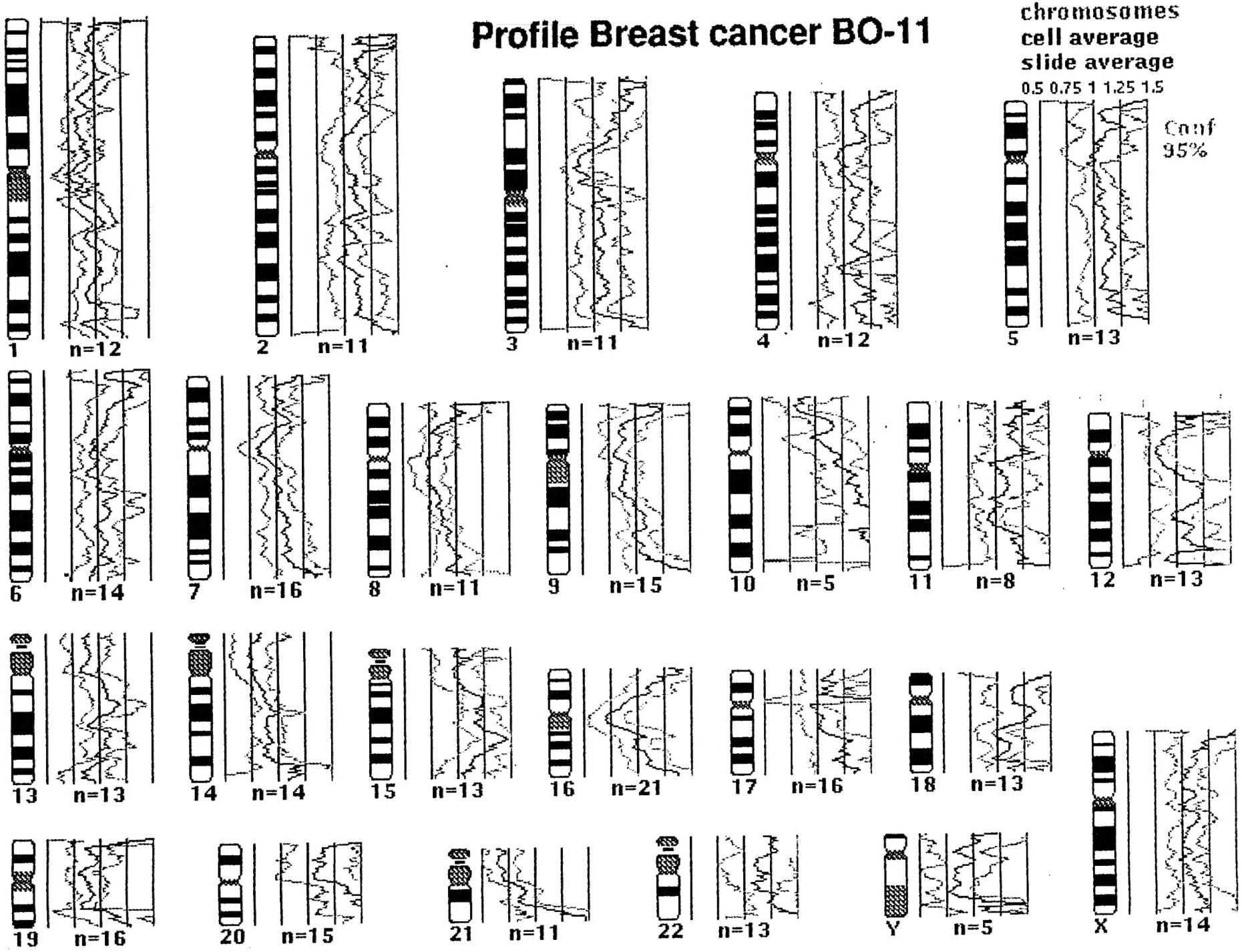

Profile Ovarian cancer BO-11

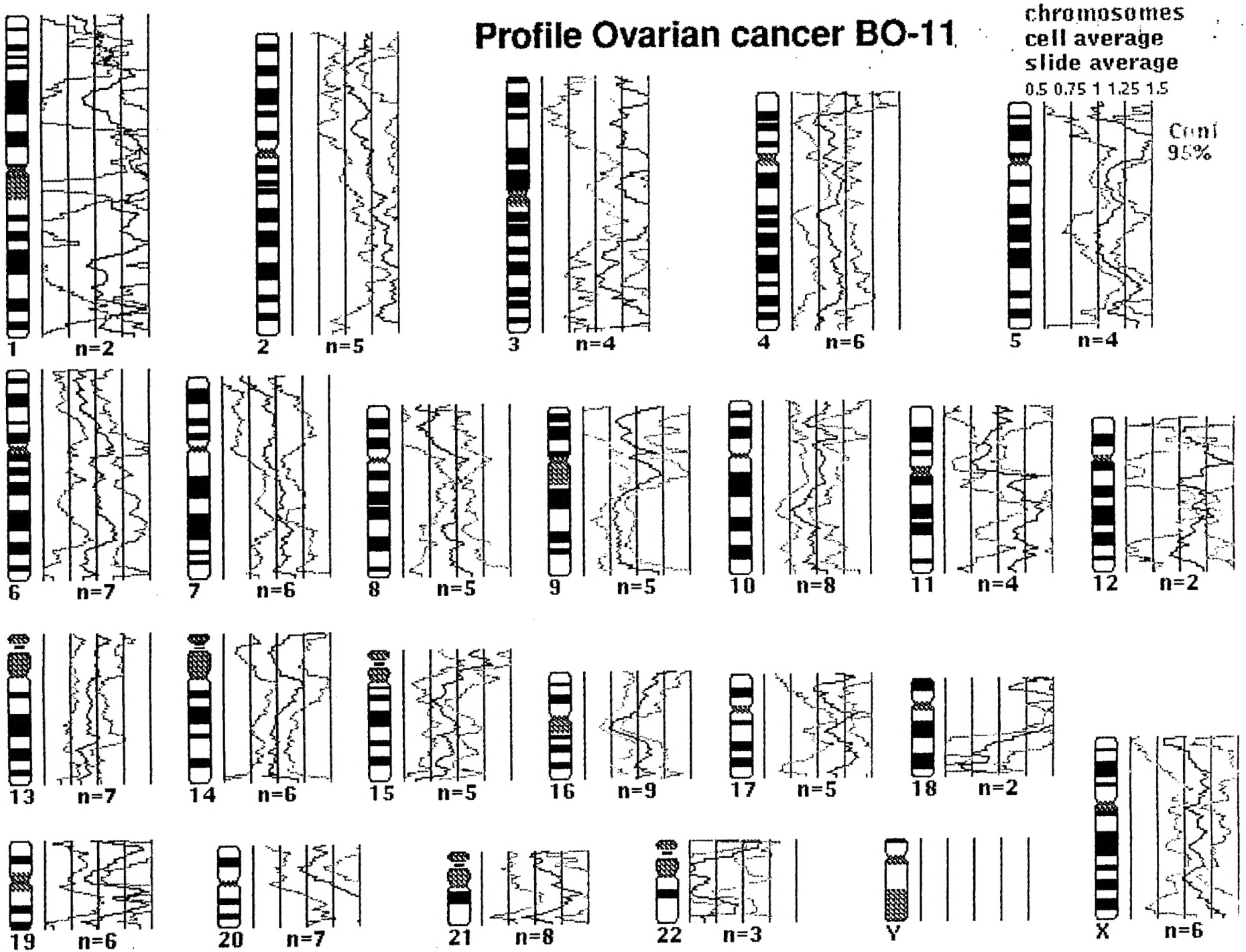

Profile Breast cancer BO-13

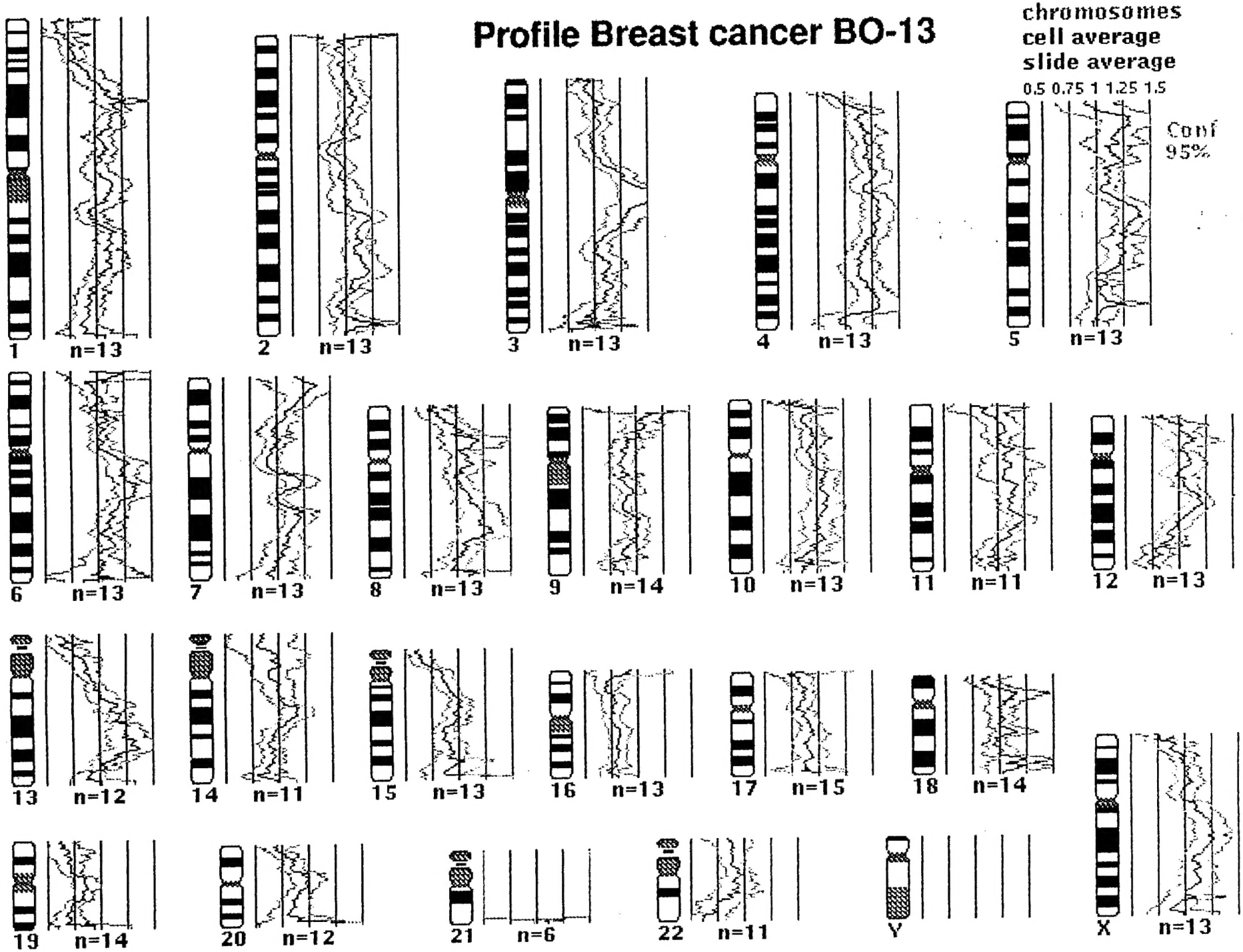

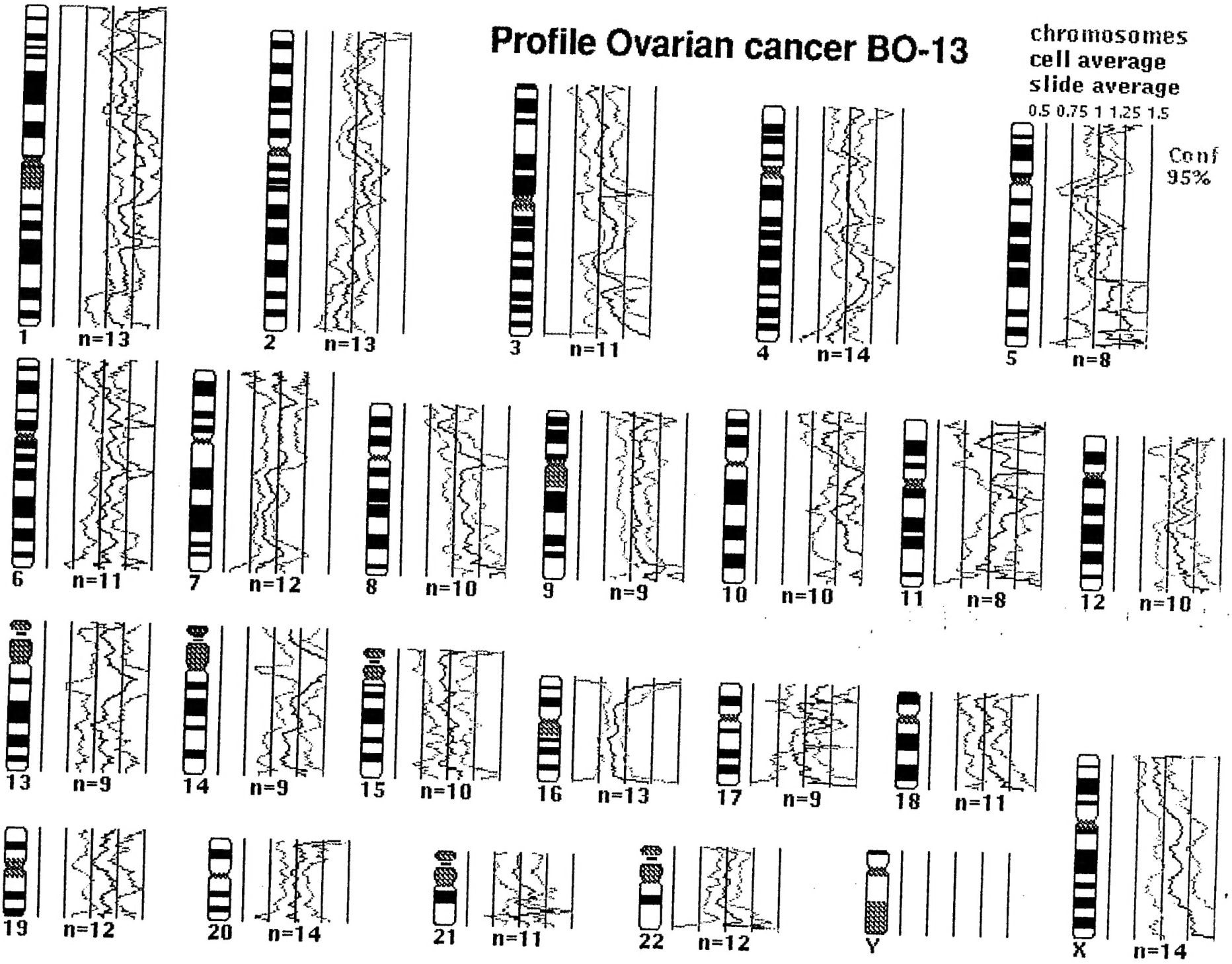
Profile Ovarian cancer BO-13
chromosomes
cell average
slide average
0.5 0.75 1 1.25 1.5
Conf
95%
1 n=13
2 n=13
3 n=11
4 n=14
5 n=8
6 n=11
7 n=12
8 n=10
9 n=9
10 n=10
11 n=8
12 n=10
13 n=9
14 n=9
15 n=10
16 n=13
17 n=9
18 n=11
19 n=12
20 n=14
21 n=11
22 n=12
Y
X n=14